MIT-3944-3
MITNE-109

A SINGLE-ELEMENT METHOD FOR HETEROGENEOUS NUCLEAR REACTORS

by

S.S. Seth, M.J. Driscoll, I. Kaplan,
T.J. Thompson and D.D. Lanning

May 1970

Contract AT(30-1)3944

U.S. Atomic Energy Commission

MASSACHUSETTS INSTITUTE OF TECHNOLOGY

Department of Nuclear Engineering

Cambridge, Massachusetts 02139

MASSACHUSETTS INSTITUTE OF TECHNOLOGY
Department of Nuclear Engineering
Cambridge, Massachusetts

A SINGLE-ELEMENT METHOD FOR HETEROGENEOUS NUCLEAR REACTORS

by

S. S. Seth, M. J. Driscoll, I. Kaplan,
T. J. Thompson and D. D. Lanning

May, 1970

MIT - 3944 - 3

MITNE - 109

AEC Research and Development Report
UC - 34 Physics
(TID-4500, 47th Edition)

Contract AT(30-1) 3944

U. S. Atomic Anergy Commission

DISTRIBUTION

MIT-3944-3 MITNE-109

AEC Research and Development Report

UC-34 Physics

1-4. U. S. Atomic Energy Commission, Headquarters
Division of Reactor Development and Technology
Reactor Physics Branch (2 copies)
Core Design Branch (1 copy)
Water Reactor Branch (1 copy)
Washington, D. C. 20545

5. U. S. Atomic Energy Commission
Savannah River Laboratory
Attn: B. C. Busche
Aiken, South Carolina 29801

6. AECL Chalk River Laboratory
Attn: C. Millar
Sheridan Park, Ontario, Canada

7. H. S. Potter, NY Patent Group
U. S. Atomic Anergy Commission
Brookhaven Office
Upton, New York 11973

8-9. U. S. Atomic Energy Commission
Cambridge Office

ABSTRACT

A "single-element" method is described for the experimental determination of the parameters Γ, η and A which characterize the neutronic properties of a fuel element in heterogeneous reactor theory. This method requires the use of only one fuel element located at the center of a tank of moderator in an exponential facility. The measurements are made outside this single fuel element and include the following quantities to which the heterogeneous fuel parameters are related: the radial distance to the thermal neutron flux peak, the inverse relaxation length of the axial flux, the cadmium ratio of gold at a given radial distance, and the ratio of the epicadmium activities (per unit isotopic weight) of gold-197 and molybdenum-98 irradiated on the fuel surface.

The single-element method was applied to 19 and 31 rod clusters of plutonium containing fuel. The reactor physics parameters of uniform lattices composed of these clusters, calculated from the measured values of Γ, η and A, show good agreement with the results of full-lattice studies of the same fuel at the Savannah River Laboratory.

It is concluded that the proposed method should increase the efficacy of heterogeneous reactor theory and make possible the evaluation of new, promising and scarce nuclear reactor fuels at very low cost.

ACKNOWLEDGEMENTS

The success of the M.I.T. Reactor Physics Project is due to the support of the U. S. Atomic Energy Commission and to the contributions of a number of individuals. The work described in this report has been performed primarily by the principal author, Shivaji S. Seth, who has submitted substantially the same report in partial fulfillment of the requirements for the degree of Doctor of Science at M.I.T.

Overall direction of the project has been shared by Professors M. J. Driscoll, I. Kaplan, D. D. Lanning and T. J. Thompson (now on leave of absence). Mr. A. T. Supple, Jr., has provided great assistance in the experimental work. The contributions of Mr. E. McFarland and Mr. T. C. Leung are specially acknowledged.

The staffs of the M.I.T. Reactor, the Reactor Machine Shop, and the Reactor Electronics Shop have provided advice and assistance. All computer calculations were done on the IBM-360 at the M.I.T. Information Processing Service Center.

Special thanks are due to Miss Marcia Clear for her unfailing patience, good humor and skill in preparing this manuscript.

TABLE OF CONTENTS

LIST OF FIGURES

LIST OF TABLES

Chapter 1

INTRODUCTION

1.1 FOREWORD

Heterogeneous nuclear reactors moderated by heavy water or graphite have been important since the early days of nuclear technology. These are, in general, well-thermalized neutron multiplying systems operating with natural or slightly enriched uranium fuel. The fuel assemblies in the reactors designed more recently are usually subdivided into clusters or annular arrays to provide for adequate cooling. The inter-array lattice spacings are large, consonant with the large migration areas of the moderators. The excellent neutron economy of these systems permits the construction of power plants that have very low fuel costs and high conversion ratios.

Although the conceptual physics problems of heterogeneous reactor lattices are generally well understood, there is still a considerable effort required to answer questions of feasibility regarding new core materials and designs, and to provide adequate and economic tools for detailed optimization. Experiments and calculations on heavy water moderated lattices have given a clear picture of the reactivity and buckling effects for the simplest case of uniform lattices of single fuel rods in D_2O (H8). This work, however, does not extend far into the range of present-day reactors. Very little work has been done, for instance, on plutonium, uranium-233, thorium, or partly burned fuels. Very few calibration experiments have been made for fuel assemblies of complex geometry with different coolants (e.g. organic,

light water, gas). Experiments with high temperature coolants are even more restricted. A deficiency in the present-day design calculations is the difficulty with which they treat complex fuel clusters; and the use of approximate methods for the calculations on fuel clusters has resulted in important errors (C2) in the calculations. Indeed, most reactor calculations contain enough approximations so that normalization by experiment is needed; and additional experimental studies are needed for each new reactor type considered.

1.2 M.I.T. REACTOR PHYSICS PROJECT

The Reactor Physics Project of the Massachusetts Institute of Technology was initiated January 1, 1968, with the objective of developing and applying single and few-rod methods for the determination of reactor physics parameters. Development of these methods should increase the ability to evaluate the reactor physics characteristics of new and promising types of reactor fuel at very low cost. Work is divided into two tasks.

Task 1 is concerned with the development of new techniques in γ-ray spectroscopy for the measurement of fuel parameters. In the first phase of this task, these techniques are applied to simulated partially burned fuel; the second phase will involve the use of actual spent fuel.

Task 2 of the project, to which this thesis is devoted, deals with the development of single-element methods and their application to fuel clusters. The first phase of this task is concerned mainly with a theoretical demonstration of the applicability of such methods,

while the later phase deals with the experimental investigation of selected plutonium fuelled single-clusters.

The annual technical reports (D6, D7) published by the project present a detailed summary of the work completed under both tasks.

1.3 THE HETEROGENEOUS REACTOR METHOD

1.3.1 A Review

Reactor calculations usually follow one of two different procedures. The more conventional one is to use multigroup multi-region diffusion theory, as applied in such computer codes as PDQ and and WHIRLAWAY. In such calculations, the heterogeneous lattice is replaced by a homogeneous multiplying medium possessing the same neutronic parameters as an infinite heterogeneous lattice. Studies (C2) have indicated, however, that this method can lead to serious errors in the reactivity of heavy water moderated lattices owing to the strongly heterogeneous nature of such lattices. The problem of calculating the critical mass and power distributions can be complicated by the use of irregular arrangements of fuel elements, control rods, dummy elements and other components for the production of isotopes. The fuel itself may consist of different types of elements, as for example, superheat and boiler elements. As irradiation proceeds, the relocation and replacement of fuel can further increase the diversity and complexity to such an extent as to make homogenized calculations highly questionable.

The second procedure based on the heterogeneous reactor theory, seems to provide a more direct treatment, which may be especially

suitable for heavy water (or graphite) moderated power reactors. The heterogeneous reactor method was first reported by Galanin (G1, G2) and Feinberg (F1) in the U.S.S.R., and by Horning (H9) in the U.S. Since then, several improvements have been made. Heterogeneous computations, as currently used, may be subdivided into "mesh methods" (finite difference methods) and "kernel methods" (source-sink methods).

The mesh method solves the differential equations of multigroup theory (usually for two groups) written as finite-difference equations, within the moderator region. Each fuel element is described by a "surface matrix" connecting the surface fluxes and their normal derivatives. The computer code HET-B2 (A1) is representative of this method.

The better known source-sink method is the more direct and convenient formulation of the heterogeneous theory. Since it has been used in the present work, this method will be described in some detail.

1.3.2 The Source-sink Method

In its kernel form, the heterogeneous reactor theory represents nuclear fuel assemblies by neutron sources and sinks, and the contribution to the neutron density at any point is expressed by means of a suitable propagation kernel and superposition. Following the notation of Feinberg (F1) and Klahr (K4), a two-dimensional assembly containing N infinitely long fuel elements may be represented by the equation:

$$\Gamma_n i_n = \sum_{n=1}^{N} \{\frac{\eta_m}{K} F^*_{nm} - f_{nm}\} i_m, \quad n = 1,2,\ldots N, \tag{1.1}$$

where i_n is the number of thermal neutrons absorbed per cm-sec in the n^{th} element,

Γ_n is $\frac{\phi_n}{\phi_n}$, with ϕ_n the asymptotic (moderator) flux at the radius of the n^{th} element,

η_m is the number of fast neutrons produced per thermal neutron absorbed in the m^{th} element,

K is the eigen-value (unity for a critical assembly),

f_{nm} is the thermal source kernel which gives the thermal flux at the n^{th} element due to a source of thermal neutrons of strength 1 neutron/(cm-sec) at the m^{th} element; the f-distribution is generally evaluated by means of simple diffusion theory.

The parameter F^*_{nm} is the "fission-to-thermal source kernel" (with resonance absorption included) which gives the thermal neutron flux at the n^{th} element due to a source of fast fission neutrons of strength 1 neutron/(cm-sec) at the m^{th} element. This factor includes moderator absorption and accounts for resonance absorption by subtracting (Eq. 1.2) a neutron sink at the resonance energy from the "fission-to-thermal source kernel", F_{nm}, which does not include resonance absorption. Thus

$$F^*_{nm} = F_{nm} - \sum_{t=1}^{N} A_t \, g_{tm} \, F^r_{nt} \tag{1.2}$$

where A_t is the ratio of resonance absorption per cm-sec in the t^{th} element at single equivalent resonance energy to the

asymptotic slowing-down density at this resonance energy,

g_{tm} is the "fission-to-resonance slowing-down kernel" giving the density of neutrons slowing down to the equivalent resonance energy per second at the t^{th} element due to a source of strength 1 neutron/(cm-sec) at the m^{th} element; a slowing-down distribution is generally taken as the weighted sum of two or three Gaussian functions, either as a convenient method of presenting the results of detailed calculations (B6) or as a purely empirical fit to experimental data (G6, G7),

F^r_{nt} is the thermal neutron flux at the n^{th} element due to a source of strength 1 neutron/(cm-sec) at the t^{th} element emitting neutrons of the equivalent resonance energy.

This formulation thus involves the use of three parameters η, Γ and A to describe a nuclear fuel element. These parameters characterize, respectively, the fast neutron source and the thermal and epithermal neutron sinks in the fuel. The formulation also involves kernel functions which describe the epithermal and thermal coupling between individual fuel elements. The resulting set of N homogeneous algebraic equations can be reduced in number to as many as the number of fuel element types by using the symmetry properties of the lattice components. The eigenvalue and eigenvector can then be obtained by the usual matrix methods.

A better understanding of the heterogeneous theory has now widened its range of validity. Klahr et al. have clarified and removed some basic restrictions, such as those on the source size and the looseness of fuel packing, which were thought to exist on the applicability of the model. Their work provides the basis for the digital computer codes HERESY I and II (K4, F2). Other codes based on the heterogeneous principle are: HETERO, of AB Atomenergi, Sweden (N1); MICRETE, of Chalk River, Canada (S2); and TATJANA and TRIHET, of Euratom (B4).

1.3.3 Advantages

Owing to their realistic treatment of the core assembly and of the discrete characteristics of the fuel and control elements, the heterogeneous calculations permit a relatively simple and accurate analysis of cores with multi-component lattices, such as seeded cores, spiked cores, lattices with fuel and control rods, and nonuniform burn-up effects. Significant results (K3, K4) include the calculation of relative absorption in the individual fuel elements, and differences in reactivity and absorption patterns among various configurations. Other applications include buildup of a lattice to criticality, power patterns for finite lattices, power flatting in spiked cores and comparison of alternative control rod patterns.

A further potential advantage of the heterogeneous method is its use of the heterogeneous fuel parameters, which if directly measured, could significantly decrease the dependence of the calculations on the cross section data.

The scope, usefulness and improved accuracy of the heterogeneous technique thus provide a strong motivation to develop this method further.

1.3.4 A Major Limitation

A major condition for the success and accuracy of the heterogeneous method is a careful determination of the three heterogeneous parameters Γ, η and A. The calculation of these parameters was, in fact, a major difficulty in the early work with the method, and much effort has been expended on the problem. Klahr et al. (K4) and Graves et al. (G7) have reported success with heterogeneous calculations based on the use of the "asymptotic" flux and a "self-consistent" procedure for evaluating the fuel parameters.

In the self-consistent procedure a set of kernel functions is used to back-calculate the fuel element parameters Γ and A from known values of the thermal utilization (f) and the resonance escape probability (p) for a uniform lattice composed of the fuel element in question. The parameters thus obtained are then used together with the original kernel functions to calculate reactivity and power distributions for configurations of interest. Values of the parameters f and p have usually been obtained in either of two ways: experimentally, from thermal and resonance flux measurements in a unit cell; analytically, from multigroup cell calculations, or in the case of p, from resonance integral formulas involving the effective surface area. The fast neutron yield factor η used in these studies is normalized so that the product (ηf) is the same as would be obtained from cell calculations.

The expressions (K4, G7) which relate Γ and A to f and p, respectively, require that (1-f) and (1-p) be known with high accuracy. In the case of D_2O moderated lattices these values are very close to zero. Hence f and p must be determined to say, one percent to ensure that the parameters Γ and A have uncertainties smaller than, say 10%. For this reason, earlier workers have found it difficult to evalute the fuel parameters in D_2O moderated assemblies. Klahr et al. have pointed out that attempts to use the measured thermal flux distributions to determine f gave poor results. On the other hand, disagreements between calculated and experimental values of buckling in some work (G7) have been ascribed primarily to errors in the cell codes used to generate the set of heterogeneous parameters for use in heterogeneous reactor calculations. The studies cited refer mainly to the relatively simple single rod lattices.

It appears, then, that in many practical lattices which would contain complex fuel clusters with nonuniform burn-up and consequent uncertain composition, reliable calculations are difficult, if not impossible. While a two-dimensional cell code is considered too unwieldy for production purposes, a code which solves an "equivalent" one-dimensional problem loses accuracy in its results. For elements consisting of 19-rod uranium-oxide clusters in heavy water, calculated and measured values of f differ by as much as 3% (H4). The high accuracy invariably associated with transport theory calculations is generally unattainable in many practical applications, either because of computational limitations, geometric complexity, or the lack of adequate nuclear data. The theoretical analysis would therefore have

to be supplemented by lattice experiments. Thus for example, in work reported on 19-rod uranium-metal clusters (T1), the value of the buckling measured in a lattice of this fuel was used to calculate the infinite-medium multiplication constant and the resonance escape probability. These in turn were used as input to the calculations with the heterogeneous reactor computer codes MICRETE and HERESY. Furthermore, this extensive experimental and calculational effort on lattices must be repeated in order to obtain the heterogeneous parameters for each different fuel type in a practical, multi-component reactor lattice.

The self-consistent procedure therefore, requires extensive experiments and calculations on uniform lattices to determine certain cell parameters (e.g. f and p); the latter, rather than the fuel parameters (Γ, η and A) themselves constitute, in effect, the input parameters to the heterogeneous calculation.

The main objective of the single-element method is the direct experimental determination of the three fuel parameters Γ, η and A. This will eliminate the indirect, uneconomical procedures currently used for their evaluation.

1.4 THE SINGLE-ELEMENT METHOD

1.4.1 Outline

The single-element method for the determination of the heterogeneous fuel parameters is developed in the present work for a cylindrical exponential facility with a single fuel element located at the center of a tank of moderator. The term "single fuel element"

is used in the present work to include all materials, i.e., fuel, cladding, coolant, etc., within the outermost boundary of a single rod or a "tight" cluster of rods. Thus in the case of the fuel clusters (Fig. 1.1), the single fuel element comprises all the individual fuel rods with their cladding and the surrounding air-gaps, and the coolant within the encompassing cluster-tubing which separates the fuel from the moderator.

The analytic formalism developed in this work makes it possible to evaluate the heterogeneous parameters - the thermal constant (Γ), the fast neutron yield (η) and the epithermal absorption parameter (A) by relating them to quantities which are measured in the moderator surrounding the single fuel element. Specifically, these measured quantities are: the radial position of the thermal neutron flux peak (X cm), the inverse relaxation length (γ cm^{-1}) of the axial flux, the cadmium ratio of gold (R) at a known radial distance (Y) from the fuel element, and the ratio (F) of the activities (per unit isotopic weight) of Au-197 and Mo-98 measured in cadmium-covered gold and molybdenum foils irradiated on the fuel surface.

These quantities are measured for tight clusters (Fig. 1.1) of 19 and 31 fuel rods typical of the clusters considered in designs of pressure-tube, D_2O moderated and cooled power reactors. The fuel composition of the elements, described in Table 1.1, simulates that of natural uranium partially burned to 5000 MWD/ton; the elements therefore contain the various isotopes of plutonium. Uniform lattices of these clusters arranged on 9.33 in. and 12.12 in. spacings in heavy water have been studied at the Savannah River Laboratory (USA).

2/3 SCALE

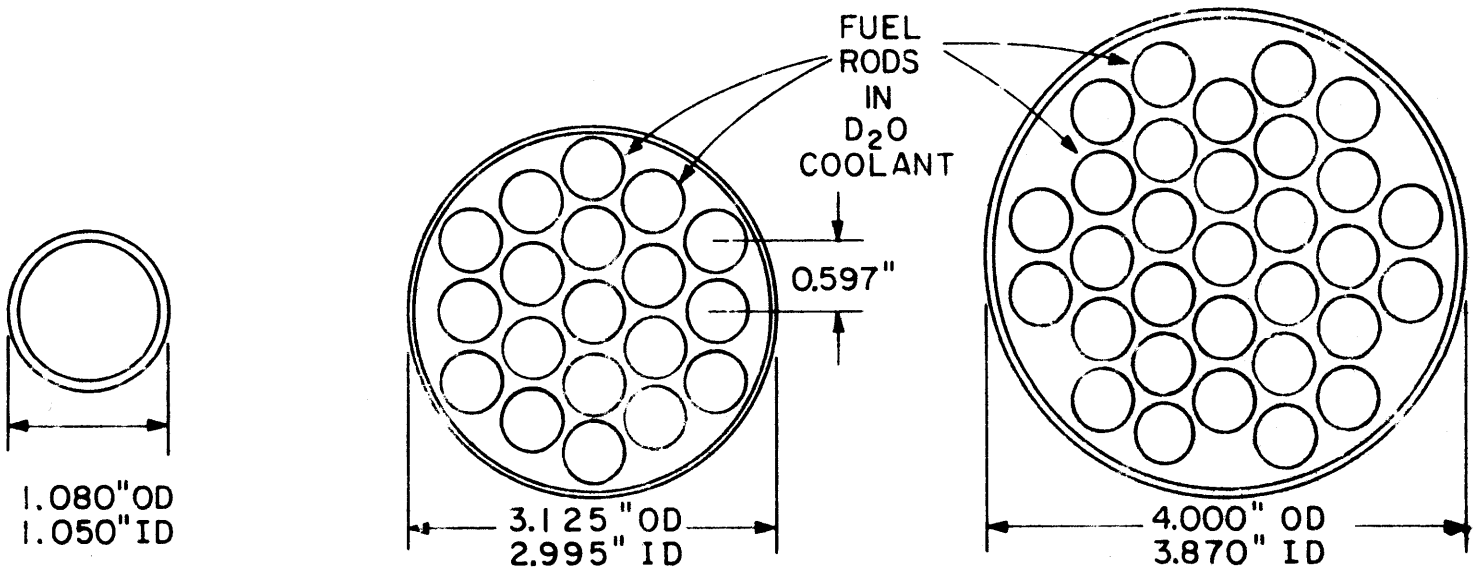

1100 Al CLADDING
(1.01-inch DIAMETER
NATURAL URANIUM)

6061 Al HOUSING TUBE
(19-ROD CLUSTER)

6061 Al HOUSING TUBE
(31-ROD CLUSTER)

FIG. 1.1 FUEL ELEMENT ARRANGEMENTS

Table 1.1

ISOTOPIC COMPOSITION* OF SIMULATED BURNED FUEL**
USED IN 19 AND 31 ROD CLUSTERS

Isotope	Wt.% of Total U + Pu
U-238	99.431
U-235	0.30
Pu-239	0.20
Pu-240	0.016
Pu-241	0.002
Pu-242	0.001

* Break-down of nuclide concentration in the clusters: Appendix G

** Type B (color code: gold),
USAEC-AECL Cooperative Program (B1)

The experimental and calculational results of these studies have been reported (B1) by the Savannah River Laboratory (SRL). Work (F4) on the same fuel has also been carried out by the Atomic Energy of Canada Limited (AECL).

The set of values of Γ, η and A, thus measured, serves to characterize the neutronic properties of the 19 and 31 rod clusters. Such a set of heterogeneous parameters for each fuel-type present in a particular multi-component lattice can thus be used in a suitable heterogeneous reactor code, such as HERESY, to give nuclear properties of the lattice in question. To provide a simple test of the methods developed, attention is restricted to the case of uniform lattices composed of the clusters described above. The measured single-element parameters are used in an expression equivalent to the four-factor formulation; values of the material buckling are then determined with the aid of age-diffusion theory. The use of this convenient procedure to test the proposed methods should give good results for the uniform lattices considered and save the cost and effort needed to apply a computer code such as HERESY. The physics characteristics of complete uniform, D_2O moderated and cooled lattices of 19 and 31-rod clusters in 9.33 in. and 12.12 in. spacings calculated from the single-element parameters are finally compared with results of the Savannah River Laboratory.

1.4.2 Highlights

The single-element method proposed in this study to directly measure the heterogeneous fuel element parameters, has features which offer valuable advantages.

1. The method requires only one fuel element. Knowledge of the physics characteristics of complete, uniform lattices made up of this fuel element can thus be obtained at greatly reduced material requirements and cost. In particular, this method can be applied to scarce, new and promising fuel-types.
2. A single rod or a single tight cluster of rods is treated as a "black-box". The method therefore seeks no information about the internal structure or composition of the fuel element. Thus, for example, a composite single fuel element could contain partially burnt, dissimilar fuel rods of uncertain isotopic composition or control rods, all arranged in any configuration with the associated structural material, "poison", fission products and coolant. In the applications of the method presented in this work, the single element is a tight cluster of 19 or 31 fuel rods with a composition simulating that of natural uranium rods partially burnt to 5000 MWD/ton; the individual rods and the cluster as a whole are contained in aluminum, and there is D_2O coolant inside the clusters.
3. The measurements are made outside the fuel: all experiments aimed at measuring quantities related to the fuel parameters are made in the moderator surrounding the single-element. There is no need to cut into the fuel cluster or otherwise perturb it. The problems of contamination and hazards from the fission products or plutonium within the fuel are thus circumvented.
4. The measurements do not depend on the microscopic nuclear data of the fuel material. Since the integral fuel parameters of the heterogeneous theory are related to certain directly measurable

quantities, which involve relative magnitudes, the method eliminates any reliance on the basic nuclear cross-sections of various isotopes in the fuel element.

5. The single-element method yields parameters which can be directly fed into an established heterogeneous formalism. The measured parameters considered in the present work have, therefore, been defined and determined so as to conform to the heterogeneous methods developed by Klahr et al. and adopted in the computer code HERESY.

1.5 ORGANIZATION OF THE REPORT

Chapter 2, which follows, describes in detail the theoretical basis underlying the measurements from which the three fuel parameters are derived. The actual experimental procedures, methods of analysis and results are presented in Chapter 3. The application of the single-element methods to uniform lattices, and subsequent comparisons with other theoretical and experimental results are given in Chapter 4. The concluding Chapter 5 is a summary of the work done. It contains several suggestions for future work. Appendix I contains a bibliography of literature on heterogeneous reactor methods.

Chapter 2

THEORY

2.1 HETEROGENEOUS FUEL ELEMENT PARAMETERS

The three fuel element parameters Γ, η and A first introduced in Chapter 1 are now defined and explained in greater detail. The term "fuel" used in the present work has the same generic definition explained earlier in Section 1.4.

A basic concept of heterogeneous reactor theory is that these parameters are independent of the inter-fuel spacing in a lattice. Data and comparisons to justify this assumption have been given in other works (D4, K3, K4, P2). Small corrections to the heterogeneous parameters are, however, necessary to take into account fuel interaction and spectral effects in a lattice. Of the three fuel parameters, η varies most with lattice spacing primarily because it has been defined here to include the fast fission factor. The other two parameters, Γ and A, vary much less with lattice spacing. The correction factors necessary to account for the above variations in the fuel parameters are discussed further in Chapter 4.

2.1.1 Thermal Constant, Γ

The thermal constant Γ is defined as the average value of the "asymptotic" thermal neutron flux in the moderator, evaluated at the fuel surface, per thermal neutron/(cm-sec) absorbed in the fuel element; it has the dimension of inverse length.

The concept of the asymptotic flux in the above definition was first introduced and explained by Klahr et al. (K3). The asymptotic

thermal neutron flux in the moderator is defined as that thermal neutron flux which would result in the moderator if the fuel element were shrunk in size to a line with its sink intensity remaining unchanged. The value of the asymptotic flux that enters the definition is obtained by extrapolating back to the surface of the fuel, the thermal diffusion theory flux in the moderator at distances of a few mean free paths or more from the fuel (Fig. 2.1). In this way, the fuel-moderator boundary transport effects do not affect the definition.

In terms of symbols, the definition of Γ is:

$$\Gamma = \frac{\phi_r(a)}{2\pi a(-J_r)_a} = \frac{\phi_r(a)}{2\pi a D(\nabla\phi_r)_a} \qquad (2.1)$$

where a is the radius of the smallest circle that completely encompasses the geometric fuel cross-section,

$\phi_r(a)$ is the radial component of the asymptotic thermal neutron flux in the moderator evaluated at r = a,

$(\nabla\phi_r)_a$ is the spatial gradient of $\phi_r(r)$ at r = a,

D is the thermal neutron diffusion coefficient of the moderator,

$(-J_r)$ is the thermal neutron current into the fuel.

The diagram in Fig. 2.1 explains the notation in relation to a single element placed in the center of a cylindrical tank of moderator.

It can readily be seen from the above definition that for a given value of the asymptotic flux, the smaller the Γ, the larger is the thermal neutron current into the fuel. In this respect, Γ

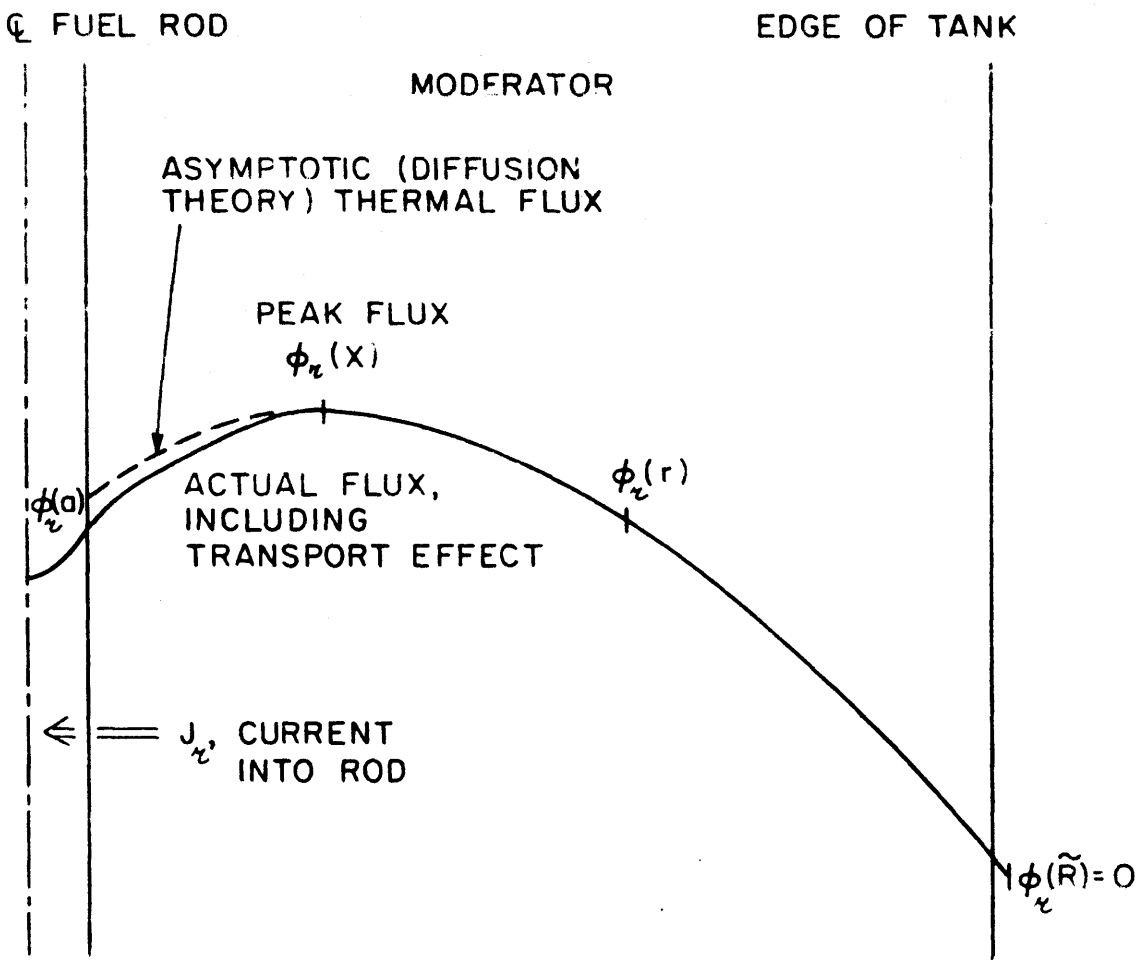

$\phi_r(a)$ = ASYMPTOTIC MODERATOR THERMAL FLUX EVALUATED AT ROD SURFACE

$|J_r|$ = NET NEUTRON CURRENT INTO THE FUEL ROD, $n / cm^2 - sec.$

a = RADIUS OF FUEL ELEMENT OR "EFFECTIVE" RADIUS IN CASE OF CLUSTER FUEL ELEMENT

X = RADIAL DISTANCE AT WHICH PEAK FLUX OCCURS

$\tilde{R}$ = EXTRAPOLATED RADIUS OF TANK

FIG 2.1 THERMAL NEUTRON FLUX DISTRIBUTION AROUND THE SINGLE FUEL ELEMENT

could be termed a "diffusional impedance" (S2).

The thermal constant Γ is related (D4) to the extrapolation distance (d) in the fuel element,

$$d = \frac{\phi_r(a)}{(\nabla\phi_r)_a}\ ; \tag{2.2}$$

$$\text{so that } \Gamma = \frac{d}{2\pi a D} = \frac{3}{2\pi a}\left(\frac{d}{\lambda_{tr}}\right), \tag{2.3}$$

since $D = \frac{\lambda_{tr}}{3}$, where λ_{tr} is the transport mean free path in the moderator.

The thermal constant Γ has been defined variously by previous workers, notably Galanin and Pilat. The relationship among these definitions and their demerits have been pointed out by Donovan (D4).

2.1.2 Fast Neutron Yield, η

The fast neutron yield η is defined as the net number of fast neutrons emerging from the fuel element per thermal neutron absorbed. The fast neutrons are a result of all the fissions: thermal, epithermal and fast, in all the fissionable nuclides in the fuel.

This definition thus differs from that of the usual fast neutron yield (η') in that it includes the epithermal and fast fission contributions to η', and the reactions which could prevent the escape of the fast neutrons from the fuel. Thus for uranium fuel containing U-235 and U-238, the relationship between η and η' is:

$$\eta = \eta'(1 + \delta_{25})\left\{1 + \frac{(\nu_{28,f} - 1 - \alpha_{28,f})}{\nu_{25,th}}\,\delta_{28}\right\} \tag{2.4}$$

where δ_{25} is the measured ratio of the epicadmium to the subcadmium fission rate in U-235,

δ_{28} is the measured ratio of total fission in U-238 to that in U-235

and other constants are defined in Appendix H.

Equation 2.4 will be used in deriving the "reference" value of η for a 1.01-in. diameter natural uranium rod (Appendix E).

For the case of an isolated single fuel element in a thermal neutron environment, the net thermal absorption per cm.-sec. of the fuel is given by $\frac{\phi_r(a)}{\Gamma}$ (Eq. 2.1). Hence it follows from the definition of η that:

$$\left.\begin{array}{l}\text{total fast neutron yield} \\ \text{per cm.-sec. from the fuel}\end{array}\right\} = \frac{\phi_r(a)}{\Gamma}\,\eta \quad . \tag{2.5}$$

2.1.3 Epithermal absorption parameter, A

Under the assumption that all the epithermal absorption occurs at a single effective resonance energy, the epithermal absorption parameter A is defined as the total epithermal absorption per cm.-sec. of the fuel element at the effective resonance energy per unit averaged asymptotic slowing down density at that effective resonance energy. A has the dimension of area. The epithermal absorption referred to includes the resonance and 1/v-absorption in all the nuclides present in the fuel. Following Klahr et al., this definition can be extended to resonance absorption at different energies (i). The definition of A^i then corresponds to the resonance absorption and the slowing down density at the i^{th} resonance.

The above definition can be applied to a unit cell of a reactor lattice in which the volume of the moderator per unit height of the fuel is V_m. If it is assumed that the asymptotic epithermal flux

$\overline{\phi}_{epi}(u)$ is constant radially throughout the cell as well as constant over all lethargies (1/E energy dependence) the asymptotic slowing down density per unit lethargy, $q_{epi}(u) = \xi\Sigma_s\overline{\phi}_{epi}(u)$ is constant. The epithermal absorption parameter A is then:

$$A = \frac{\text{epithermal absorption}}{q_{epi}(u)} = \frac{V_f \sum_i N_f^i RI_f^i \overline{\phi}_{epi}}{\xi \Sigma_s \overline{\phi}_{epi}}, \qquad (2.6.1)$$

so that $$A = \frac{V_f \sum_i N_f^i RI_f^i}{\xi\Sigma_s}, \qquad (2.6.2)$$

where V_f is the volume of fuel element per unit length,

N_f^i is the concentration of the i^{th} nuclide in the fuel,

RI_f^i is the resonance integral (including 1/v-absorption) of the i^{th} nuclide,

$\overline{\phi}_{epi}$ is the average asymptotic epithermal neutron flux per unit lethargy,

$\xi\Sigma_s$ is the slowing down power of the moderator.

If only one neutron is slowing down in the moderator volume of the unit cell of unit height, the slowing down density is $1/V_m$. Hence the total epithermal absorption per cm.-sec. in the unit cell per unit source neutron is: A/V_m; (2.7.1)

and the probability that a source neutron escapes epithermal absorption (resonance escape probability) is:

$$p = 1 - \frac{A}{V_m}. \qquad (2.7.2)$$

2.2 EXPERIMENTAL PARAMETERS

This section presents the set of quantities to be directly measured. These will be related to the three heterogeneous parameters in subsequent sections. The sketch in Fig. 2.2 should aid in understanding the experimental arrangement and the basis for the theoretical model.

The single element in question is located at the center of a cylindrical tank of moderator. A J_0-shaped source of thermal neutrons at the lower end of the tank sets up an axial exponential flux gradient in the moderator. The single element, playing the dual role of a source of fast neutrons and a sink of thermal and resonance neutrons, superimposes its neutronic proprties upon the unperturbed thermal neutron distribution.

A set of four quantities is measured:

1. X(cms): position of the peak of the thermal neutron flux distribution in the moderator.
2. $\gamma(cm^{-1})$: inverse relaxation length of the axial flux.
3. R: cadmium ratio in gold at a measured radial distance Y(cms).
4. F: ratio of the activities (per unit isotopic weight) of Au-197 and Mo-98 measured in cadmium-covered gold and molybdenum foils irradiated on the fuel surface.

It is shown in what follows that whereas the measurement of F alone suffices to determine A, all of the other three experimental quantities: X, γ and R are directly or indirectly involved in the determination of the other two parameters Γ and η.

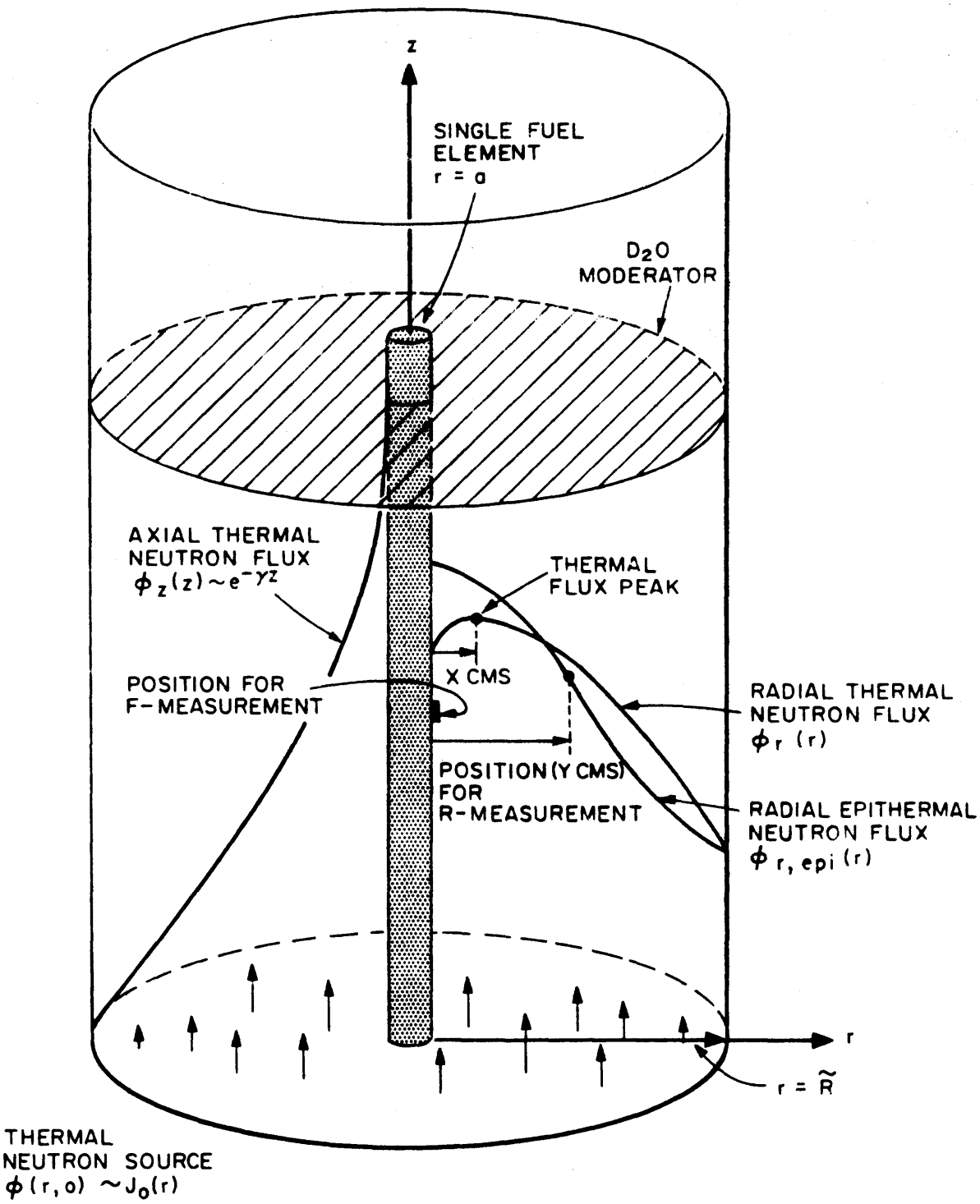

FIG. 2.2 THE SINGLE ELEMENT MODEL

2.3 DETERMINATION OF Γ

In the "self-consistent" procedure (K3) the value of Γ is obtained rather indirectly from a previously known value of the thermal utilization. A method for a direct evaluation of Γ is presented in this section. A new method (B2) which also employs only a single fuel assembly, makes use of neutron-wave propagation methods to measure Γ (actually, Galanin's thermal constant, γ); the stated uncertainty in the result, however, is 8% and its deviation from the calculated value is about 25%.

The proposed procedure for obtaining a theoretical expression for Γ consists of first deriving the shape of the thermal neutron flux distribution, and then using the condition that the flux passes through a maximum at the measured distance X. To evaluate Γ completely, however, values of both η and A are necessary (Eq. 2.36). Final comments regarding the determination of Γ are made in Section 2.4.3.

2.3.1 Thermal Neutron Flux Distribution

Consider a unit volume of the moderator located around a point (r,z) with respect to coordinate axes located at the base of the fuel element in the center of the moderator tank. The r and z components are measured, respectively, along the radius and the axis of the tank. The system has azimuthal symmetry. The balance of thermal neutrons in this unit volume of the moderator (Fig. 2.2), may be described by the following diffusion equation:

$$D\nabla^2\phi(r,z) - \Sigma_{am}\phi(r,z) + Q(r,z,\tau_{th}) = 0, \tag{2.8}$$

where $$\nabla^2 \equiv \frac{1}{r}\frac{\partial}{\partial r}\left(r\frac{\partial}{\partial r}\right) + \frac{\partial^2}{\partial z^2}, \tag{2.8.1}$$

$\phi(r,z)$ is the thermal neutron flux at the point (r,z),

Σ_{am}, D are the macroscopic absorption cross-section and the diffusion coefficient, respectively, for thermal neutrons in the moderator,

$Q(r,z,\tau_{th})$ is $Sq_r(r,\tau_{th})$, (2.8.2)
the contribution of fast neutrons slowing down from the single-element to thermal energies at the point (r,z);

S is $\frac{\phi(a,z)\eta}{\Gamma}$, the single element fast neutron source (Eq. 2.5) at age $\tau = 0$; and

$q_r(r,\tau_{th})$ is the slowing-down density of thermal neutrons ($\tau = \tau_{th}$) at the point (r,z) arising from a uniform cylindrical fast neutron source ($\tau = 0$) of unit intensity and of radius, a, located at $(0,z)$ in the presence of resonance absorption in the source element at a single effective energy E_r ($\tau = \tau_r$). This slowing-down density is derived in Section 2.3.4.

The flux and neutron densities are now separated into their radial and axial components (written with subscripts, r and z, respectively). Assuming that the z-components decay exponentially with an inverse relaxation length, γ, it follows that:

$$\phi(r,z) = \phi_r(r) \cdot \phi_z(0)e^{-\gamma z}, \tag{2.8.3}$$

$$Q(r,z,\tau_{th}) = \frac{\phi_r(a)\phi_z(0)e^{-\gamma z}}{\Gamma}\,\eta\; q_r(r,\tau_{th}). \tag{2.8.4}$$

Substitution for $\phi(r,z)$ and $Q(r,z,\tau_{th})$ from Eqs. 2.8.3 and 2.8.4 into 2.8 and dividing throughout by $\phi(0)e^{-\gamma z}$ gives:

$$\frac{1}{r}\frac{\partial}{\partial r}\left[r\frac{\partial}{\partial r}\phi_r(r)\right] + \gamma^2\phi_r(r) - \frac{\Sigma_{am}}{D}\phi_r(r) + \frac{Q_r(r,\tau_{th})}{D} = 0 \tag{2.8.5}$$

This equation may be written:

$$\mathcal{L}\{\phi_r(r)\} + \frac{Q_r(r,\tau_{th})r}{D} = 0 \tag{2.9}$$

where $\mathcal{L}$, the linear differential operator

$$\equiv \frac{\partial}{\partial r}\left(r\frac{\partial}{\partial r}\right) + \alpha^2 r, \tag{2.9.1}$$

$$\alpha^2 \equiv \gamma^2 - \frac{\Sigma_{am}}{D} = \gamma^2 - \frac{1}{L_0^2}, \tag{2.10}$$

and L_0 is the thermal neutron diffusion length in the moderator;

$Q_r(r,\tau_{th})$ is $S_r q_r(r,\tau_{th})$, with

$$S_r = \frac{\phi_r(a)\eta}{\Gamma}, \text{ and} \tag{2.11}$$

$q_r(r,\tau_{th})$ the radial component of $q_r(r,z,\tau_{th})$ is evaluated in Section 2.3.4.

Equation 2.9 is an inhomogeneous differential equation with the following homogeneous mixed boundary conditions at the fuel surface (r = a) and at the "extrapolated" outer moderator boundary ($r = \tilde{R}$):

$$r = a, \quad \phi_r(a) - 2\pi a D(\nabla\phi_r)_a \Gamma = 0 \text{ (Eq. 2.1)}; \tag{2.12}$$

$$r = \tilde{R}, \quad \phi_r(\tilde{R}) = 0. \tag{2.13}$$

The use of the Green's function technique (H6) to solve Eq. 2.9 gives a closed functional representation of the solution. Physically, the method consists of obtaining the thermal neutron field caused by the distributed source by first calculating the effects of each elementary portion of the source and then adding them all up.

The Green's function $G(r,\xi)$ is the field at the point, r, caused by a unit point source at ξ. $G(r,\xi)$ is symmetric under the interchange of r and ξ. It is continuous at $r = \xi$, but has a discontinuity there in its derivative, of magnitude, $-\frac{1}{\xi}$, in the present case. It satisfies the equation,

$$\mathcal{L}\{G\} = 0 \tag{2.14}$$

within the intervals of definition, $r<\xi$ and $r>\xi$, with the prescribed homogeneous conditions (Eqs. 2.12 and 2.13) at the end points of the intervals, $r = a$ and $r = \tilde{R}$. Under the assumption that the function $G(r,\xi)$ exists, the original formulation (Eq. 2.9) can be transformed to an equivalent integral equation:

$$\phi_r(r) = \int_a^{\tilde{R}} G(r,\xi)\, \frac{Q_r(\xi,\tau_{th})}{D}\, \xi d\xi$$

$$= \frac{S_r}{2\pi D} \int_a^{\tilde{R}} G(r,\xi)\, q_r(\xi,\tau_{th})\, 2\pi\xi\, d\xi \qquad (2.15)$$

which is the solution to the problem.

To obtain the Green's function in question, let u(r) and v(r) be nontrivial solutions of Eq. (2.14) which respectively satisfy the boundary conditions at r = a and r = $\tilde{R}$. Then,

$$G = \begin{cases} c_1 u(r), & r<\xi \\ c_2 v(r), & r>\xi \end{cases} \qquad (2.15.1)$$

where c_1 and c_2 are constants. The general solution of the associated equation, $\mathcal{L} y = 0$, with $\mathcal{L}$ defined by Eqs. 2.10 and 2.9.1, is:

$$y = a_1 J_0(\alpha r) + a_2 Y_0(\alpha r). \qquad (2.15.2)$$

Substitution of the condition (Eq. 2.12) at r = a gives u(r), and that at r = $\tilde{R}$ (Eq. 2.13) gives v(r). The results are:

$$u(r) = \{Y_o(\alpha r) - e_1 J_0(\alpha r)\}, \qquad r<\xi \qquad (2.16.1)$$

$$v(r) = \{J_0(\alpha r) - e_2 Y_0(\alpha r)\}, \qquad r>\xi \qquad (2.16.2)$$

where
$$e_1 = \frac{Y_0(\alpha a) + 2\pi D\, \Gamma\, \alpha a\, Y_1(\alpha a)}{J_0(\alpha a) + 2\pi D\, \Gamma\, \alpha a\, J_1(\alpha a)}, \qquad (2.17.1)$$

$$e_2 = \frac{J_0(\alpha\tilde{R})}{Y_0(\alpha\tilde{R})}. \qquad (2.17.2)$$

The constants c_1 and c_2 appearing in Eqs. 2.15.1 are determined with the use of the conditions of the continuity of G and of

the discontinuity in its derivative at $r = \xi$. Thus,

$$c_2 v(\xi) - c_1 u(\xi) = 0,$$

$$c_2 v'(\xi) - c_1 u'(\xi) = -\frac{1}{\xi} .$$

Then substituting Eqs. 2.16 in the above gives:

$$c_1 = -\frac{v(\xi)}{L} , \qquad c_2 = -\frac{u(\xi)}{L} , \tag{2.18}$$

where $$L = -\frac{2}{\pi}\{1 - e_1 e_2\} , \tag{2.19}$$

e_1, e_2 being defined in Eqs. 2.17. With these relations, the Green's function is completely determined. Substitution in Eqs. 2.15.1 gives:

$$G(r,\xi) = \begin{cases} -\frac{1}{L} v(\xi)\, u(r), & r<\xi \\ -\frac{1}{L} u(\xi)\, v(r), & r>\xi \end{cases} \tag{2.20}$$

where the constant L and the functions u, v are described by Eqs. 2.19 and 2.16 respectively.

With $G(r,\xi)$ evaluated, the thermal neutron flux distribution is determined by Eq. 2.15. The range of integration is broken into two parts: a to r, and r to $\tilde{R}$, with appropriate values of the Green's function taken from Eqs. 2.20. This substitution gives:

$$\phi_r(r) = -\frac{S_r}{2\pi DL}\left\{ v(r) \int_a^r u(\xi)\, q_r(\xi,\tau_{th})\, 2\pi\xi\, d\xi \right. \\ \left. + u(r) \int_r^{\tilde{R}} v(\xi)\, q_r(\xi,\tau_{th})\, 2\pi\xi\, d\xi \right\} . \tag{2.21}$$

Since $u(\xi)$ and $v(\xi)$ are known through Eq. 2.16,

$$\phi_r(r) = - \frac{S_r}{2\pi DL} \Big[\{J_o(\alpha r) - e_2 Y_0(\alpha r)\}\{I_Y(a,r) - e_1 I_J(a,r)\} + \{Y_0(\alpha r) - e_1 J_0(\alpha r)\}\{I_J(r,\tilde{R}) - e_2 I_Y(r,\tilde{R})\} \Big] , \tag{2.22}$$

where the integrals I_J and I_Y are:

$$I_J(\ell_1,\ell_2) = \int_{\ell_1}^{\ell_2} J_0(\alpha\xi)\, q_r(\xi,\tau_{th})\, 2\pi\xi\, d\xi , \tag{2.23.1}$$

$$I_Y(\ell_1,\ell_2) = \int_{\ell_1}^{\ell_2} Y_0(\alpha\xi)\, q_r(\xi,\tau_{th})\, 2\pi\xi\, d\xi . \tag{2.23.2}$$

The integrals I_J and I_Y are evaluated in Section 2.3.5.

At the fuel surface, Eq. 2.22 gives:

$$\phi_r(a) = - \frac{S_r}{2\pi DL} \{Y_0(\alpha a) - e_1 J_0(\alpha a)\}\{I_J(a,\tilde{R}) - e_2 I_Y(a,\tilde{R})\} . \tag{2.24}$$

With the Bessel relation:

$$J_1(\alpha a)Y_0(\alpha a) - J_0(\alpha a)Y_1(\alpha a) = \frac{2}{\pi\alpha a} , \tag{2.25}$$

Eq. 2.24 simplifies to:

$$\phi_r(a) = - \frac{S_r}{2\pi DL} \frac{4D\Gamma \{I_J(a,\tilde{R}) - e_2 I_Y(a,\tilde{R})\}}{\{J_0(\alpha a) + 2\pi D\, \Gamma\, \alpha a\, J_1(\alpha a)\}} . \tag{2.26}$$

Denoting by $\hat{\phi}_r(r)$ the value of the radial component of the thermal neutron flux relative to its magnitude at r = a, it follows that:

$$\hat{\phi}_r(r) = \frac{4D\Gamma \{I_J(a,\tilde{R}) - e_2 I_Y(a,\tilde{R})\}}{\{J_0(\alpha a) + 2\pi D\, \Gamma\, \alpha a\, J_1(\alpha a)\}} \times$$

$$\Big[\{J_0(\alpha r) - e_2 Y_0(\alpha r)\}\{I_Y(a,r) - e_1 I_J(a,r)\}$$

$$+ \; Y_0(\alpha r) - e_1 J_0(\alpha r)\}\{I_J(r,\tilde{R}) - e_2 I_Y(r,\tilde{R})\} \Big] \; . \qquad (2.27)$$

This radial flux shape may be distorted through two effects: presence of higher harmonics and a "reflector" effect due to the back-scattering of epithermal neutrons. These effects have been investigated previously (P1) for the M.I.T. subcritical facility and shown to leave the "purity" of the flux distributions unaffected, at least in the limiting case where uniform lattices or a tank of pure moderator are involved.

2.3.2 Expression for Γ

One relation which expresses Γ in terms of the known quantities is clearly given by Eq. 2.26. Thus, substitution for S_r and L from Eqs. 2.11 and 2.19 respectively, and solving Eq. 2.26 for Γ gives:

$$\Gamma = \frac{\eta \{I_J(a,\tilde{R}) - e_2 I_Y(a,\tilde{R})\} - \{J_0(\alpha a) - e_2 Y_0(\alpha a)\}}{2\pi D\, \alpha a \{J_1(\alpha a) - e_2 Y_1(\alpha a)\}} , \qquad (2.28)$$

where $e_2 = J_0(\alpha\tilde{R}) \; / \; Y_0(\alpha\tilde{R})$.

The above equation affords a method for the evaluation of Γ, without the knowledge of X, from the measurement of γ (or α) alone. The determination of Γ by this equation is, however, inaccurate and sensitive to errors in the measurement of γ.

Other expressions for Γ are based upon the measurement of both γ and X. The analytic expression for $\hat{\phi}_r(r)$ in Eq. 2.27 can be

differentiated to meet the condition that:

$$\text{at } r = X, \ \frac{d}{dr} \{ \hat{\phi}_r(r) \} = 0 \ . \tag{2.29}$$

Differentiation of the integrals I_J and I_Y in Eq. 2.27 can be accomplished by using the Leibnitz rule. Thus for example,

$$\frac{d}{dr} [I_J(a,r)] = J_0(\alpha r) \, q_r(r,\tau_{th}) \, 2\pi r \ . \tag{2.30}$$

Then, substitution for $\hat{\phi}_r(r)$ from 2.27 into 2.29, and simplification, shows that:

$$\{J_1(\alpha X) - e_2 Y_1(\alpha X)\}\{I_Y(a,X) - e_1 I_J(a,X)\}$$

$$+ \{Y_1(\alpha X) - e_1 J_1(\alpha X)\}\{I_J(X,\tilde{R}) - e_2 I_Y(X,\tilde{R})\} = 0 \tag{2.31}$$

The only unknown in the above equation, contained in e_1, is Γ, which can therefore be explicitly expressed in terms of the other known or measurable quantities. Omitting the algebra, the final expression is:

$$\Gamma = \frac{\{J_0(\alpha a) - e_3 e_4 \, Y_0(\alpha a)\}}{2\pi D \, \alpha a \, \{Y_1(\alpha a) \, e_3 e_4 - J_1(\alpha a)\}} \ , \tag{2.32}$$

where

$$e_3 = \frac{\left[\frac{e_2}{e_4} I_J(a,X) + e_2 \, I_Y(X,\tilde{R}) - I_J(a,\tilde{R})\right]}{\left[e_2 \, I_Y(a,\tilde{R}) - e_4 \, I_Y(a,X) - I_J(X,\tilde{R})\right]} \ , \tag{2.33}$$

$$e_4 = \frac{J_1(\alpha X)}{Y_1(\alpha X)} \ , \tag{2.34}$$

and e_1, e_2 are as defined in Eqs. 2.17.

The above relation for Γ is cumbersome to use and gives inaccurate results because of its sensitivity to small errors in γ. An expression for Γ which is more convenient to use, can be obtained by returning to Eq. 2.31 to eliminate the integrals which range to the moderator tank boundary $\tilde{R}$. Splitting the range of integration in the integrals of Eq. 2.26, substituting for S_r, and rearranging gives:

$$\{I_J(X,\tilde{R}) - e_2 I_Y(X,\tilde{R})\} = -\frac{L\pi}{2}\frac{1}{\eta}\{J_0(\alpha a) + 2\pi D\,\Gamma\,\alpha a\, J_1(\alpha a)\} - \{I_J(a,X) - e_2 I_Y(a,X)\} . \tag{2.35}$$

Substitution of the left-hand side of this equation into Eq. 2.31 and solving for Γ gives:

$$\Gamma = \frac{\eta\left[I_J(a,X) - \frac{J_1(\alpha X)}{Y_1(\alpha X)} I_Y(a,X)\right] - \left[J_0(\alpha a) - \frac{J_1(\alpha X)}{Y_1(\alpha X)} Y_0(\alpha a)\right]}{2\pi D\,\alpha a\left[J_1(\alpha a) - \frac{J_1(\alpha X)}{Y_1(\alpha X)} Y_1(\alpha a)\right]} \tag{2.36}$$

The physical understanding of this relation is sought in the next section. Except for the presence of the unknown fuel parameter η, the above expression involves geometric and neutronic constants which are well known; and the quantities X and γ which are directly measured. Section 2.3.6 attempts to show that any transport correction which may be applied to the measured value of X is negligible. The slowing-down density of fast neutrons from the fuel element, $q_r(r,\tau)$ which occurs in the integrals I_J and I_Y is discussed in Section (2.3.4). This discussion is followed by the evaluation of these integrals.

Solving Eq. 2.36 simultaneously with the expression for η (Eq. 2.75) developed in Section 2.4.2 gives the two fuel parameters Γ and η (further comments in Section 2.4.3).

2.3.3 Physical Basis of the Expression for Γ

If Eq. 2.36 for Γ is simplified with the use of a line-source, infinite-medium age kernel for $q_r(r,\tau)$ (Eq. 2.56) and several approximations for the Bessel functions and for the evaluation of integrals I_J and I_γ, the expression for Γ may be written as:

$$\Gamma \simeq \frac{1}{\pi X^2 \, D\alpha^2} - \frac{\eta \, e^{\gamma^2 \tau_{th}}}{4\pi\tau \, D\alpha^2} \tag{2.37}$$

Noting that $\alpha^2 = \gamma^2 - \frac{\Sigma_{am}}{D}$, further rearrangement shows:

$$\frac{\phi_r(a)}{\Gamma} + \Sigma_{am}\phi_r(a) \, \pi X^2 = D\gamma^2\phi_r(a) \, \pi X^2 + \frac{\phi_r(a)\eta}{\Gamma} \frac{e^{\gamma^2 \tau_{th}}}{4\pi\tau} \pi X^2, \tag{2.38}$$

where Eq. 2.37 has been multiplied throughout by $\phi_r(a)$. When each term in this equation is "spelled out",

$$\begin{bmatrix}\text{Thermal}\\ \text{absorption}\\ \text{in single}\\ \text{element}\end{bmatrix} + \begin{bmatrix}\text{Thermal}\\ \text{absorption}\\ \text{in}\\ \text{moderator}\end{bmatrix} = \begin{bmatrix}\text{Axial}\\ \text{thermal}\\ \text{in-leakage}\end{bmatrix} + \begin{bmatrix}\text{Thermal contribu-}\\ \text{tion of fast}\\ \text{neutrons from the}\\ \text{single-element}\end{bmatrix} \tag{2.39}$$

Thus, Eq. 2.38 is a simple statement of the thermal neutron balance in a pill-box of radius X cms surrounding the single fuel element.

2.3.4 The Slowing-down Density $q(r,z,\tau)$

It is important to obtain a sufficiently accurate slowing-down age kernel, which is to be used to evaluate the contribution of fast

neutrons in the expression for Γ (Section 2.3.1), and to relate the measured cadmium-ratio to η (Section 2.4).

The slowing-down density of neutrons of age τ at a point (r,z), in the moderator, arising from a uniform, cylindrical source of unit untensity and of radius a in a moderator tank of finite radius $\tilde{R}$ in the absence of any resonance absorption is denoted by $q_0(r,z,\tau)$. First an expression for $q_0(r,z,\tau)$ is developed with the use of age theory. The effect on q_0 of the resonance absorption in the source element at an effective age τ_r is evaluated later, in Section 2.3.4.1. The function $q_0(r,z,\tau)$ must satisfy the basic age equation,

$$\nabla^2 q_0(r,z,\tau) = \frac{\partial q_0(r,z,\tau)}{\partial \tau} \tag{2.40}$$

where $\nabla^2 \equiv r\frac{\partial}{\partial r}\left(r\frac{\partial}{\partial r}\right) + \frac{\partial^2}{\partial z^2}$.

Under the assumption that the z-component, $q_{0,z}$ of the slowing-down density "dies away" exponentially and that it can be separated from its radial component $q_{0,r}$, it follows that:

$$q_0(r,z,\tau) = q_{0,r}(r,\tau)\, q_{0,z} e^{-\gamma z}. \tag{2.41}$$

Substituting this expression in Eq. 2.40 and simplifying gives:

$$\frac{\partial^2}{\partial r^2} q_{0,r}(r,\tau) + \frac{1}{r}\frac{\partial}{\partial r} q_{0,r}(r,\tau) + \gamma^2 q_{0,r}(r,\tau) = \frac{\partial}{\partial \tau} q_{0,r}(r,\tau). \tag{2.42}$$

This equation must be solved with the boundary conditions that $q_{0,r}(r,\tau)$ be finite at the source and vanish at the moderator tank boundary ($r = \tilde{R}$).

The effect of a cylindrical shell element of the source located at r = r' is considered first. Following the general methods outlined in Ref. C1, the solution q_0 may be expressed as:

$$q_{0,r}(r',r,\tau) = u + w \tag{2.43}$$

where u is the solution for a unit "instantaneous" source ($\tau = 0$) on the cylindrical surface at r = r' in an infinite medium; and w satisfies:

$$\frac{\partial^2 w}{\partial r^2} + \frac{1}{r}\frac{\partial w}{\partial r} - \frac{\partial w}{\partial \tau} + \gamma^2 w = 0, \tag{2.44}$$

and is to be such that $q_{0,r}$(= u + w) satisfies the boundary conditions. The solution for u is (C1);

$$u = \frac{1}{4\pi\tau} e^{-(r^2+r'^2)/4\tau} I_0\left(\frac{rr'}{2\tau}\right) e^{\gamma^2\tau}. \tag{2.45}$$

Denoting the Laplace transforms of $u(r,\tau)$, $w(r,\tau)$ by $\bar{u}(r,s)$, $\bar{w}(r,s)$ respectively, and $\sqrt{s}$ by μ,

$$\bar{u} = \frac{1}{2\pi} I_0(\mu r') K_0(\mu r), \qquad \text{when } r>r'; \tag{2.46}$$

and $\bar{w}$ satisfies:

$$\frac{d^2\bar{w}}{dr^2} + \frac{1}{r}\frac{d\bar{w}}{dr} - \mu^2\bar{w} = 0. \tag{2.47}$$

The solution of Eq. 2.47 which is finite at the origin is:

$$\bar{w} = A_w I_0(\mu r).$$

The value of the arbitrary constant A_w is obtained from the condition that:

$$\bar{q}_{0,r} = \bar{u} + \bar{w} = 0, \text{ at } r = \tilde{R}, \tag{2.49}$$

so that

$$A_w = - \frac{I_0(\mu r')K_0(\mu\tilde{R})}{2\pi I_0(\mu\tilde{R})} .$$

Equation 2.49 then gives:

$$q_{0,r}(r',r,s) = \frac{I_0(\mu r')}{2\pi I_0(\mu\tilde{R})} \{I_0(\mu\tilde{R})K_0(\mu r) - I_0(\mu r)K_0(\mu\tilde{R})\}, r>r'. \tag{2.50}$$

The transformation $\bar{q}_{o,r}$ in Eq. 2.50 to $q_{0,r}$ is accomplished by the use of the Inversion Theorem for the Laplace transformation, which states that:

$$q_{0,r}(r',r,\tau) = \frac{1}{2\pi i} \int_{\gamma'-i\infty}^{\gamma'+i\infty} e^{\lambda\tau} \bar{q}_{0,r}(r',r,\lambda)\, d\lambda, \tag{2.51}$$

where γ' is large enough that all singularities of $\bar{q}$ lie to the left of the line $(\gamma-i\infty, \gamma'+i\infty)$; λ is written in place of $s(=\mu^2)$ to signify that $\bar{q}$ is to be regarded as a function of a complex variable.

The integral in Eq. 2.51 can be evaluated by the usual methods of complex variable theory. The zeros of $I_0(\mu\tilde{R})$ are at $\mu = \pm i\alpha_n$, where $\pm\alpha_n$, $(n = 1,2...)$ are the roots of the equation:

$$J_0(\alpha\tilde{R}) = 0. \tag{2.52}$$

Thus the integrand in Eq. 2.51 is a single valued function of λ with a row of poles along the negative real axis. The range of integration in the integral of Eq. 2.51 is completed into a contour

not passing through any pole, by a large circle of radius R'. The integral over this contour vanishes in the limit at R' tends to ∞. Thus in the limit, the integral is equal, by Cauchy's theorem, to $(2\pi i)$ times the sum of the residues at the poles of the integrand. The final result of these standard manipulations is:

$$q_{0,r}(r',r,\tau) = \frac{1}{\pi\tilde{R}^2} \sum_{n=1}^{\infty} \frac{J_0(\alpha_n r')}{J_1^2(\alpha_n \tilde{R})} J_0(\alpha_n r)\ e^{(\gamma^2-\alpha_n^2)\tau}. \tag{2.53}$$

For a uniform unit source, extending from r = 0 to r = a,

$$q_{0,r}(r,\tau) = \frac{1}{\pi a^2} \int_0^a q_{0,r}(r',r,\tau)\ 2\pi r'\ dr'; \tag{2.54}$$

so that

$$q_{0,r}(r,\tau) = \frac{2}{\pi\tilde{R}^2} \sum_{n=1}^{\infty} \frac{J_1(\alpha_n a)\ J_0(\alpha_n r)}{\alpha_n a\ J_1^2(\alpha_n \tilde{R})} e^{(\gamma^2-\alpha_n^2)\tau}, \tag{2.55}$$

$\pm\alpha_n$, (n = 1,2...) being the roots of:

$$J_0(\alpha\tilde{R}) = 0. \tag{2.52}$$

Equation 2.55 when substituted into Eq. 2.41 then gives the complete slowing down density $q_0(r,z,\tau)$, in the basence of any resonance absorption.

The age-kernel developed above for a source of finite size in a finite moderator is a substitute for the simple line source, infinite-medium age kernel:

$$q^{\infty}_{0,r}(r,\tau) = \frac{e^{-r^2/4\tau}}{4\pi\tau}. \tag{2.56}$$

Less than five terms of the series in Eq. 2.55 are usually sufficient for satisfactory convergence. The graph in Fig. 2.3 is a comparison of Eq. 2.56 with Eq. 2.55 evaluated for the 31-rod fuel cluster. The study shows that the slowing-down densities and their cumulative contribution (for example, in the integrals of Eq. 2.63) for large size elements in a finite tank could deviate significantly from predictions of Eq. 2.56. As will be seen, this error could be important owing to the sensitivity of the final results to small errors in the fuel parameter η.

2.3.4.1 Effect of Epithermal Absorption on $q_{0,r}(r,\tau)$

All epithermal absorption in the single element is assumed to occur at an age τ_r, corresponding to an effective resonance energy E_r. The slowing-down density of neutrons of this energy at the fuel element surface from a unit intensity fast neutron source ($\tau = 0$) located within the same element, is $q_{0,r}(a,\tau_r)$. Hence, according to the definition of the epithermal absorption parameter A, the net epithermal absorption in the fuel element is equal to $A\, q_0(a,\tau_r)$. The negative contribution, $\Delta q(r,\tau)$, to neutrons of age τ at a distance r from the element, due to this epithermal sink, is

$$\Delta q(r,\tau) = A\, q_{0,r}(a,\tau_r)\, q_{0,r}(r,\tau-\tau_r), \tag{2.57}$$

so that

$$q_r(r,\tau) = q_{0,r}(r,\tau) - \Delta q(r,\tau), \tag{2.58}$$

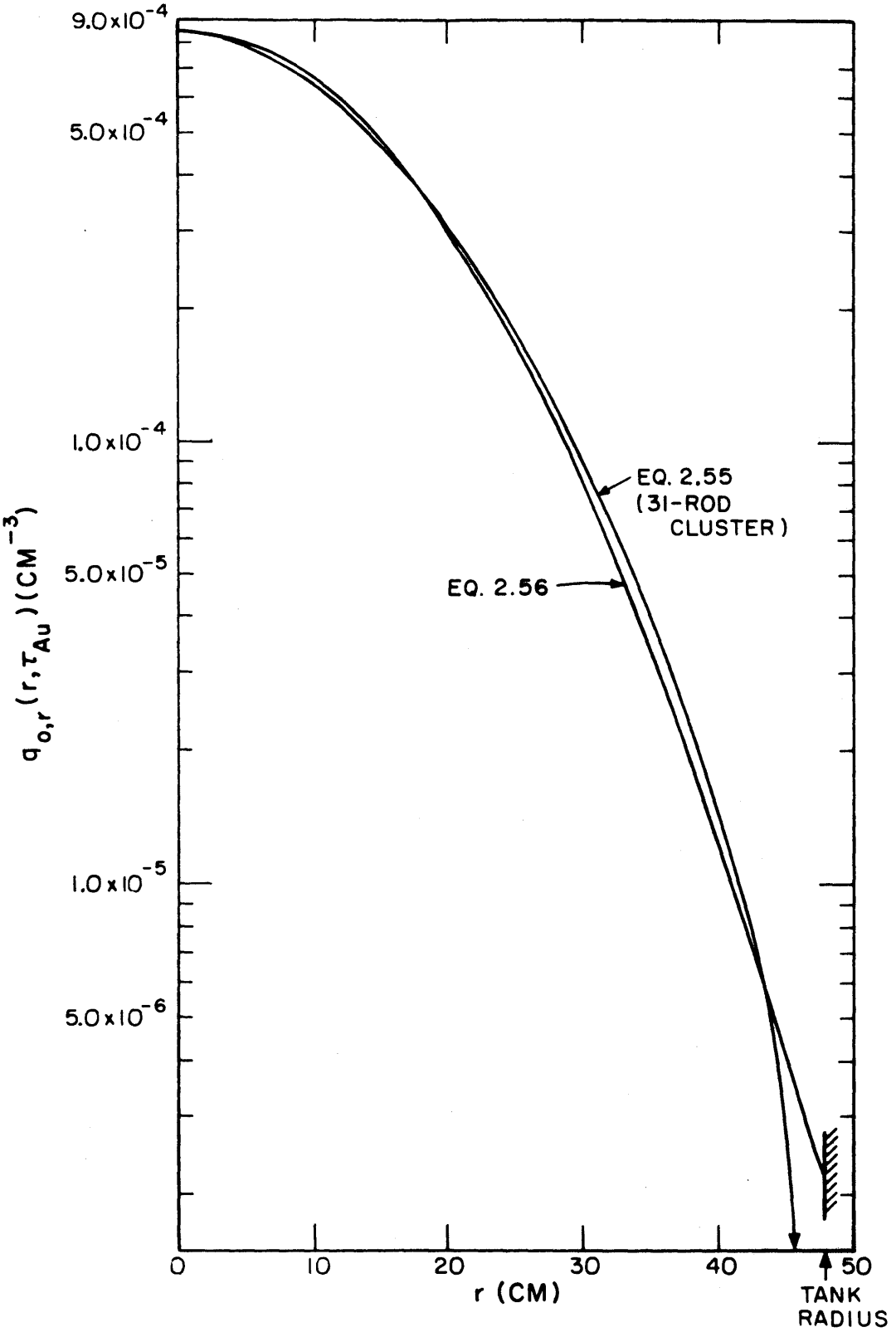

FIG. 2.3 COMPARISON OF SLOWING DOWN AGE KERNELS ($\tau = 95\ CM^2$)

or

$$q_r(r,\tau) = q_{0,r}(r,\tau) - A\, q_{0,r}(a,\tau_r)\, q_{0,r}(r,\tau-\tau_r), \quad \tau>\tau_r \tag{2.59}$$

Substitution for $q_{0,r}$'s from Eq. 2.55 into the last equation gives:

$$q_r(r,\tau) = \sum_{n=1}^{\infty} C_n(\tau)\, J_0(\alpha_n r), \tag{2.60}$$

where

$$C_n(\tau) = \frac{2J_1(\alpha_n a)\, e^{(\gamma^2-\alpha_n^2)\tau}}{\pi R^2\, \alpha_n a\, J_1^2(\alpha_n \tilde{R})} \left[1 - A\, q_{0,r}(a,\tau_r)\, e^{-(\alpha^2-\alpha_n^2)\tau_r}\right] \tag{2.61}$$

As pointed out earlier, n is less than 5. The epithermal absorption parameter A, which occurs in the definition of C_n, is determined independently (Section 2.5).

This prescription for $q_r(r,\tau)$ will be used in all the subsequent work.

2.3.5 The Integrals I_J and I_Y

With the expression for $q_r(r,\tau)$ at hand, the evaluation of the integrals I_J and I_Y defined in Eq. 2.23 presents no difficulty. Thus from Eqs. 2.23 and 2.60,

$$I_J = \sum_{n=1}^{\infty} C_n(\tau_{th}) \int_{\ell_1}^{\ell_2} J_0(\alpha\xi)\, J_0(\alpha_n\xi)\, 2\pi\xi\, d\xi, \tag{2.62.1}$$

$$I_Y = \sum_{n=1}^{\infty} C_n(\tau_{th}) \int_{\ell_1}^{\ell_2} Y_0(\alpha\xi)\, J_0(\alpha_n\xi)\, 2\pi\xi\, d\xi, \tag{2.62.2}$$

where ℓ_1 and ℓ_2 are the limits of integration: $\ell_1 = a$, and $\ell_2 = X$ or $\tilde{R}$. With the use of standard Bessel function identities,

$$I_J = \sum_{n=1}^{\infty} \frac{2\pi C_n(\tau_{th})}{(\alpha_n^2-\alpha^2)} \left[\{\alpha_n\xi\ J_1(\alpha_n\xi)J_0(\alpha\xi) - \alpha\xi\ J_0(\alpha_n\xi)J_1(\alpha\xi)\}_{\ell_1}^{\ell_2} \right], \quad (2.63.1)$$

$$I_Y = \sum_{n=1}^{\infty} \frac{2\pi C_n(\tau_{th})}{(\alpha_n^2-\alpha^2)} \left[\{\alpha_n\xi\ J_1(\alpha_n\xi)Y_0(\alpha\xi) - \alpha\xi\ J_0(\alpha_n\xi)Y_1(\alpha\xi)\}_{\ell_1}^{\ell_2} \right] \quad (2.63.2)$$

The above relations complement Eqs. 2.27 and 2.36 which describe, respectively, the thermal neutron flux distribution and the basis for the measurement of Γ.

2.3.6 Transport Correction to X

The measured radial distance of the thermal neutron flux peak (X_T) corresponds to the actual flux, which includes the contribution of transport effects at the fuel-moderator interface. The expression for Γ in Eq. 2.36, however, requires the radial distance X to correspond to the maximum of the asymptotic thermal flux in the moderator. The difference (X_T - X) can be investigated, (D4) with the use of a simplified model which approximates the transport kernel by a sum of the diffusion and the first-flight kernels (Appendix B). The actual flux $\phi_r^T(r)$ may then be written

$$\phi_r^T(r) = \phi_r(r) - \frac{S_L}{4r}\ e^{-\frac{\pi r}{2\lambda}} \quad (2.64)$$

where $\phi_r(r)$ is the asymptotic diffusion flux (Eq. 2.27), S_L is the thermal neutron sink, and λ is the mean free path of thermal neutrons in D_2O. Since $\phi_r^T(r)$ passes through a maximum at $r = X_T$,

$$\left(\frac{d\phi_r}{dr}\right)_{r=X_T} + \frac{S_L}{4X_T}\left(\frac{1}{X_T} + \frac{\pi}{2\lambda}\right) e^{-\frac{\pi X_T}{2\lambda}} = 0. \quad (2.65)$$

If the transport effects are considered, then

$$\left(\frac{d\phi_r}{dr}\right)_{r=X} = 0, \tag{2.66}$$

which, of course, is the same as Eq. 2.29. Together, Eqs. 2.65 and 2.66 provide a way to express X in terms of X_T. A simple computer program FLIC uses this procedure to calculate the magnitude of the error involved. An approximate relation (D4) between X and X_T is:

$$\frac{X_T^2-X^2}{X^2} = \frac{\pi D}{2}\left(\frac{1}{X_T}+\frac{\pi}{2\lambda}\right) e^{-\frac{\pi X_T}{2\lambda}} \tag{2.67}$$

For the cases of interest in the present study, in which X_T>10 cms, the error is less than about 0.25%, and may therefore be neglected in comparison with the experimental error.

2.4 DETERMINATION OF η

In most of the previous work on heterogeneous reactor methods, the fast neutron yield η is never measured directly. In the self-consistent procedure (G7), for example, its value is taken to be such that (ηf) agrees with the results of cell calculations. In previous work at M.I.T. (D4), η has been obtained directly from integral parameter measurements which require the irradiation of uranium foils within the fuel. But this procedure violates one of the basic premises of the single element model, namely that measurements be made outside the fuel element to avoid the problems of contamination and radiation hazard due to plutonium and fission products.

A recent effort at M.I.T. undertook to evaluate the use of the pulsed-neutron technique to obtain η from the change $\Delta\lambda$ in the fundamental mode time decay constant due to insertion of a single fuel element into the moderator tank. This method (L1) appears not to be feasible because of the lack of sufficiently precise methods to determine $\Delta\lambda$. A second attempt was based upon the underlying correspondence (O1) between the pulsed-neutron approach and axial buckling measurements which yields a relation between η and the perturbation in axial buckling due to the presence of the single-element. This method, however, gave grossly inaccurate results.

Another approach similar to the above in respect to its reliance on axial buckling measurements to determine η, is discussed briefly in the next section. The cadmium-ratio technique actually used in the present study will be discussed thereafter.

2.4.1 The Determination of η from the Axial Buckling

The possibility of obtaining Γ and η from measurements of X and γ alone can be seen from equations already derived in Section 2.3.

Observation of Eqs. 2.28 and 2.36 shows that the right hand sides of both equations, each being equal to Γ, can be equated. This results in an expression which gives η in terms only of the measured quantities γ (or α) and X. Thus,

$$\eta = \frac{\dfrac{2}{\pi\alpha a}\left[\dfrac{J_1(\alpha X)}{Y_1(\alpha X)} - \dfrac{J_0(\alpha\tilde{R})}{Y_0(\alpha\tilde{R})}\right]}{J_1(\alpha a)\,(I_2 - I_1) - Y_1(\alpha a)\left[I_2\dfrac{J_1(\alpha X)}{Y_1(\alpha X)} - I_1\dfrac{J_0(\alpha\tilde{R})}{Y_0(\alpha\tilde{R})}\right]} \tag{2.68}$$

where

$$I_1 = I_J(a,x) - \frac{J_1(\alpha x)}{Y_1(\alpha x)} I_Y(a,x), \qquad (2.69.1)$$

and

$$I_2 = I_J(a,\tilde{R}) - \frac{J_0(\alpha \tilde{R})}{Y_0(\alpha \tilde{R})} I_Y(a,\tilde{R}). \qquad (2.69.2)$$

An approximate version of this equation and further deductions from it which may be used to calculate the perturbation in radial buckling are given in Appendix A.

Values of η calculated for the clusters, using the above exact equation, are about 5% higher than those obtained with the cadmium ratio technique (Section 2.4.2). Though the method is generally very sensitive to errors in γ, it does show that in principle, Γ and η can be inferred from two measurements of X and γ (or α), or as is pointed out in Section 2.4.3, in measurements of any two of the three experimental parameters X, γ and R.

2.4.2 The Determination of η from the Gold Cadmium Ratio, R

Since the epithermal neutron field around the single fuel element results entirely from the slowing-down of fast neutrons produced in the element, the measurement of the epithermal neutron flux at a certain radial distance Y should provide a way to estimate its source strength, which is proportional to η.

The epithermal flux is estimated by measuring the cadmium-ratio in gold foils irradiated at a radial distance Y from the single element. Gold is chosen because it has a large absorption resonance at 4.9 ev., which makes it ideal for cadmium-ratio measurements in a

weak epithermal flux field such as in the present application. Under the assumption that most of the epithermal absorption in gold occurs at its single large resonance at 4.9 ev. ($\tau_{Au} = 95 cm^2$), the slowing-down density $Q_{epi}(Y,\tau_{Au})$ at a distance Y, (large enough to neglect any source effects) is conveniently given by age theory. The applicability of age theory in the region of the moderator where the experiments may be conducted has been verified (L1) with multigroup diffusion theory calculations.

The number of neutrons of age τ_{Au} slowing down to the point (Y,z) is then (Eq. 2.8.2):

$$Q_{epi}(Y,z,\tau_{Au}) = \frac{\phi(a,z)\eta}{\Gamma} q_r(Y,\tau_{Au}). \tag{2.70}$$

If the z-component of the neutron densities is accounted for as before (Section 2.3.1),

$$Q_{epi,r}(Y,\tau_{Au}) = \frac{\phi_r(a)\eta}{\Gamma} q_r(Y,\tau_{Au}), \tag{2.71}$$

where $q_r(Y,\tau_{Au})$ is given by Eq. 2.60. It follows that

$$\phi_{epi,r}(Y,\tau_{Au}) = \frac{Q_{epi,r}(Y,\tau_{Au})}{\xi\Sigma_s} = \frac{\phi_r(a)\eta}{\Gamma} \frac{q_r(Y,\tau_{Au})}{\xi\Sigma_s} . \tag{2.72}$$

The measured cadmium-ratio R is the ratio of the total neutron activity in a "bare" gold foil to its epithermal component measured in a cadmium-covered gold foil. The ratio is measured at a position whose radial distance from the fuel element is Y. Hence,

$$\frac{1}{R-1} = \frac{\phi_{epi,r}(Y,\tau_{Au})}{\phi_r(Y)} \frac{\sigma_{epi}}{\sigma_{th}} K , \tag{2.73}$$

where σ_{epi} is the effective absorption cross section of gold integrated over all epithermal energies;

σ_{th} is the effective absorption cross section of gold integrated over all thermal energies;

K is $\frac{(R-1)_0}{(R-1)}$, the ratio for an infinitely thin foil to that for the foils of finite thickness actually used in the experiment; this is the self-shielding correction necessary to account for the effect of the foil thickness.

Substitution for $\phi_{epi,r}$ from Eq. 2.72 gives a direct relation between η and the gold cadmium ratio R:

$$\eta = \frac{\sigma_{th}\ \xi\Sigma_s}{\sigma_{epi}\ K}\ \frac{\Gamma\hat{\phi}_r(Y)}{q_r(Y,\tau_{Au})}\ \frac{1}{(R-1)}\ , \tag{2.74}$$

where $\hat{\phi}_r(Y)$ is given by Eq. 2.27.

The above equation, which could in principle permit an absolute determination of η, involves several parameters, each with its attendant experimental uncertainty. The use of a comparison method, which is based upon η_{st} for some "reference" fuel element (1.01 in diameter natural uranium rod in this work), eliminates this problem.

Denoting the quantities corresponding to the reference fuel element by the subscript "st", and dividing Eq. 2.74 by the same equation written for η_{st},

$$\eta = H\left[\frac{\Gamma\ \hat{\phi}_r(Y)}{q_r(Y,\tau_{Au})\ (R-1)}\right], \tag{2.75}$$

where

$$H = \frac{\eta_{st}\, q_{r,st}(Y,\tau_{Au})\ (R-1)_{st}}{\Gamma_{st}\ \hat{\phi}_{r,st}(Y)} \tag{2.76}$$

Except for the factor $\{\Gamma\hat{\phi}_r(Y)\}$ which requires the knowledge of Γ, the quantities in Eq. 2.75 are known. The value of $q_r(Y,\tau_{Au})$ supplied by Eq. 2.60 is known for a predetermined value of A, and (r-1) is, of course, one of the direct measurements of the single-element model. The quantity H may be called the "Single Element Constant", since it involves all the three heterogeneous fuel parameters Γ, η and A. Its value, defined in Eq. 2.76 is determined by the reference value of η_{st} (1.375, Appendix E), and by measurements and calculations made on the reference fuel element.

2.4.3 Comments Regarding the Determination of Γ and η

A simple way to obtain Γ and η is to solve Eq. 2.36 and 2.75 simultaneously. Equation 2.36 involves η explicitly, and a substitution for it from Eq. 2.75 gives a relation between Γ and the measured quantities X, γ and R:

$$\Gamma = \frac{\left[J_0(\alpha a) - \frac{J_1(\alpha X)}{Y_1(\alpha X)}\, Y_0(\alpha a)\right]}{\left[I_1 \frac{H\hat{\phi}_r(Y)}{q_r(Y,\tau_{Au})(R-1)} - 2\pi D\, \alpha a \left[J_1(\alpha a) - \frac{J_1(\alpha X)}{Y_1(\alpha X)}\, Y_1(\alpha a)\right]\right]}, \tag{2.77}$$

where

$$I_1 = I_J(a,x) - \frac{J_1(\alpha X)}{Y_1(\alpha X)}\, I_Y(a,X). \tag{2.69.1}$$

This value of Γ when substituted into Eq. 2.75 gives η.

The quantity $\hat{\phi}_r(Y)$, which is the thermal neutron flux at Y relative to its value on the fuel surface, can be calculated from Eq. 2.27. The calculation, however, involves the unknown parameter Γ. This problem is met by carrying out a few iterations on Eq. 2.77. The steps of the iteration involve calculating a value of Γ from an initial value of $\hat{\phi}_r(Y)$; then using this value of Γ to improve $\hat{\phi}_r(Y)$ from Eq. 2.27. This procedure is repeated until Γ, η and $\hat{\phi}_r(Y)$ converge to their final values. In the present work, $\hat{\phi}_r(Y) \simeq 1$, and only four iterations are sufficient for the convergence of these parameters separately to within 0.5% of their final values.

The simple coupling between Γ and η also involves the third parameter A through the presence of the factor $q_r(Y,\tau_{Au})$ and the integrals I_J and I_Y. However, the determination of A, discussed in the following section, is independent of Γ and η; and A can be evaluated before proceeding to obtain Γ and η from the experimental measurements.

The method of obtaining the fuel parameters Γ and η thus involves the use of three experimental quantities X, γ and R. In theory, two of these are sufficient. Thus if η is obtained from Eq. 2.68 and this value substituted into 2.36 to determine Γ, a measurement of R is unnecessary. Again, if γ (or α) is not known, iterations among Eq. 2.68, 2.75 and 2.77 can determine a value for α, which can then be used to calculate Γ and η. Similarly, the use of Eqs. 2.28 and 2.75 for a known value of γ obviates the need to know X. However, the additional third measurement helps to relax the severe conditions on the degree of accuracy required for single-element experiments. On the

other hand it appears that there is incentive to increase the accuracy of measurements and thereby decrease the number of experimental parameters.

A computer code THINK has been written to carry out all the manipulations described in the previous sections and to arrive at the final values of the single-element parameters Γ and η.

2.5 DETERMINATION OF A

Contemporary methods of evaluating A involve a back calculation from a known value of the resonance escape probability for uniform lattice cells made up of the fuel element in question. At M.I.T. Donovan (D4) has shown how A could be inferred from in-rod foil activation. This method is, however, incompatible with a major objective of the present work - namely, of performing experiments outside the fuel element. Recently, McFarland (M1) has carried out experiments and numerical computations in support of a new method for the determination of A. This method will be developed in the following sections.

2.5.1 Motivation for the Method

Several assumptions are now made for developing a simple basis for the proposed method of evaluating A. The single element in the center of the moderator tank is treated as a line source of fast neutrons of unit intensity. The slowing-down of these neutrons in the surrounding moderator is described by age-theory. All epithermal absorption in the fuel occurs at a single effective resonance energy E_r (age τ_r).

If $q_1(0,\tau_1)$, $q_r(0,\tau_r)$ and $q_2(0,\tau_2)$ are the slowing-down densities of neutrons at ages τ_1, τ_r and τ_2 respectively ($\tau_1<\tau_r<\tau_2$), which arrive at the fuel element, it follows that:

$$q_1(0,\tau_1) = \left(\frac{e^{-r^2/4\tau_1}}{4\pi\tau_1}\right)_{r=0} = \frac{1}{4\pi\tau_1} , \tag{2.78}$$

and $$q_r(0,\tau_r) = \frac{1}{4\tau\pi_r} , \text{as above} , \tag{2.79}$$

By definition of A (eq. 2.7), the epithermal absorption in the fuel is $\frac{A}{4\pi\tau_r}$;
therefore,

$$q_2(0,\tau_2) = \frac{1}{4\pi\tau_2} - \frac{A}{4\pi\tau_r} \frac{1}{4\pi(\tau_2-\tau_r)} , \tag{2.80}$$

as in Eq. 2.59. Consequently,

$$\frac{q_2(0,\tau_2)}{q_1(0,\tau_1)} = \frac{\tau_1}{\tau_2} - A\frac{\tau_1}{\tau_r} \frac{1}{4\pi(\tau_2-\tau_r)} . \tag{2.81}$$

Or, since the ratio (q_2/q_1) is proportional to the ratio (f_c) of the corresponding fluxes,

$$f_c = K_1 - A\,K_2 \tag{2.82}$$

where K_1 and K_2 are constants which involve the values of τ_1, τ_2 and τ_r.

The last equation shows that the flux ratio f_c is a linearly decreasing function of the parameter A, and its measurement could provide a way to infer the value of A. This simple model, however, does not account for the finite size of the fuel element and the complexities in neutron resonance cross-sections. Consequently,

Eq. 2.82 can go no further than merely supplying a physical basis to the proposed method.

2.5.2 Exact Relationship between f_c and A

The computer code ANISN (E1, E2, B5) is used to study the deviations from the simple Eq. 2.82, and to establish a better correspondence between the flux ratio f_c and the epithermal absorption parameter A. (A superior method, purely experimental, which does not involve the use of ANISN is suggested in Chapter 5.)

ANISN is a one-dimensional, 16 group, S_N transport program. Its use to simulate the single-element experiment has been discussed in adequate detail by Donohew (D3) and by McFarland (M1). Neutron energy groups 12 ($3 \leq E \leq 10$ev.), and 9 ($100 \leq E \leq 550$ ev.) of the ANISN program span an energy range which accounts for about 90% of the epithermal absorption in U-238 (Fig. 2.6). The ratio of the ANISN computed neutron fluxes in these two groups can therefore be chosen to correspond to the ratio f_c of Eq. 2.82.

A series of ANISN "runs" are made for each fuel element tested: namely, the natural uranium rod, the 19-rod cluster and the 31-rod cluster. For each fuel-type, different values of the ratio f_c are obtained by varying the epithermal absorption parameter A. The different A's corresponding to a certain fuel element are generated by varying the absorption cross-section in each epithermal group by a multiplicative shielding factor χ. The size and geometry of the fuel are maintained. To be sure that the χ-factors provide A's in the range of interest, the central value, χ_M, for each fuel element is estimated

from the relation:

$$\chi_M = \frac{ERI^{238}}{RI_\infty^{238}}, \tag{2.83}$$

where RI_∞^{238} is the infinite-dilution resonance integral of U-238; and ERI^{238}, the effective resonance integral of the cylindrical fuel element (Appendix F) is obtained with the use of Hellstrand's correlation (H3). The value of A for each case is then given by Eq. 2.6:

$$A = \frac{V_f N^{238} RI_\infty^{238}}{\xi \Sigma_s} \chi + \sum_{i, i \neq U\text{-}238} A^i \tag{2.84}$$

The plots in Fig. 2.4 show the variation of the epithermal flux ratio f_c at the fuel surface as a function of the epithermal absorption parameter for each of the three fuel elements. These curves follow approximately, the behavior predicted by Eq. 2.82. However, the curves differ among themselves with respect to their slopes and intercepts. As will be seen, these differences are probably due to geometric (i.e., finite size) effects rather than to differences in neutron spectra.

The curves of Fig. 2.4 indicate that if f_c, or an experimental quantity proportional to it, can be determined to within 1% (a typical standard derivation for foil activations), the value of A can be predicted to within 4%. This result should be compared with the knowledge (from Eq. 2.7.2) that for the lattices of interest where the resonance escape probability (p) is quite large an error of 10% in A causes an uncertainty in p which is only about 1%. Thus an experimental evaluation of the epithermal flux ratio on the surface of a

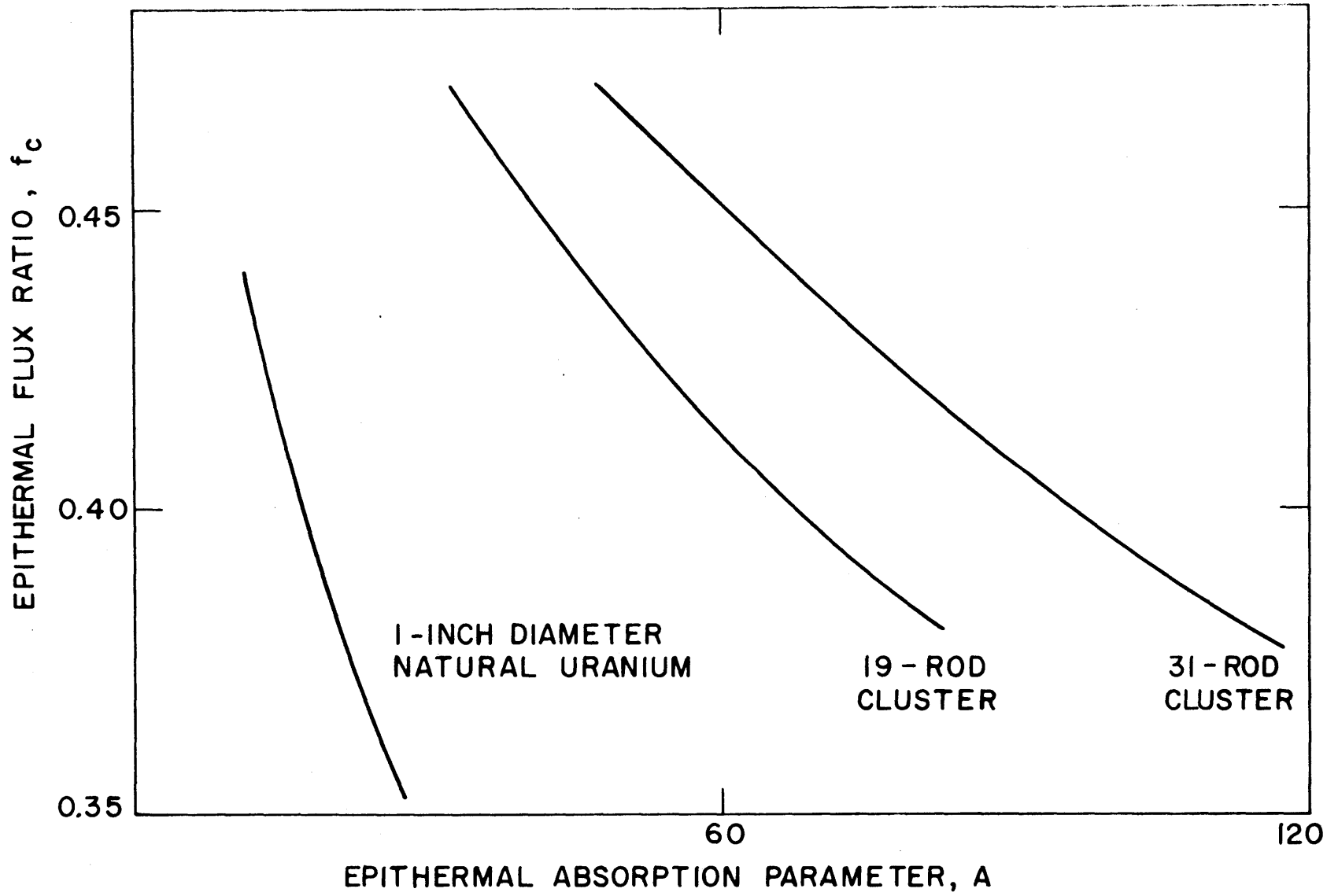

FIG. 2.4 EPITHERMAL FLUX RATIO (f_c) VERSUS EPITHERMAL ABSORPTION PARAMETER (A)

given fuel element could be related to the required parameter A with adequate accuracy, provided a characteristic curve such as that depicted in Fig. 2.4 is generated for the fuel-type in question.

It may be noted that a computer-aided study (D6), such as that discussed above, has also been carried out to relate A to a value of f_c which is calculated at a relatively large radial distance into the moderator (20 cms). The relationship thus obtained can be readily interpreted theoretically. It cannot, however, be used to advantage since this ratio f_c, calculated at a large distance from the fuel, is extremely insensitive to fuel changes.

2.5.3 Normalization of f_c

The discussion in the previous section points to the feasibility of obtaining A from the ratio, f_c, of two fluxes corresponding to energies which span the major epithermal absorption region.

In the experimental work of McFarland (M2), molybdenum-98, which has an absorption resonance at 470 ev., and gold-197, which has one at 4.9 ev., were used to detect (Table 3.3) the relative flux levels of group-9 and group-12 which are used to calculate f_c from the ANISN code. Figure 2.6 shows the cumulative absorption in U-238 versus the neutron energy. These calculations used the partial ERI(E) data (G4) for a 1 in. diameter natural uranium rod and corresponding ANISN-fluxes. The graph shows that the choice of gold-197 with its resonance below the lowest lying and the largest U-238 resonance (at 6.7 ev.), and of molybdenum-98, with its resonance above the four major U-238 resonances, should account

satisfactorily for most epithermal absorption. This range would, however, be inadequate for fuels with a large concentration of Pu-240 which has a large resonance cross-section at 1 ev. The use of a detector with resonance energy much higher than that of molybdenum-98 would have to include the effect of first-flight captures in the fuel, which (D6) can be a large fraction of the epithermal captures for an isolated single fuel element. The two detector materials Mo-98 and Au-197 have the further advantage that they have nearly identical half lives (67 hours), which simplifies measured-activity corrections, and both are relatively strong resonance absorbers as compared to their 1/v-absorption.

The measured ratio, F, of the epithermal activities of Mo-98 and Au-197 foils, irradiated on the fuel surface can be related to the ratio (f_e) of the corresponding epithermal fluxes. This ratio f_e, however, is not equal to the ANISN-computed flux ratio f_c. There are several reasons to account for the inequality of f_e and f_c. Thus, for example, the method of obtaining f_e from the measured ratio F involves the use of foil parameters, such as self-shielded resonance absorption cross sections, whose values are uncertain. Further, the ANISN-computations for f_c are inexact; firstly, the fuel clusters are cylindricized and homogenized; and secondly, the energy group structure in ANISN is so coarse that the resonance absorption in each group is considerably smeared out. The constant shielding factor χ introduced to account for the overall effect, provides only a rough approximation, and should really be different for the various energy groups because resonance self-shielding varies with energy (lower

resonances shielded more). There is thus considerable scope for improving the procedures for the determination of f_c and f_e.

A suitable way to account for the different between f_e and f_c, and to minimize uncertainties such as those described above, is first to normalize f_c for a "reference" fuel, and then to determine the f_c's of unknown fuels relative to this reference value. This is effectively done as follows. A standardization factor, c, is defined so that:

$$c = \frac{f_c}{f_e} , \tag{2.85}$$

which is assumed independent of the fuel type. The value of c can then be found by measuring f_e^{st} for a reference fuel element, whose epithermal absorption parameter, A^{st}, and consequently the ratio f_c^{st}, obtained from its characteristic curve (Fig. 2.4), are known. The "reference" fuel chosen is again, as in the case for η, the 1.01 in. diameter natural uranium rod. From Eq. 2.84 and the standard Hellstrand correlation for the resonance integral of metallic uranium rods (H3), the value of A^{st} for the natural uranium rod is found to be 20.39 cm^2 (Appendix F). Corresponding to this value of A^{st}, the ANISN-generated characteristic curve (Fig. 2.4) gives the value of f_c^{st} as 0.3872. The measured value of f_e^{st} (0.9510, Appendix D) then determines the standardization factor c (equal to 0.4072).

The ratio f_c, and correspondingly, the parameter A for the fuel element in question, can then be obtained by measuring the ratio f_e on the rod surface and relating it to f_c with Eq. 2.85. In summary, this standardization method for the calculation of f_c and A insures

that if the same step-by-step procedure is carried out for the standard 1.01 in. diameter natural uranium fuel, the value of A so obtained in the "accepted" one (A^{st}).

2.5.4 Summary Procedure to Evaluate A

The steps to evalute the epithermal absorption parameter A may be briefly outlined as follows:

1. The epithermal activity ratio, F, is first measured on the surface of the unknown fuel element. The experimental procedure for measuring F, and the method for deducing from it the experimental epithermal flux ratio f_e, is discussed in Section 3.7.
2. The ratio f_e is then normalized with the use of Eq. 2.85. This gives the related epithermal flux ratio f_c corresponding to the ANISN-computations (step 3).
3. In parallel with the above experimental investigation, numerical studies are carried out to obtain the characteristic f_c vs. A curve for the fuel element in question. This is done by varying the epithermal absorption in the manner described in Section 2.5.2 and computing the corresponding value of f_c with the ANISN computer program. This results in a curve such as in Fig. 2.4.
4. The final step is to refer to the curve obtained in step 3, and to look up the value of the epithermal absorption parameter A which corresponds to the normalized ratio f_c of step 2.

2.5.5 Effects of Spectral Differences

The definition of A involves the incident epithermal neutron flux and the epithermal neutron slowing down density at the fuel

surface (Eq. 2.6). Since these are characteristic of the particular neutron energy distribution, a question arises whether the epithermal absorption parameter A for the fuel element would be different if the incident neutron spectrum were altered.

According to a simple model, which assumes that all epithermal absorption occurs at a single, effective, narrow resonance (width: Δu_r) at lethary u_r (age τ_r), A may be written as:

$$A = \frac{V_f \sum_i N_f^i \sigma_a^i(u_r)\, \phi(u_r)\, \Delta u_r}{\xi \Sigma_s\, \phi(u_r)}$$

$$= \frac{V_f}{\xi \Sigma_s} \sum_i N_f^i\, \sigma_a^i(u_r)\, \Delta u_r, \qquad (2.86)$$

where the notation conforms to Eq. 2.6. This would imply that if the resonance absorption can be shown to occur at the same effective lethargy u_r so that $\sigma_a^i(u_r)$ is the same, then the parameter A should be independent of the neutron spectrum $\phi(u_r)$. However owing to the serious assumptions made, the above conclusion cannot be generally accepted and a deeper investigation is needed.

In the present work, the above conclusion is tested only for the spectral difference between the case of the single-element experiment, where the fuel element is isolated in the moderator, and the case of a uniform lattice. Figure 2.5 shows the difference in neutron spectra between the two cases for the 1-inch diameter natural uranium fuel. The single-element and lattice results shown in the figure are obtained from the multigroup computer programs SRA (D3) and LASER (P3) respectively. It can be seen that, whereas the

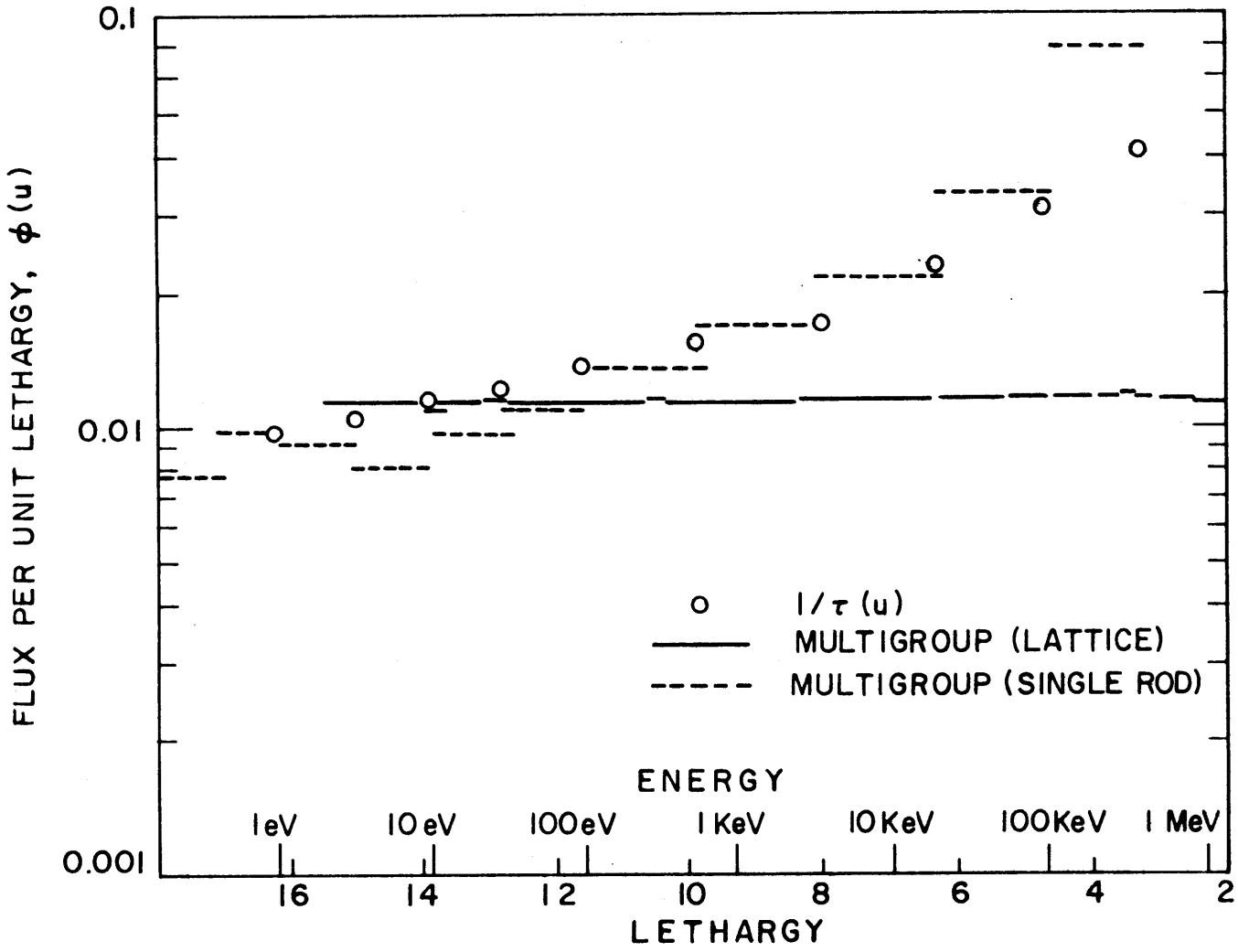

FIG. 2.5 COMPARISON OF EPITHERMAL SPECTRA

lattice flux is constant over lethargy (1/E neutron energy dependence), the lethargy dependence of the flux which the fuel "sees" in a single-element experiment varies as $1/\tau(u)$ - a result which would follow from age theory.

The implication of Eq. 2.86 for the two cases described above is checked by computing the effective age (τ_r) of U-238 absorptions. In general,

$$\bar{\tau}_r = \frac{\int \mathrm{ERI}(u)\ \phi(u)\ \tau(u)\ du}{\int \mathrm{ERI}(u)\ \phi(u)\ du} \tag{2.87}$$

The values of $\tau(u)$ used in the above equation are calculated from the LASL group cross-section set (R1). The partial ERI(u) data for the natural uranium rod is obtained from Gosnell (G4). The effective age, τ_r, for the single-element is obtained in two ways: in one, $\phi(u)$ varies as $1/\tau(u)$; in the other, it is taken from 16-group ANISN-calculations. The two results for τ_r are: 79.6 cm^2 and 77.3 cm^2 respectively. The effective age τ_r for the lattice is obtained by treating $\phi(u)$ as a constant; the result is 81.2 cm^2. The agreement among all these results shows that the effective age (or lethargy) of epithermal capture in the fuel element is very nearly the same if the single element is isolated in a moderator tank, or if it is placed in a uniform lattice. This result then leads to the conclusion (from Eq. 2.86) that the A-value is not perturbed, at least for this particular spectral difference.

Other pertinent evidence bearing on this point may be obtained from the comparison of the fractional U-238 epithermal absorption in

the uranium rod as a function of energy for the two cases of interest, namely, the single-element experiment for which $\phi(u) \simeq 1/\tau(u)$, and the uniform lattice for which $\phi(u) \simeq$ constant. Again, the calculations use the partial ERI(u) data of Gosnell. Figure 2.6 shows that about 90% of the U-238 epithermal absorption occurs between about 5 ev. and 500 ev. in both cases. This fact, and the similar shape of the two curves, again indicates that the differences between the single element and lattice experiments may not be substantial.

The above study to determine any effect on A due to change in the neutron energy spectrum has been done mainly with the natural uranium fuel rod. The work needs to be generalized to fuels of difference sizes and composition. Both types of evidence presented do, however, strongly support the notion that the parameter A measured in single element experiments could be used for lattice-cell calculations.

2.6 SUMMARY

The analytic formalism developed in this chapter provides the means to determine the heterogeneous fuel parameters Γ, η and A from single-element experiments. The epithermal absorption parameter, A, is obtained from the epithermal activity ratio, F, measured on the fuel surface. The other two parameters, Γ and η can then be calculated from Eqs. 2.77 and 2.75 with the knowledge of the values of A, the moderator properties, D, τ, τ_{Au} and τ_r, and the experimental parameters, X, γ and R. The measurement of the four experimental parameters X, γ, R and F is described in the next chapter. The subject methods are applied

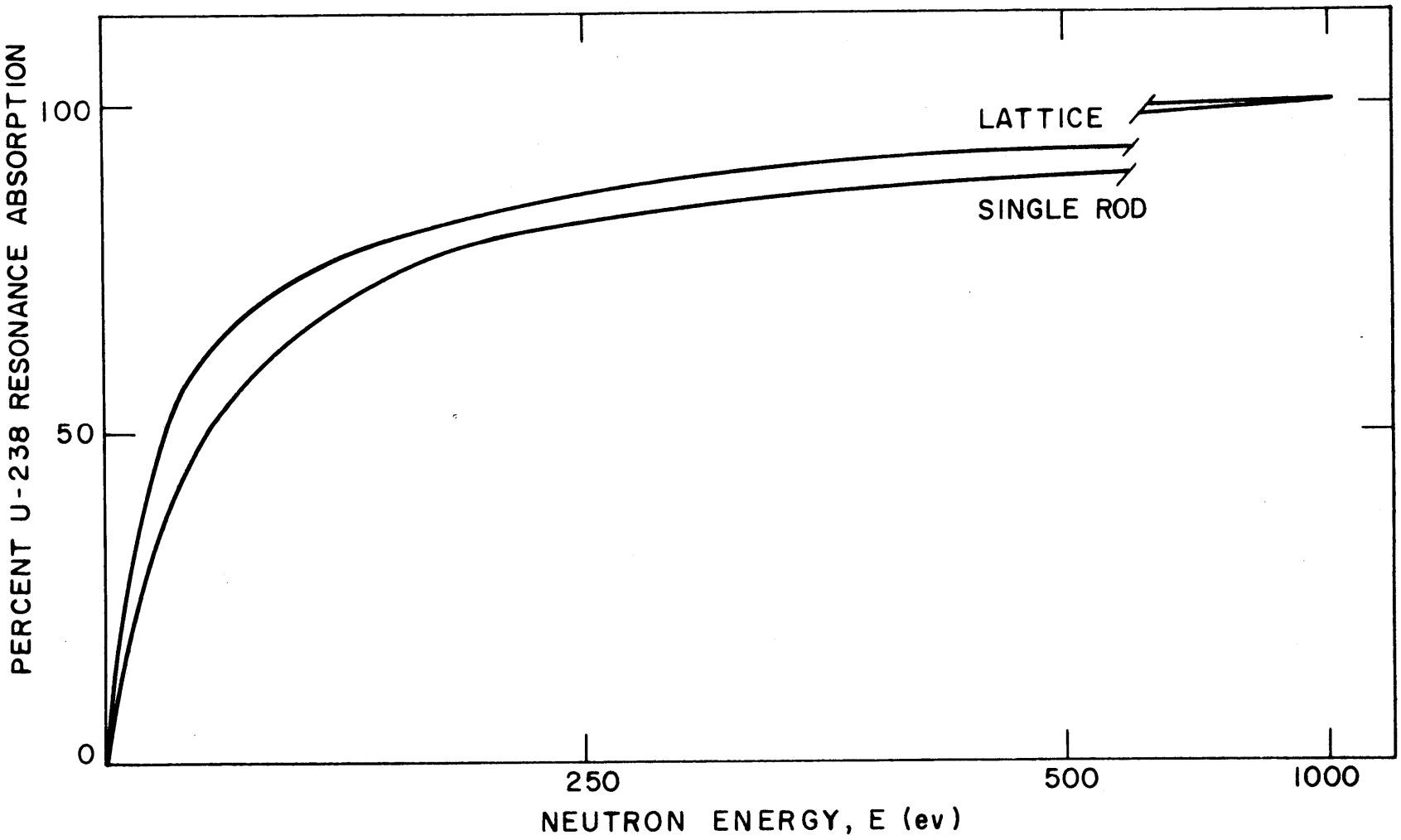

FIG. 2.6 CUMULATIVE U-238 RESONANCE ABSORPTION IN A LATTICE AND AROUND A SINGLE FUEL ELEMENT VERSUS ENERGY

to the plutonium containing single-clusters of 19 and 31 rods. The results of the study to determine the sensitivity of the fuel parameters Γ, η and A to the uncertainties in experimental measurements are given in Section 3.10.

Chapter 3

EXPERIMENTS, ANALYSIS AND RESULTS

3.1 INTRODUCTION

The experimental determination of the four quantities X, γ, R and F introduced in Section 2.1 is discussed in this chapter. The results of the measurements for the natural uranium rod, and 19 and 31-rod UO_2-PuO_2 clusters, are then used with the theoretical formalism developed in the previous chapter to calculate the heterogeneous parameters Γ, η and A for the three fuel elements. The sensitivity of these fuel parameters to the uncertainties in the experimental measurements is discussed in the final section of this chapter.

3.2 M.I.T. EXPONENTIAL FACILITY

All single element experiments are performed in the D_2O-moderated exponential tank at the M.I.T. Reactor. A detailed description of the facility is given in a report (T2) of the M.I.T. Heavy Water Lattice Research Project.

The source neutrons for the exponential facility originate in the M.I.T. Reactor, pass through a thermal column to the graphite lined cavity ("hohlraum") where they are reflected upwards into the D_2O-filled exponential tank (Fig. 3.1). The entering neutron flux is so shaped that its radial intensity varies as J_0. With the reactor operating at 5MW., the thermal neutron flux at the bottom of the tank is approximately 6×10^9 neutrons/(cm^2-sec). It is highly thermalized, with a gold cadmium-ratio of about 3500.

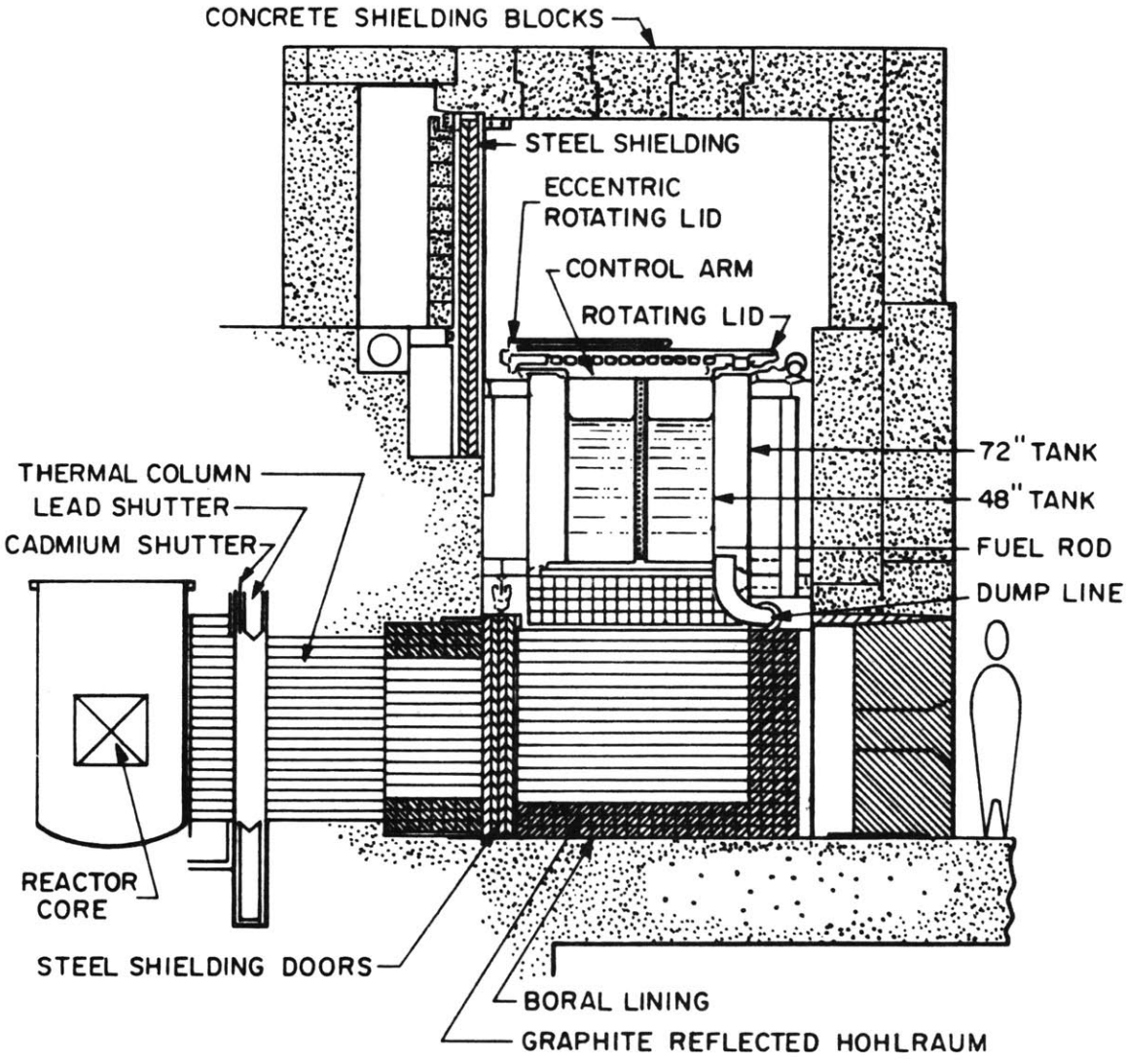

FIG. 3.1 VERTICAL SECTION OF THE SUBCRITICAL ASSEMBLY

The exponential tank, which is 36 inches in diameter, is lined on the radial periphery with 0.020 in. thick cadmium so that it approximates a bare (unreflected) system. The tank is filled with D_2O (purity: 99.7%) to a depth of approximately 52 inches. The mean temperature of the moderator for most of the single element experiments is close to 80°F.

The test fuel element is located at the center of the tank. The foil holders essential to the experiments are suspended from a sturdy aluminum girder which rests horizontally along a diameter on top of the exponential tank. A dry nitrogen atmosphere maintained above the moderator level prevents D_2O-contamination by H_2O. Access to the tank is achieved through a glove box located on the smaller of the two eccentrically rotating circular lids on top of the facility.

The "equilibrium" region of the exponential assembly, where the epithermal and thermal fluxes are proportional to each other (constant cadmium ratio), begins approximately 14 inches from the bottom of the tank. All experiments are made in this region.

3.3 SINGLE ELEMENTS

The three fuel elements tested in this work are: a 1.01-in. diameter natural uranium metal rod (reference element), a 19-rod UO_2-PuO_2 cluster and a 31-rod UO_2-PuO_2 cluster. The fuel within these clusters simulates natural uranium partially burned to 5000 MWD/ton. The geometric characteristics and the fuel composition of the clusters are described in Fig. 1.1 and Table 1.1. Details regarding the fuel rods within the clusters appear in Table 3.1. The concentration of all

Table 3.1

DESCRIPTION OF FUEL AND CLADDING

FUEL*				CLADDING		
Material	Wt.% Fissile	Fuel column density (g/cm^3)	Diameter (in.)	Material	Outer diameter (in.)	Thickness (in.)
U-Metal	0.71(U-235)	18.9	1.01	100 Aℓ	1.01	0.014
UO_2-PuO_2 (pellets)	0.30(U-235) 0.25(Pu-239)	10.25	0.5	6063-T Aℓ	0.547	0.02

*Isotopic composition: Table 1.1 and Appendix G.

isotopes in the homogenized clusters are given in Appendix G. The fuel rods of the clusters(classification: type B) are on loan from the Savannah River Laboratory, and have been previously investigated (B1, F4) under the USAEC/AECL Cooperative Program. Further details, such as the results of chemical analysis on the fuel and the fuel design features, may be found in Ref. B1. All three investigators, SRL, AECL, and M.I.T., have used the same fuel arrangement of Fig. 1.1 within the simulated calandria/pressure tube.

3.3.1 Some Features of the Cluster Design

The aluminum structural parts of the 19 and 31-rod clusters and the arrangement for central vertical suspension of the single elements in the D_2O tank have been designed and built at the M.I.T. Reactor Machine Shop. Schematic sideviews of the individual fuel rod and the cluster assembly are shown in Fig. 3.2. The fuel rods and the aluminum housing-tube are kept in position by two aluminum plates at the top and bottom of the fuel. The weight of the fuel assembly is borne mainly by the top plate, which supports the steel-pins threading the top adapters of the fuel rods. Holes at the lower end of the housing-tube give a free passage for the surrounding D_2O moderator to enter the cluster. The top plate is connected to a support plate with four screws, and the weight of the whole assembly hangs vertically from a universal joint bolted at one end to the support plate and welded at the other to a steel knob. In the vertically suspended position of the cluster, this knob rests on a steel-cross which is centered on the central rectangular (7 in. x

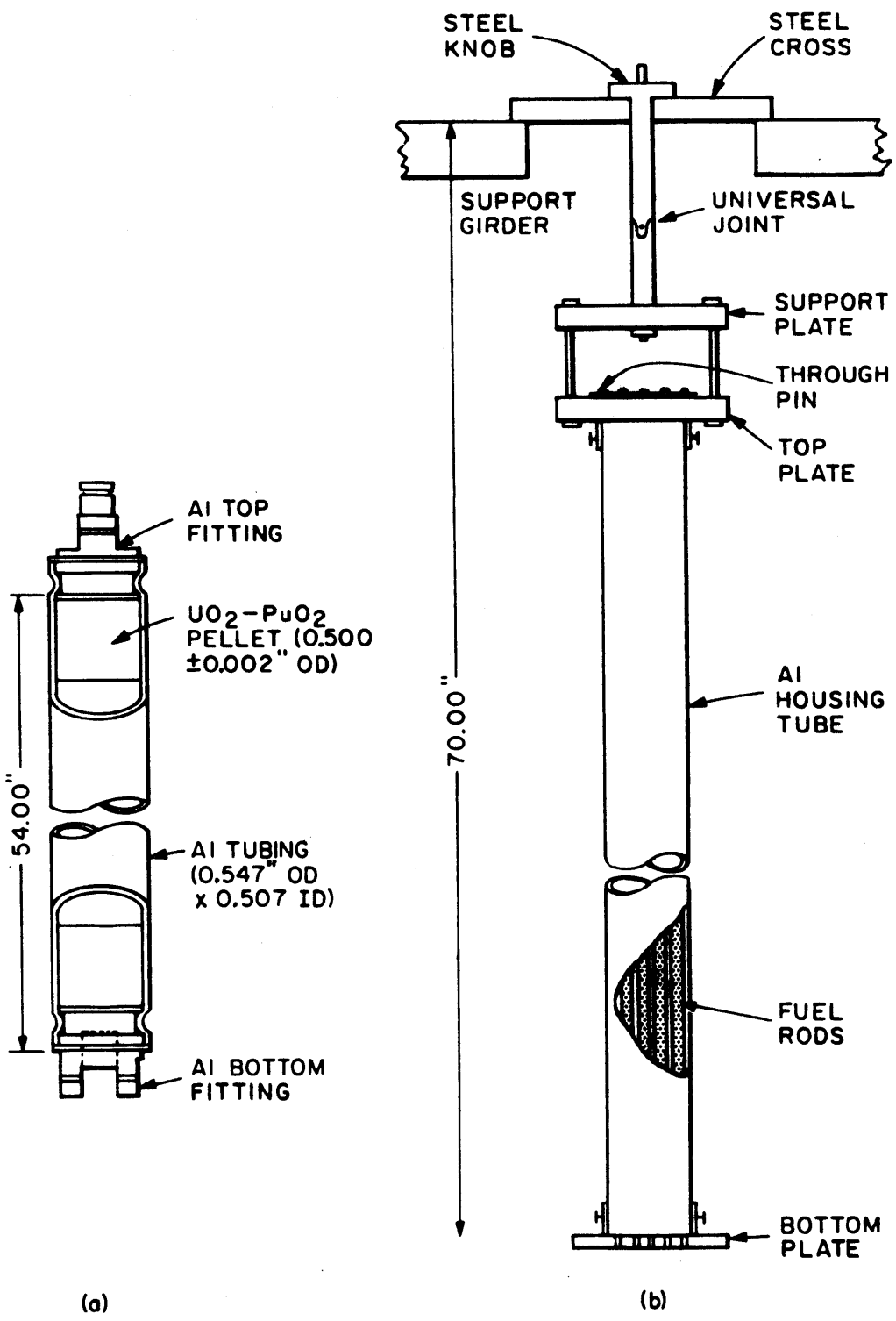

FIG. 3.2 SCHEMATIC SIDE-VIEW
(a) FUEL ROD (TYPE B)
(b) FUEL CLUSTER

6.5 in.) gap of the support girder. By lifting and turning the steel knob, the cluster can be rotated without disturbing its own central position.

3.3.2 S.R.L. and M.I.T. Cluster Differences

The design and construction of the M.I.T. clusters is similar to that of the S.R.L. clusters. The only dissimilarity between the M.I.T. and S.R.L. clusters is related to the slight differences in the outer aluminum tubings. These are tabulated in Table 3.2.

Table 3.2

HOUSING TUBE DIFFERENCES BETWEEN S.R.L. AND M.I.T. CLUSTERS

Cluster		Aℓ Housing Tube Outer Diameter (in.)	Aℓ Housing Tube Thickness (in.)
19-rod	M.I.T.	3.125	0.065
	S.R.L.	3.080	0.030
31-rod	M.I.T.	4.000	0.065
	S.R.L.	4.000	0.050

3.4 DETERMINATION OF X

The distance X to the thermal neutron flux peak is obtained by activating gold foils along a horizontal radial traverse with the fuel element placed vertically along the central axis. The γ-ray activities of the gold foils are counted, corrected and curve-fitted. The position of the maximum of this measured activity distribution

corresponds to the radial distance X of the peak of the thermal neutron flux. A sample data set obtained with each fuel element is presented in Appendix D.

3.4.1 Foil Irradiation

Gold foils of high purity, each 1/16 in. in diameter and .01 in. thick, are punched, cleaned, weighed and catalogued. The variation in weights among the foils is less than 1%. Such uniformity of foil weights is desirable because it makes certain corrections such as gamma-ray self-shielding negligible. Several of these foils (about 14 in number) are mounted, 1/4 in. apart along a long, thin aluminum holder, and positioned to straddle the flux peak. The holder is suspended along a radial direction with aluminum chains which hang from the girder. During the irradiation, the holder rests horizontally against the single fuel element. Figure 3.3 is a sketch of a set of two such aluminum holders suspended on opposite sides of the fuel.

Typically, the irradiation lasts for about 4 hours. The gold foils are then demounted and counted for their γ-ray activities. Four such independent "runs" are made for each single element. The cluster orientation is altered and the two holders are interchanged for different "runs".

3.4.2 Activity Measurement

The activation product Au-198 in the irradiated gold foils emits, primarily, gamma rays of energy 411 kev., with a convenient 2.7 day half-life. Figure 3.4 is a block diagram of the standard NaI-detector counting set up. The gold foils mounted on circular planchets are

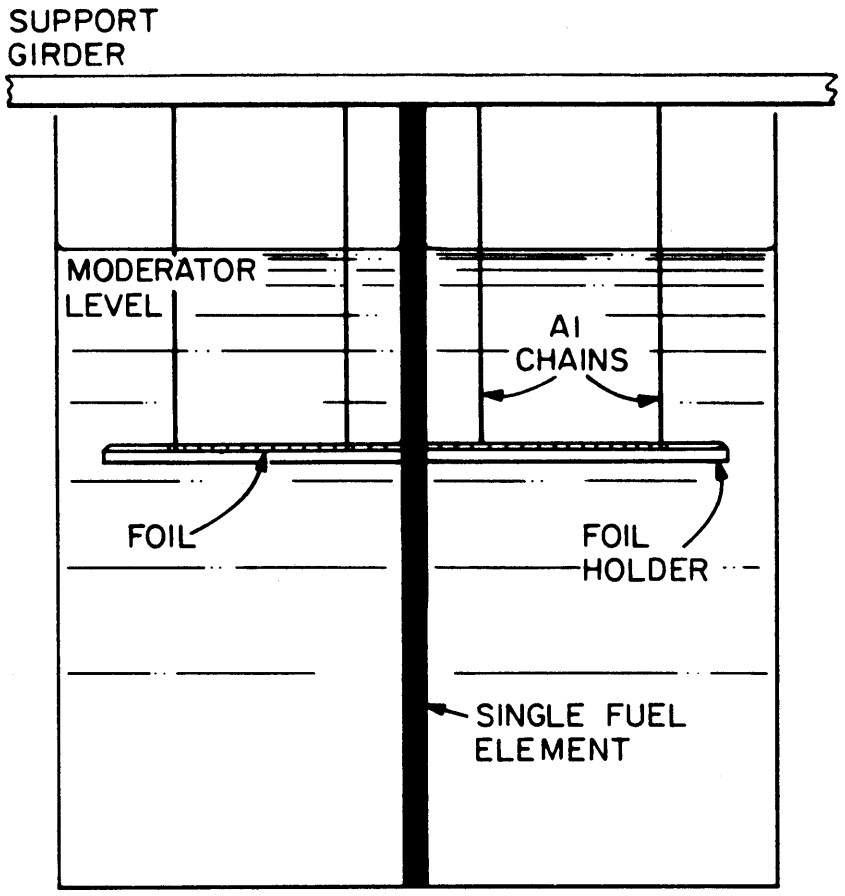

FIG. 3.3 POSITION OF RADIAL FOIL HOLDERS

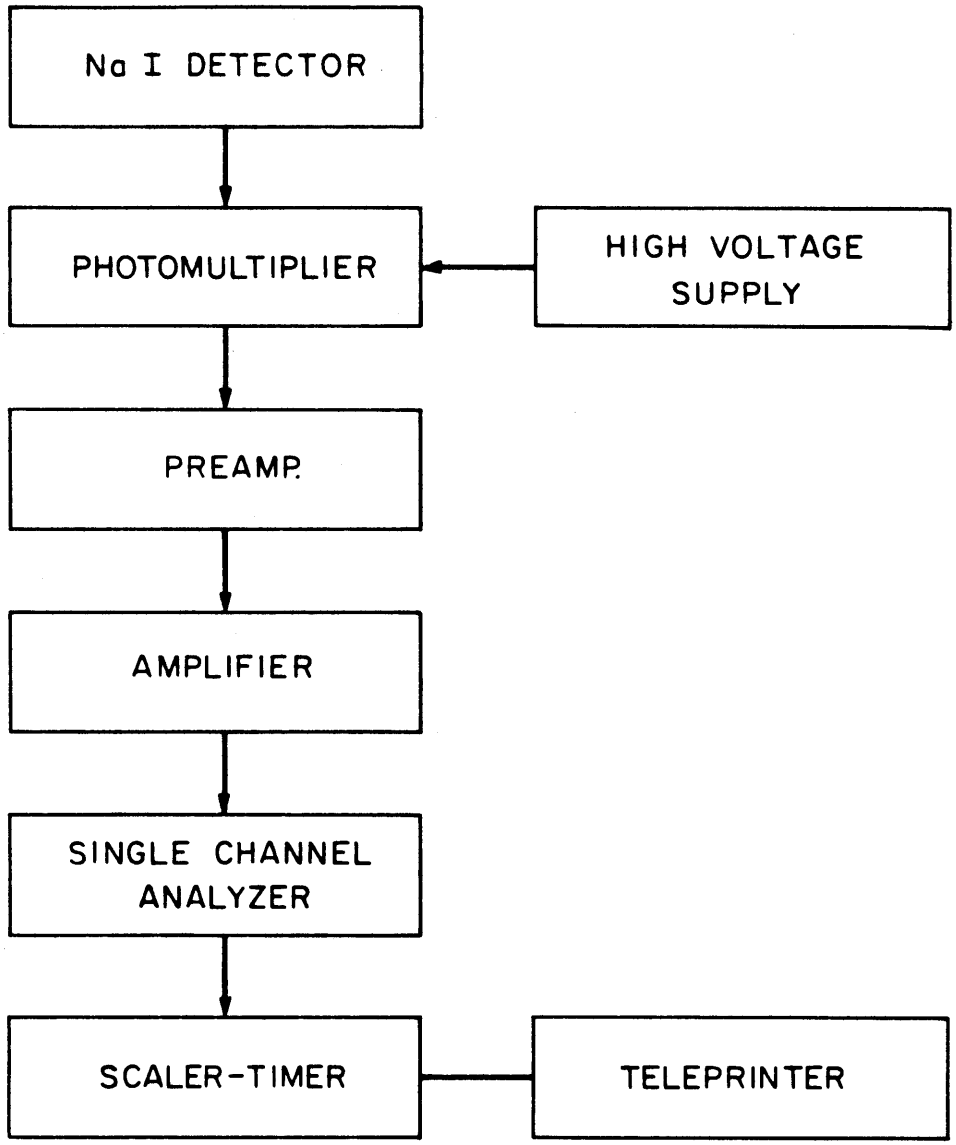

FIG. 3.4 SCHEMATIC SET UP OF COUNTING EQUIPMENT

stacked in an automatic sample changer coupled to the electronic system. The single channel analyzer settings, calibrated with an irradiated sample foil, are set to admit the desired 411 kev. γ-ray photopeak.

Approximately 400,000 counts are accumulated per foil to insure very good statistics. The raw data as printed out by the counting apparatus are corrected for foil weight, dead time, counting time, background activity and decay during counting. This is accomplished by the computer program ACTVTY whose output lists the corrected counts per minute per milligram for each foil.

3.4.3 Curve-fitting for X

When the fast neutron source effect of the fuel element on the thermal neutron distribution is neglected, the radial variation of the thermal flux, or of the activity induced by it, is given by:

$$\phi(r) = B_1 J_0(\alpha r) - B_2 Y_0(\alpha r). \tag{3.1}$$

For small values of the argument (αr) the above equation may be written in the form:

$$\phi(r) = c_1 + c_2 \ell nr + c_3 r^2. \tag{3.2}$$

The corrected activities of gold foils obtained from ACTVTY are fitted to Eq. 3.2 by means of the computer code THERMAX using the least-square technique (H7). The distance X to the position of zero gradient of $\phi(r)$ is obtained from Eq. 3.2. Thus:

$$X = (-c_2/2c_3)^{1/2} \tag{3.3}$$

The program also computes the standard error in X from the root-mean-square of the curve-fit. At larger radial distances, the approximations used to derive Eq. 3.2 fail; while in the proximity of the fuel, the transport effects affect the accuracy of the curve.

The values of X obtained for different angular orientation of the clusters show no systematic trend. The final X-values for the three single-elements are given in Table 3.4.

3.5 DETERMINATION OF γ

The inverse relaxation length, γ, also termed as the die-away constant, determines the variation of the vertical component of the flux. It is measured by irradiating gold foils along a vertical traverse. The induced activities are counted, corrected and fit to a sinh-distribution to give γ corresponding to the best-fit of the experimental data.

3.5.1 Foil Irradiation

Gold foils (about 14 in number), 1/8 in. in diameter and .01 in. thick, are spaced 2 in. apart and positioned on vertical foil holders made of aluminum. Each of these foil holders has a flexible joint at the top. This keeps it vertically straight when suspended from the support girder. Two such holders are placed on opposite sides of the fuel rod (Fig. 3.5), about 8.5 in. from the center, and irradiated simultaneously with the radial holders for X-measurement. The procedures for irradiating the foils and counting and correcting the induced activities are the same as those described earlier in Section 3.4.

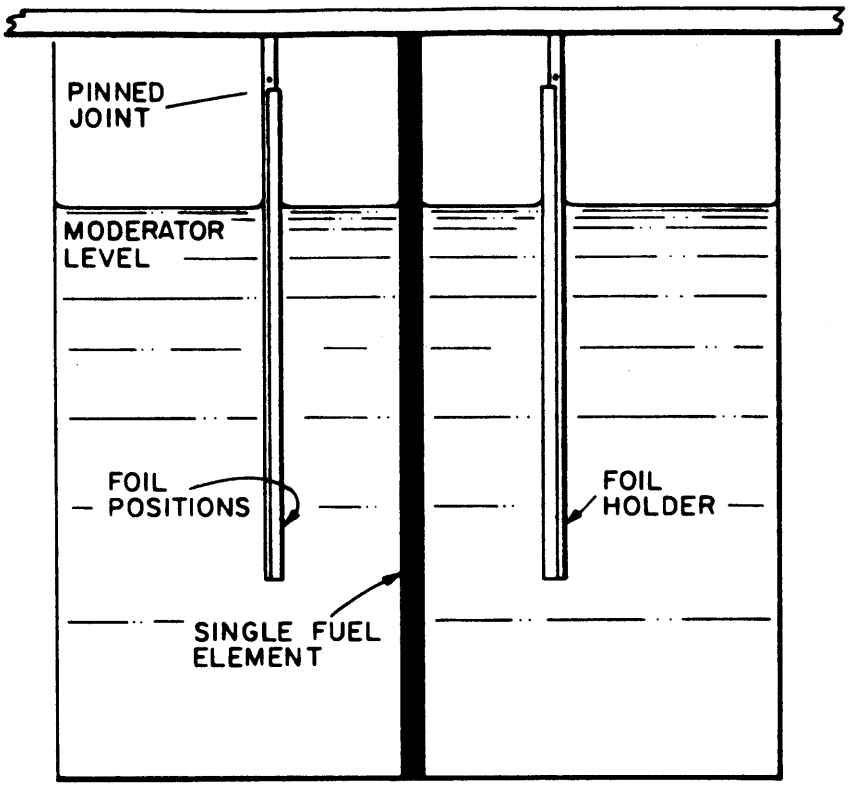

FIG. 3.5 POSITION OF VERTICAL FOIL HOLDERS

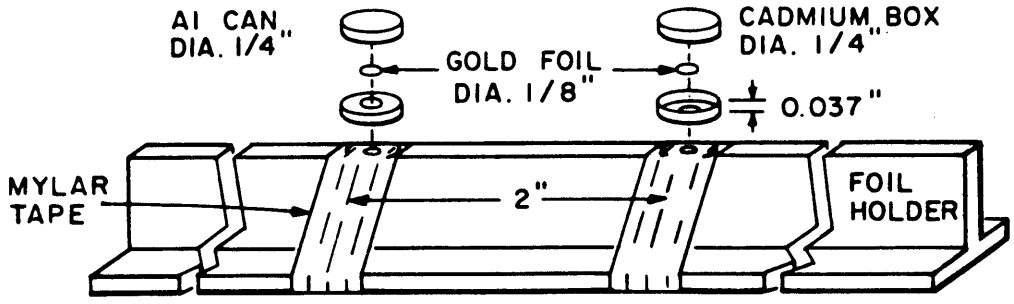

FIG. 3.6 MOUNTING OF FOILS FOR MEASUREMENT OF R

3.5.2 Curve-fitting for γ

The corrected activities of the gold foils, irradiated along axial traverses in the "equilibrium" region of the tank, are expected to follow the axial flux distribution

$$\phi(z) = A' \sinh \gamma(h'-z), \tag{3.4}$$

where h' is the extrapolated height at which the neutron fluxes of all energies are assumed to vanish.

The computer code AXFIT, used to analyze and curve-fit the axial distributions, has been studied and reported in great detail by Palmedo (P1). The code least-square fits the experimental activities to a function of the form of Eq. 3.4 for various values of h', each time dropping a specified number of end points. The "best" value of γ is deduced by comparing the probable errors of γ and by considering the axial distribution of the residuals of the experimental and fitted fluxes. The fitting process weights the experimental activities inversely as the square of the values of corresponding fluxes.

The details of the theoretical basis and of the operation of AXFIT are described in Ref. P1. A typical set of data is given in Appendix D, and the final results appear in Table 3.4

3.6 DETERMINATION OF R

The gold cadmium-ratio, R, at a radial distance, Y, from the single element is directly measured by irradiating at that distance, two similar gold foils, one of which is covered with cadmium. R is then the ratio of the corrected activities of, respectively, the bare and

the cadmium-covered foils. The cadmium ratio experiments were made by Leung (L1).

3.6.1 Foil Irradiation

Each irradiation for the R-measurement (Fig. 3.6) involves two pairs of similar gold foils irradiated on each of the two vertical foil holders placed at a predetermined radial distance Y on opposite sides of the fuel element. The distance Y is equal to 21 cms. for the natural uranium rod, and to 23 cms. for the two clusters. The foils are spaced 2 in. apart and mounted alternately in aluminum cans and cadmium boxes. The aluminum cans insure local displacement of the moderator equivalent to that by the cadmium boxes. The irradiation procedure, and the methods for counting and correcting the gold foil activities are the same as those used for the measurement of γ.

To insure that sufficient activity is accumulated on the cadmium covered foils, the foils are irradiated for about 10 hours. The activities of the bare foils are too high to be counted immediately after irradiation. They are therefore allowed to "cool" for two to three days to minimize counter dead-time corrections.

Two experimental runs, which result in eight sets of R values, are made for each single element. Again, the sample data are shown in Appendix D, and the final results are tabulated in Table 3.4.

3.6.2 Height Correction

Each bare foil is at a distance Δz (2 in.) above its paired cadmium covered foil. Since the flux has an exponential distribution in an axial direction, a multiplicative correction factor,

is applied to the activity of each bare foil.

Note that other corrections such as those due to the finite thickness of the foils and the presence of cadmium covers, are eliminated in the comparison method (Eq. 2.75).

3.7 DETERMINATION OF F AND f_e

Cadmium-covered pairs of natural molybdenum and dilute gold foils (Table 3.3) are simultaneously activated in the neutron flux on the surface of each single-element. These foils are later counted for the induced activities in Au-197 and Mo-98. The measured ratio F of the correct activities per unit weight of the two isotopes thus obtained is then related to the epithermal flux ratio, f_e. Experiments and calculations related to f_c are due to McFarland (M1).

3.7.1 Foil-packet Irradiation

The molybdenum used for the foils is natural molybdenum metal which contains 23.78% by weight of the desired isotope Mo-98. The diluted gold foil is 1.24% by weight of Au-197 in aluminum. Both foils are 1/4 in. in diameter, the Mo-foil being 0.025 in. thick and and Au-foil, 0.003 in. The use of dilute gold reduces resonance self-shielding and lowers the gold activity so that the total counts and the counting times for both foil-types are comparable.

Three packets, each consisting of an Mo-foil and an Au-foil placed "back-to-back", are enclosed in a cadmium can of walls at least 0.030 in. thick. These packets are taped directly to the fuel surface. The packets are spaced about 4 in. apart, the lowest one being located about 20 in. from the bottom of the tank. The configuration and order of the foils within a cadmium can and the

manner in which this can is taped to the fuel is the same for all the packets in the various irradiation runs. The duration of the irradiation of the foils is about 36 hours.

3.7.2 Activity Measurement

All the foils are "counted" with standard NaI gamma counting equipment, the same as that shown schematically in Fig. 3.4. Because of their relatively smaller activation cross section and gamma-yield (Table 3.3), the molybdenum activities are low; consequently, a well-type NaI crystal is used which provides a much larger solid angle for counting. The crystal is surrounded with approximately 12 inches of lead shielding to maintain a very low background.

All the foils are integral counted with the baseline just below the gold gamma-ray photopeak of 412 kev. The electronic set-up is checked periodically for drift with a standard Cs-137 gamma source. The low activity of the Mo-foils is the controlling factor in the determination of the length of the counting intervals. A statistically good value of about 50,000 is obtained for the total counts collected per foil during counting times of approximately 60 minutes. The measured activities are corrected for weight and background and residual activities according to standard prescriptions. The half-lives of the gold and molybdenum foils have been measured experimentally, and found to be nearly identical, thus alleviating the need for half-life corrections. Further details on the activity measurement are to be found in Ref. M1. Values of the ratio F of the corrected activities per unit isotopic weight of Au-197 and Mo-98 measured for the three single

Table 3.3

PROPERTIES OF Au-197 AND Mo-98

Property	Au-197	Mo-98
Isotopic abundance, wt %	100	23.87
Resonance neutron energy, ev.	4.9	480
Effective resonance integral, barns	1490	8.9
2200 (m/s) cross section	94	0.13
Gamma energy, kev	412	740, 780
Gamma yield, %	100	15
Half-life, hrs.	65	67

elements are given in Appendix D. Average values are shown in Table 3.4.

3.7.3 Relating F to f_e

The epithermal flux ratio f_e is related to the measured activity ratio F:

$$f_e = \frac{\phi_{Au}}{\phi_{Mo}} = \frac{M_{Au}}{M_{Mo}} \frac{RI_{Mo}}{RI_{Au}} \frac{u_{Au}}{u_{Mo}} Y_\gamma F, \qquad (3.5)$$

where M_{Au}, M_{Mo} are, respectively, the molecular weights of infinite-Au-197 and Mo-98,

RI_{Au}, RI_{Mo} are the infinite-dilution resonance integrals of Au and Mo in barns,

u_{Au}/u_{Mo} is the ratio of lethargies at Au and Mo resonances; this factor corrects the resonance integrals for the $1/\tau(u)$ neutron energy spectrum on the single element surface (Appendix C),

Y_γ is the ratio of the yields of γ rays of energies above 412 kev. (gold photopeak) from Mo-98 and Au-197 respectively.

The procedure for the calculation of f_c and A requires a value of f_e relative to that for the "reference" element (natural uranium rod). Consequently the uncertainties in the constants which appear in Eq. 3.5 are eliminated provided that the experimental methods for the test and reference fuel elements are the same. Values of f_e are given in Appendix D.

Table 3.4

VALUES OF THE EXPERIMENTAL PARAMETERS

Single Element Type	X cm	γ^2, cm^{-2}	R	F
Nat. U rod ("reference")	9.70 ±0.08	2488.5 ±9.2	122.18 ±2.2	361.6 ±0.5
19-rod PuO_2-UO_2 cluster	13.16 ±0.14	2417.6 ±6.7	77.69 ±0.44	397.15 ±10.6
31-rod PuO_2-UO_2 cluster	14.77 ±0.21	2388.2 ±11.6	58.41 ±0.56	389.9 ±5.0

3.8 MODERATOR PARAMETERS

The theoretical methods (Chapter II) developed to interpret the single-element experiments require the knowledge of thermal neutron properties of the moderator, namely, the diffusion area, L_0^2, and the diffusion coefficient, D.

L_0^2 is related to α^2 and γ^2 (Eq. 2.10):

$$\frac{1}{L_0^2} = \gamma^2 - \alpha^2 .$$

The determination of L_0^2 consists, therefore, in measuring the radial buckling, α^2, and the (square, γ^2, of the) inverse relaxation length γ, in the tank filled with the D_2O moderator alone. The determination of α and γ consists in the measurement of the radial and axial fluxes in the moderator and fitting them, respectively, to J_0 and sinh-distributions.

The radial flux measurement for the determination of α is made by irradiating gold foils, 1/8 in. in diameter and 0.010 in. thick, spaced 1.5 in. apart on an aluminum holder suspended horizontally along a tank diameter. The methods for irradiating, and for counting and correcting the induced activities are the same as those used for measuring X. The measured activities are fitted, according to the least-square criterion, to the theoretical flux distribution given by

$$\phi_r(r) = A\, J_0\Big[\, \alpha(r-c) \,\Big], \tag{3.6}$$

where the "best" values of A and α are determined in the fitting process. The analysis is repeated for different preset values of c, the center of the distribution, and of the number of experimental

points to be used in the fit. The analytical methods and the computer code RADFIT used for obtaining α have been described by Palmedo (P1).

The method for the determination of γ is the same as that used in the single-element experiments (Section 3.4).

The results of two independent measurements for α and of four for γ, in D_2O moderator of 99.7 mole-% purity, are:

$$\alpha^2 = (2516.8 \pm 12.5) \times 10^{-6} \quad cm^{-2}$$

$$\gamma^2 = (2628.4 \pm 10.5) \times 10^{-6} \quad cm^{-2}$$

The moderator properties L_0^2 and D deduced from these results are given in Table 3.5. The effect on these results of the variations in moderator temperature has not been taken into account.

3.9 CALCULATION OF Γ, η, A

The first step in the evaluation of the heterogeneous fuel parameters is to obtain the epithermal absorption parameter A. The measured value of f_e for the single element is multiplied by the standarization factor c (equal to 0.4073; Section 2.5.3) to give the corresponding ANISN computed ratio f_c. This ratio is then related (Section 2.5.3) to the desired value of A, from the f_c versus A curves (Fig. 2.4).

The knowledge of A permits the calculation of the coefficients C_n (Eq. 2.61) and the integrals I_J and I_γ which occur in the expressions for Γ (Eq. 2.36) and the thermal neutron flux distribution $\hat{\phi}_r(r)$ (Eq. 2.27). Given the experimental parameters X, γ (or α; Eq. 2.10) and R, and the moderator data (Table 3.5), Eqs. 2.36 and 2.75 can be solved simultaneously (Section 2.5.4) to calculate Γ and η. The values

Table 3.5

MODERATOR PROPERTIES*

L_0^2	=	8958.2	cm^2
D	=	0.84	cm
τ_{th}	=	118.8	cm^2
τ_{Au}	=	95.0	cm^2
τ_r	=	80.0	cm^2

*Notation according to Appendix H

Table 3.6

HETEROGENEOUS FUEL PARAMETERS

Fuel Type	Γ	η	A
Nat. U rod ("reference")	0.9546	1.375*	20.39*
19-rod UO_2-PuO_2 cluster	0.4707	1.3643	52.5
31-rod UO_2-PuO_2 cluster	0.3313	1.4017	81.50

* "Reference" values (Appendices E and F)

of $\hat{\phi}_r(Y)$, arrived at after iterations between Eqs. 2.27 and 2.77, for the three fuel elements: Nat. U metal rod, and 19 and 31-rod UO_2PuO_2 clusters, are respectively, 1.097, 1.134 and 1.238.

The final values of Γ, η and A are tabulated in Table 3.6.

3.10 SENSITIVITY OF THE HETEROGENEOUS PARAMETERS

Figures 3.7, 3.8 and 3.9 illustrate the dependence of the heterogeneous fuel parameters Γ, η and A on the experimentally measured quantities X, γ, R and F.

The typical experimental error in measuring F (Table 3.4) leads to an uncertainty of about 8% in the determination of A. The other two heterogeneous parameters Γ and η depend upon all four measured quantities. The order of the gross error associated with Γ and η can be established by compounding the separate effects on them of the uncertainties in X, γ, R and F. The effects on Γ and η due to the typical errors (Table 3.4) in the measured values of the four experimental parameters are readily seen from the linear plots of Figs. 3.7 and 3.8. Combining these effects separately for Γ and η shows that the uncertainties associated with their determination are about 5% and 3% respectively. These composite errors are, of course, not independent of each other and cannot themselves be directly compounded to give gross error in a quantity, such as the multiplication constant or the buckling of a reactor lattice, which depends upon both the parameters Γ and η.

Observation of the sensitivity curves shows that the uncertainty in X-measurement is important to the accuracy with which Γ and η can

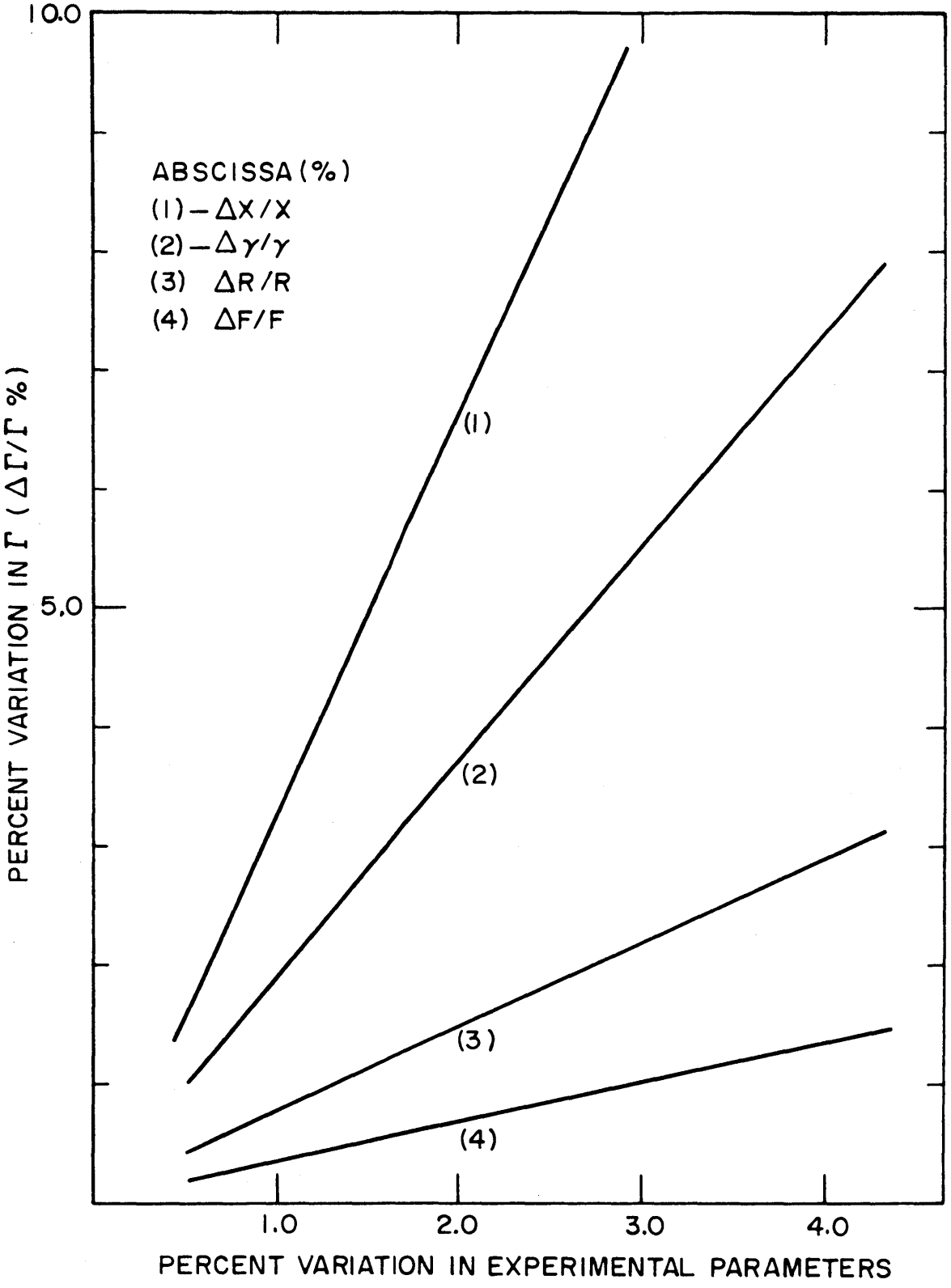

FIG. 3.7 SENSITIVITY OF Γ

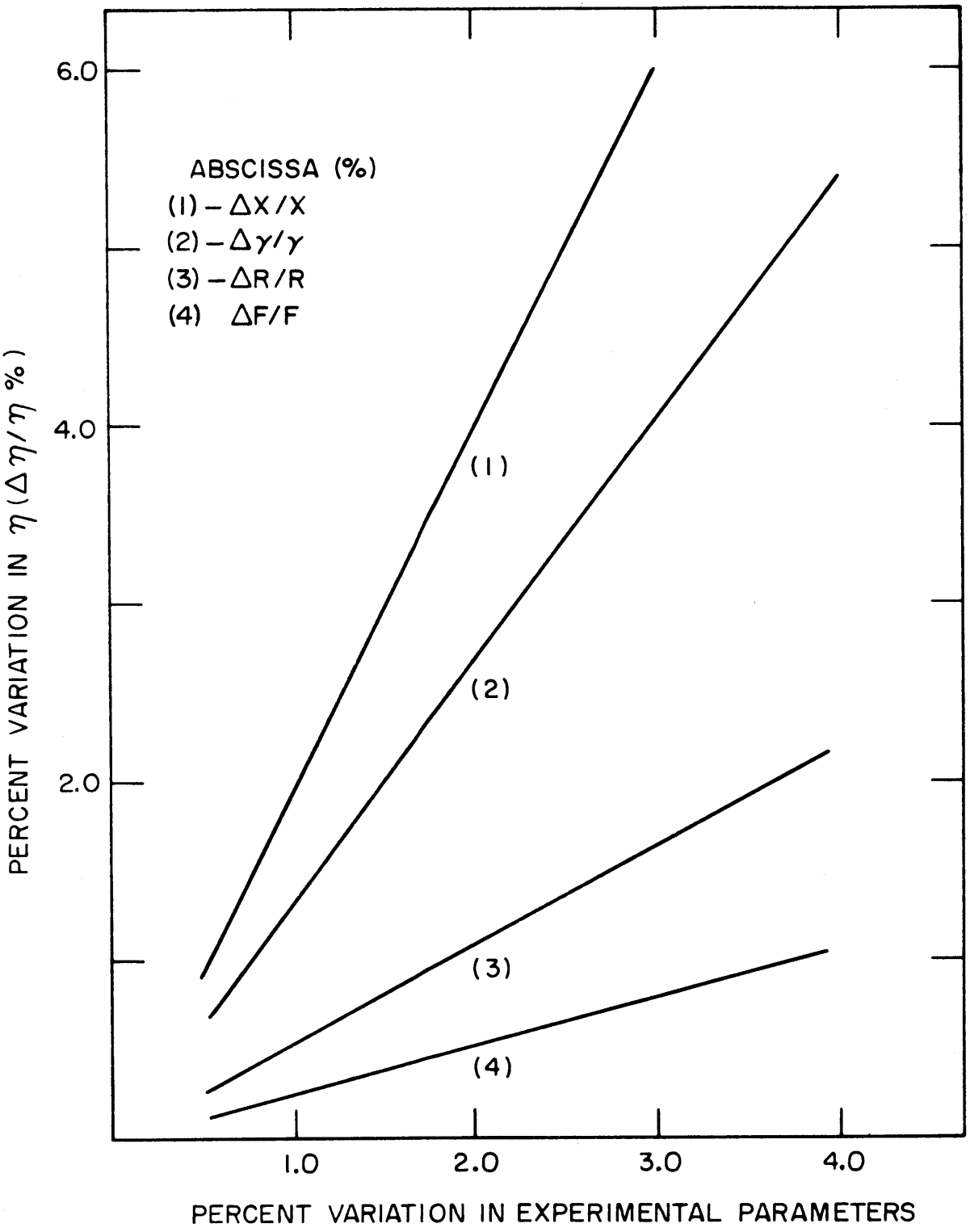

FIG. 3.8 SENSITIVITY OF η

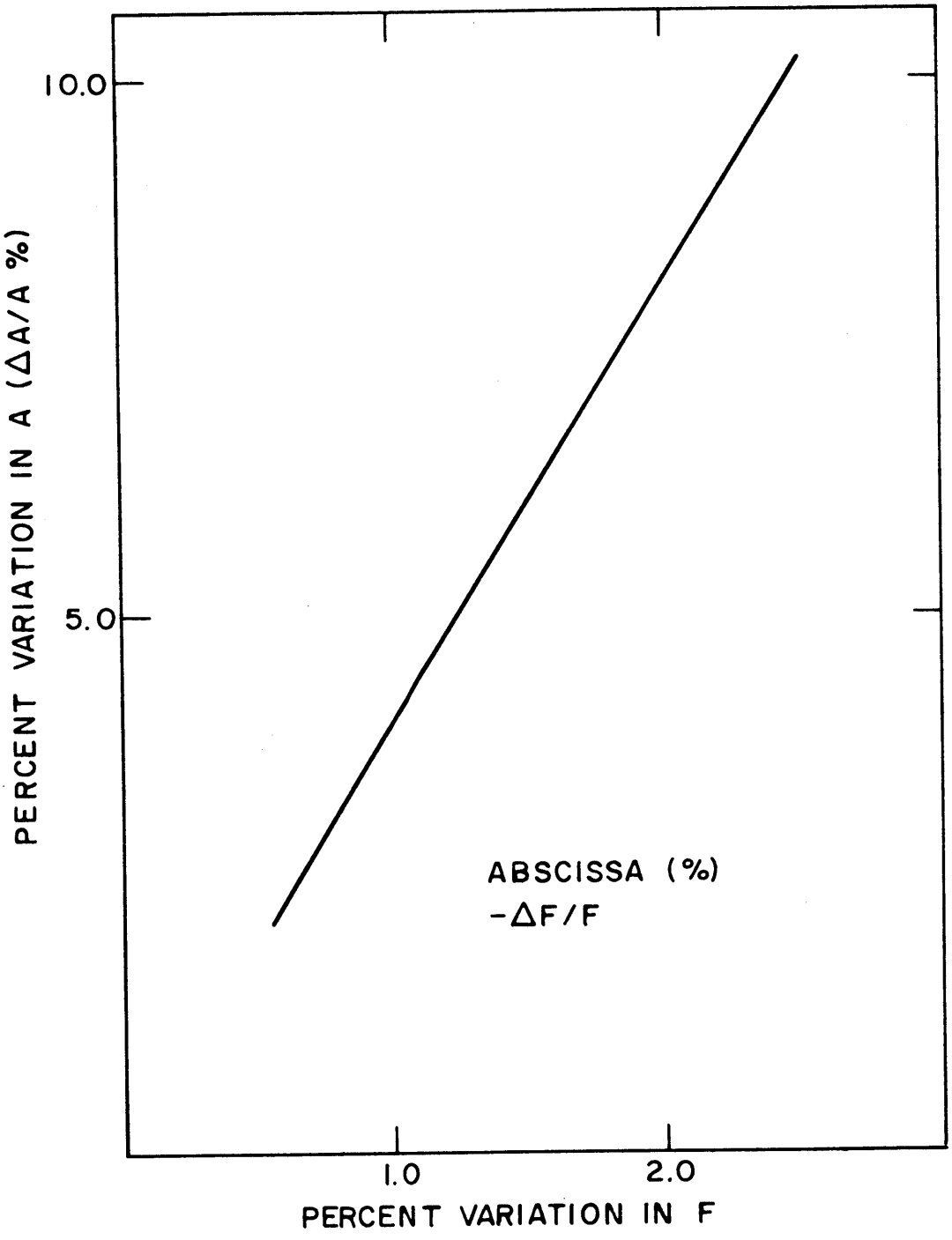

FIG. 3.9 SENSITIVITY OF A

be determined. Improvements should, therefore, be made in the techniques for measuring X. The largest percentage of error, however, is associated with the value of F measured for the 19-rod cluster. It is shown in Fig. 4.4 that the value of the material buckling calculated from the four experimental parameters is most sensitive to the ratio F. Hence, it is also important to increase the accuracy in the measurement of F. Increasing the number of independent determinations of F can considerably reduce the error.

The significance of the errors in experimental measurements becomes clearer in the next chapter where the heterogeneous fuel parameters Γ, η and A are used in a calculation for the material bucklings of uniform lattices. Some suggestions for improving the experimental methods are included in the final chapter.

Chapter 4

APPLICATION TO UNIFORM LATTICES

4.1 INTRODUCTION

The previous chapters show how the characteristic heterogeneous parameters Γ, η and A of a fuel element can be determined by interpreting simple experiments which directly measure the four quantities X, γ, R and F. The three fuel parameters are thus determined for the 19 and 31-rod PuO_2-UO_2 clusters typical of those heavy water reactor designs which use the pressure tube concept. These parameters completely "define" the particular fuel cluster in question. Such a set of heterogeneous parameters for each different fuel (or control) element in a multi-component lattice can then be used with the heterogeneous source-sink formalism (Section 1.3) to carry out overall reactor calculations for a given non-uniform core configuration.

The purpose of this part of the work, however, is not to perform a detailed core calculation such as that indicated above; but only to provide a simple test for the measured values of Γ, η and A. Attention is therefore restricted to the case of uniform D_2O-moderated lattices composed of a single fuel-type which in the present case is the 19 or the 31-rod PuO_2-UO_2 fuel cluster. The lattices have a triangular arrangement; the spacing between fuel elements is 9.33 in. for the 19-rod clusters and 9.33 in. and 12.12 in. for the 31-rod clusters. These particular lattices have been extensively investigated at the Savannah River Laboratory (SRL).

For the sake of simplicity, the three heterogeneous fuel parameters are directly related to the conventional reactor physics parameters: the thermal utilization, the neutron reproduction factor and the resonance escape probability; and the material buckling then calculated from the age-diffusion equation. For uniform lattices, this convenient procedure should give satisfactory results and save the cost and effort involved in the use of a heterogeneous reactor code such as HERESY. The lattice results obtained from the single element parameters Γ, η and A are compared with the corresponding theoretical and experimental values obtained with conventional methods at SRL.

4.2 THERMAL UTILIZATION, f_Γ

The thermal utilization can be derived by using the Poisson summation (P2) to determine the thermal flux at the surface of a fuel element from the contributions of the other fuel elements, and then relating these surface fluxes to the fuel absorptions through the thermal constant Γ. In the case of a uniform lattice, this can also be derived by using the Wigner-Seitz formalism of a unit cell centered about a fuel element.

$$f_\Gamma = \frac{\text{fuel absorption}}{\text{fuel absorption + moderator absorption}} , \tag{4.1}$$

$$\frac{1}{f_\Gamma} = 1 + \frac{\text{moderator absorption}}{\text{fuel absorption}} , \tag{4.2}$$

The fuel absorption in the above expression includes absorption in cladding, coolant and air-gaps associated with a composite fuel element; in this sense, f_Γ differs from the conventional definition

of the thermal utilization. The fuel absorption in a unit lattice cell follows from the definition (Eq. 2.1) of Γ and is equal to $\frac{\phi_r(a)}{\Gamma}$.

The moderator absorption to be substituted into Eq. 4.2 may be considered to be made up of two parts: (1) moderator absorption calculated on the assumption of a flat flux in the moderator whose value equals that at the fuel surface $\phi_r(a)$. This component of the moderator absorption is equal to $V_m\Sigma_{am}\phi_r(a)$, V_m being the moderator volume in the unit cell, (2) "excess" moderator absorption due to the moderator thermal flux in excess of $\phi_r(a)$.

Then from Eq. 4.2,

$$\frac{1}{f_\Gamma} = 1 + \Gamma\Sigma_{am}V_m + (E\text{-}1) \tag{4.3}$$

where (E-1) denotes the "excess" moderator absorption per fuel absorption. Diffusion theory gives the following result (W2) for (E-1):

$$(E\text{-}1) = \frac{\kappa_m^2(b^2-a^2)}{2(\kappa_m a)}\left[\frac{I_1(\kappa_m b)K_0(\kappa_m a) + I_0(\kappa_m a)K_1(\kappa_m b)}{I_1(\kappa_m b)K_1(\kappa_m a) - I_1(\kappa_m a)K_1(\kappa_m b)}\right] \tag{4.4}$$

where κ_m is the inverse diffusion length in the moderator, and "a", "b" refer to the fuel and unit cell radii, respectively. The above relation may be usefully approximated (W2) and expressed in terms of the volume fraction of fuel in the unit cell, V_f/V_c, denoted by v:

$$(E\text{-}1) = \frac{V_m}{4\pi L_0^2}\left[\frac{v}{2} - \frac{3}{2} - \frac{\ell n\ v}{(1-v)}\right] \tag{4.5}$$

Table 4.1 lists the values used for the constants in the above equations and the results for f_Γ. The derivation of Eq. 4.3 disregards the slight variation in Γ due to changes in the lattice

Table 4.1

RESULTS FOR THERMAL UTILIZATION, f_Γ

Lattice	b, cms	a, cms	v	V_m, cm^2	Γ, cm^{-1}	(E-1)	f_Γ
19-rod cluster 9.33 in. pitch	12.44	3.97	0.102	436.7	0.4707	0.00416	0.9793
31-rod cluster 9.33 in. pitch	12.44	5.08	0.167	405.1	0.3313	0.00279	0.9863
31-rod cluster 12.12 in. pitch	16.16	5.08	0.099	739.3	0.3313	0.00717	0.9733

D_2O purity: 99.75 mole %

$\Sigma_{am} = 0.825 \times 10^{-4}$ cm^{-1}

$L_0^2 = 10178$ cm^2

spacing and the attendant spectral changes. Frech (F3) has shown experimentally that the change in effective neutron temperature is directly proportional to the volume fraction of fuel; hence it is conceivable that a correction could be developed to account for spectral hardening. However, because of the experimental uncertainty of about 5% in the determination of Γ, it is questionable whether such an effort is warranted.

4.3 FAST NEUTRON YIELD, η

The single element heterogeneous fuel parameter η, which is measured in the present work, gives the total number of fast neutrons produced in all the fissions occuring within the fuel element per thermal neutron absorbed. It does not, however, include the effect of those fast and epithermal neutrons which arrive at this fuel element from other fuel elements. Hence the expression for η_L, which includes the effect of lattice interaction, is obtained by adding to η for the single (subscript: "0") element, the number of fast neutrons born in the element ("0") due to fissions by fast and epithermal neutrons produced per thermal neutron absorption in other (subscript: "j") elements. Thus,

$$\eta_L = \eta + V_f \, (\nu N RI_f)^{epi} \sum_{j,j\neq 0} \phi_{0j}^{epi} + V_f \, (\nu N \bar{\sigma}_f)^{fast} \sum_{j,j\neq 0} \phi_{0j}^{fast} \qquad (4.6)$$

In the above equation, V_f is the fuel volume, and the products $(N \nu RI_f)^{epi}$, $(N \nu \bar{\sigma}_f)^{fast}$ are, respectively, the number of neutrons

produced per unit volume, per unit flux, in all the epithermal and fast fissions in all the uranium and plutonium isotopes present in the fuel assembly; ϕ_{0j}^{epi} and ϕ_{0j}^{fast} are, respectively, the contributions of the j^{th} element to the epithermal and fast neutron fluxes at the zero-th ("0") element. The age kernel and the uncollided flux kernel (Appendix B) are used for the respective propagation of the epithermal and fast neutrons over the distance r_{0j}, from the j^{th} fuel element to the 0^{th}. Thus, the flux contributions in Eq. 4.6 are:

$$\phi_{0j}^{epi} = \frac{\eta}{\xi\Sigma_s} \frac{e^{-r_{0j}^2/4\tau_{ef}}}{4\pi\tau_{ef}}, \tag{4.7}$$

where $(\xi\Sigma_s)$ is the slowing down power of the moderator, τ_{ef} is the age of fission neutrons to the effective energy of epithermal fissions, and

$$\phi_{0j}^{fast} = \eta \frac{e^{-\frac{\pi}{2}\frac{r_{0j}}{\lambda_f}}}{4r_{0j}}, \tag{4.8}$$

where λ_f is the mean free path of the fast neutrons in the moderator. Substituting Eqs. 4.7 and 4.8 into Eq. 4.6,

$$\eta_L = \eta \left[1 + V_f \frac{(\nu N RI_f)^{epi}}{\xi\Sigma_s} \sum_{j,i\neq 0} \frac{e^{-r_{0j}^2/4\tau_{ef}}}{4\pi\tau_{ef}} + V_f \frac{(\nu N \bar{\sigma}_f)^{fast}}{4} \sum_{j,j\neq 0} \frac{e^{-\frac{\pi}{2}\frac{r_{0j}}{\lambda_f}}}{r_{0j}} \right] \tag{4.9}$$

If the corrections to η due to epithermal and fast interactions are denoted by $\Delta\eta_{epi}$ and $\Delta\eta_{fast}$ respectively, then it follows that:

$$\eta_L = \eta + \Delta\eta_{epi} + \Delta\eta_{fast} \tag{4.10}$$

The summations of the age and uncollided flux kernels in Eq. 4.9 are carried out by the methods of Ref. H5. These are discussed briefly in the next two subsections. The numerical values used in the present work for all the nuclear constants appearing in Eq. 4.9 are tabulated in Table 4.2. Calculated values of $\Delta\eta_{epi}$, $\Delta\eta_{fast}$ and η_L for the three lattices of present interest are given in Table 4.3 In the calculations for the material buckling of the lattices (Section 4.6), $\Delta\eta_{epi}$ and $\Delta\eta_{fast}$ are to be corrected, respectively, for epithermal and fast neutron leakage. These terms are thus multiplied (W2) by $e^{-B_m^2\tau_{ef}}$ and $e^{-B_m^2\lambda^2/3}$ respectively. The effect of these further corrections in the present cases is to decrease η_L only by a small fraction of one percent.

4.3.1 Summation of the Age Kernel

The infinite array of identical fuel elements, arranged in a triangular lattice with fuel spacing, p_0, is depicted in Fig. 4.1. The origin of the coordinates x and y, offset at 60°, is located at the center of the "zero-th" fuel element. The radial distance, r_{0j}, of the j^{th} fuel element from the origin is then given by:

$$r_{0j}^2 = x^2 + y^2 + xy, \tag{4.11}$$

Since the fuel elements are located at a constant spacing p along the coordinate axes,

$$x = mp_0; \quad y = np_0, \tag{4.12}$$

where m and n are integers. Thus,

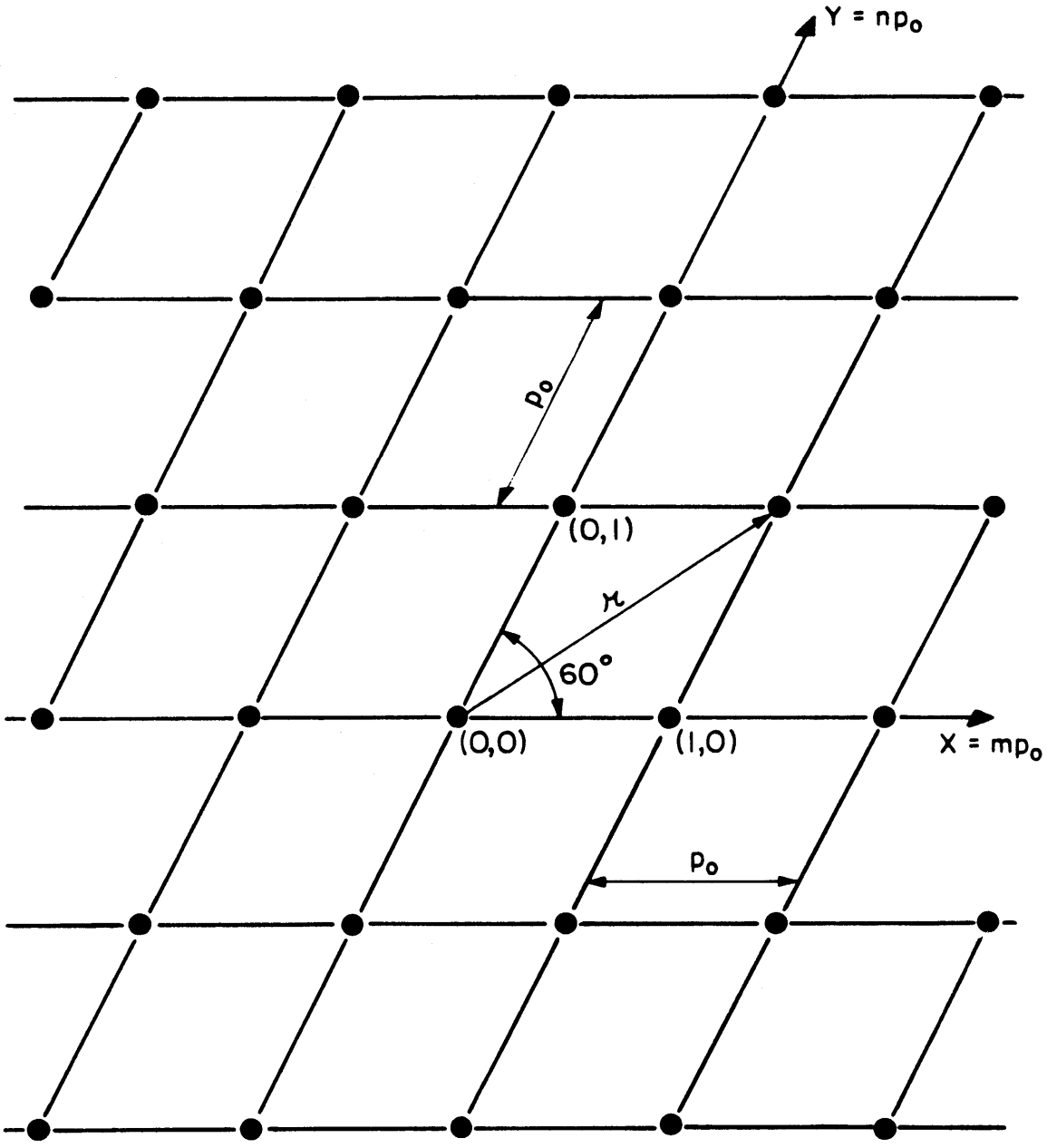

FIG. 4.1 LATTICE ARRAY FOR AGE KERNEL SUMMATION

$$r_{0j}^2 = m^2p_0^2 + n^2p_0^2 + mnp_0^2 \quad . \tag{4.13}$$

Denoting the required summation of the age kernel which appears in the second term of Eq. 4.9 by S_e:

$$S_e = \sum_{j,j\neq 0} \frac{e^{-r_{0j}^2/4\tau_{ef}}}{4\pi\tau_{ef}} \quad . \tag{4.14}$$

It is convenient first to sum the kernel with the contribution of the center fuel element included. Substituting for r_{0j}^2, this summation (S_0) is:

$$S_0 = \frac{1}{4\pi\tau_{ef}} \left[\sum_{m=-\infty}^{\infty} e^{-\frac{m^2p_0^2}{4\tau_{ef}}} \sum_{n=-\infty}^{\infty} e^{-\frac{(n^2p_0^2+mnp_0^2)}{4\tau_{ef}}} \right] . \tag{4.15}$$

Use of the Euler-McLaurin sum formula (D1) yields

$$\sum_{n=-\infty}^{\infty} e^{-\frac{(n^2+mn)p_0^2}{4\tau_{ef}}} = 2\int_0^{\infty} e^{-\frac{(n^2+mn)p_0^2}{4\tau_{ef}}} dn$$

$$= \frac{\sqrt{4\pi\tau_{ef}}}{p_0} e^{\frac{m^2p_0^2}{16\tau_{ef}}} , \text{ Ref. B3.} \tag{4.16}$$

Substitution of this result in Eq. 4.15 gives:

$$S_0 = \frac{1}{p_o\sqrt{4\pi\tau_{ef}}} \sum_{m=-\infty}^{\infty} e^{-\frac{3m^2p_o^2}{16\tau_{ef}}} \quad . \tag{4.17}$$

On again applying the Euler-McLaurin sum formula to evaluate the summation over the index, m, it follows that:

$$\sum_{m=-\infty}^{\infty} e^{-\frac{3m^2p_0^2}{16\tau_{ef}}} = 2\int_0^{\infty} e^{-\frac{3m^2p_0^2}{16\tau_{ef}}}\,dm = \frac{1}{p_0}\sqrt{\frac{16\pi\tau_{ef}}{3}} \quad , \tag{4.18}$$

Thus,

$$S_0 = \frac{2}{\sqrt{3}}\,\frac{1}{p_0^2} = \frac{1}{V_c} \quad , \tag{4.19}$$

where V_c is the area of the unit cell in the lattice.

The required sum S_e is then obtained by subtracting from S_0 the contribution of the center rod, which is: $\frac{1}{4\pi\tau_{ef}}$; hence

$$S_e = \left(\frac{1}{V_c} - \frac{1}{4\pi\tau_{ef}}\right) . \tag{4.20}$$

4.3.2 Summation of the Uncollided Flux Kernel

The desired summation in Eq. 4.9 is denoted by S_f:

$$S_f = \sum_{j,j\neq 0} \frac{e^{-\frac{\pi}{2}\frac{r_{0j}}{\lambda_f}}}{r_{0j}} , \tag{4.21}$$

and is to be evaluated over a triangular lattice array. It is convenient to bracket the desired value of S_f between the results which would be obtained by summing the kernel over circumscribed and inscribed rings (Fig. 4.2).

Each of the successive pairs (index: n) of circumscribed and inscribed rings has 6n elements. The radius of a circumscribed ring is (np_0) and the kernel summation carried out over all the successive circumscribed rings provides a lower limit for the value of S_f. On the other hand, the summation over the successive inscribed rings, each of whose radius is $(\frac{\sqrt{3}}{2}\,np_0)$ gives the corresponding upper limit for the required result.

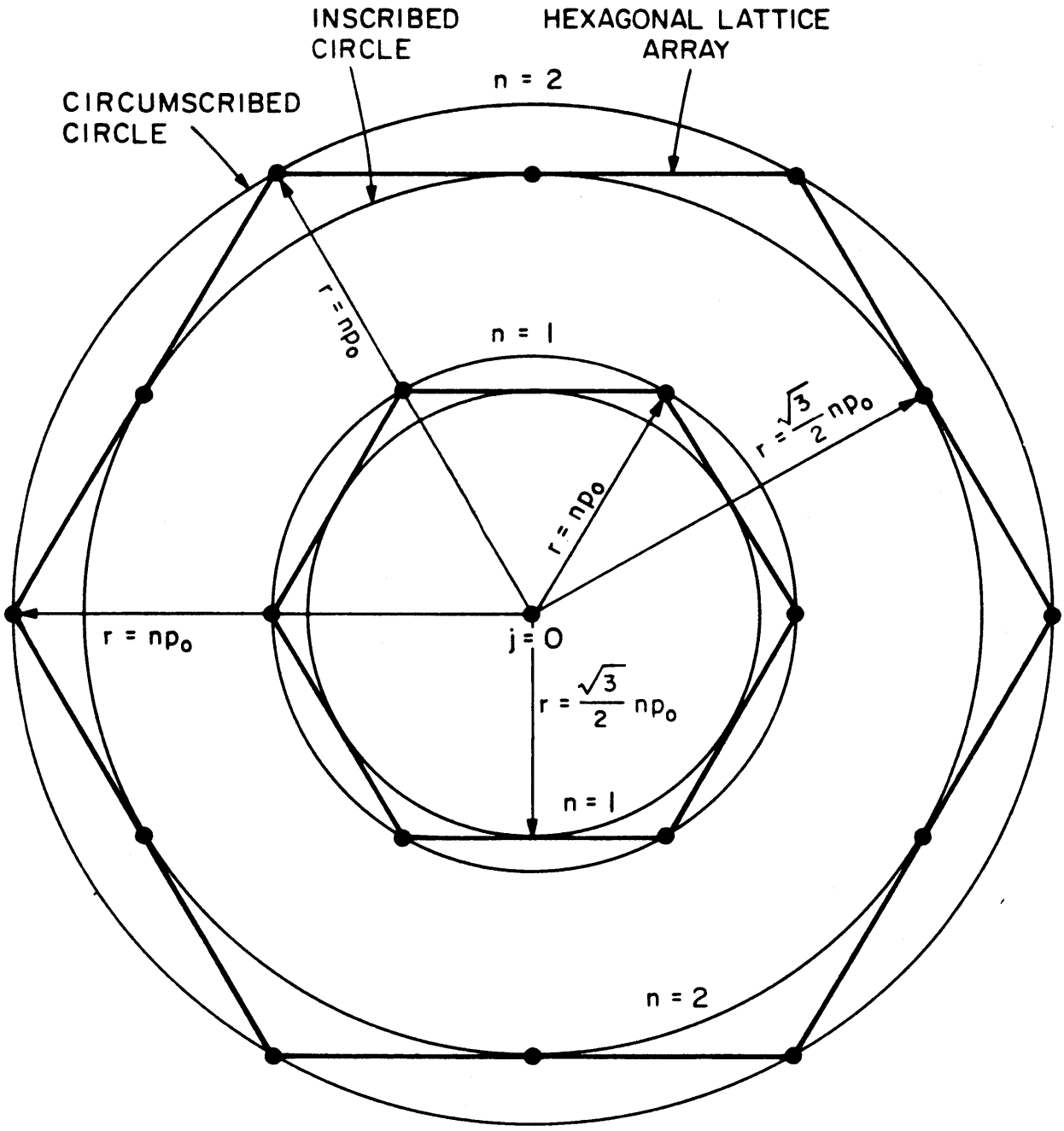

FIG. 4.2 LATTICE ARRAY FOR UNCOLLIDED FLUX KERNEL SUMMATION

Substituting for r_{0j} in Eq. 4.21 and adding up the contribution of the 6n fuel elements in each circumscribed ring,

$$S_f > \sum_{n=1}^{\infty} \frac{e^{-\frac{\pi}{2}\frac{np_0}{\lambda_f}}}{np_0} 6n = \frac{6}{p_0} \sum_{n=1}^{\infty} e^{-\frac{\pi np_0}{2\lambda_f}} \quad (4.22)$$

Then the Euler-McLaurin sum formula (D1) gives:

$$S_f > \frac{6}{p_0} e^{-\frac{\pi p_0}{2\lambda_f}} \left\{\frac{2\lambda_f}{\pi p_0} + \frac{1}{2} + \frac{\pi p_0}{24\lambda_f} + \ldots\right\} \quad (4.23)$$

Since the volume fraction of fuel, v_c in this case is:

$$v_c = \lim_{n\to\infty} \frac{6\pi a^2 \sum_{n-1}^{n} n}{\pi p_0^2 n^2} = \frac{3a^2}{p_0^2}, \quad (4.24)$$

$$S_f > \left(\frac{4\lambda_f v_c}{\pi a^2} + \frac{\sqrt{3v_c}}{a} + \frac{\pi}{4\lambda_f}\right) e^{-\frac{\pi\sqrt{3}a}{2\lambda_f\sqrt{v_c}}} \quad (4.25)$$

The use of the same procedure for the case of inscribed rings yields

$$S_f < \frac{6}{p_0} e^{\frac{\pi p_0}{2\lambda_f}} + \sum_{n=2}^{\infty} \frac{4\sqrt{3}}{p_0} e^{-\frac{\pi\sqrt{3}}{4}\frac{np_0}{\lambda_f}}, \quad (4.26)$$

where the first ring is treated correctly as a circumscribed circle. The application of the Euler-McLaurin formula gives

$$S_f < \frac{6}{p_0} e^{-\frac{\pi p_0}{2\lambda_f}} + \frac{4\sqrt{3}}{p_0} e^{-\frac{\pi\sqrt{3}p_0}{2\lambda_f}} \left(\frac{4\lambda_f}{\pi\sqrt{3}p_0} + \frac{1}{2} + \frac{\pi\sqrt{3}p_0}{48\lambda_f}\right). \quad (4.27)$$

Table 4.2

VALUES OF THE FAST AND EPITHERMAL NUCLEAR CONSTANTS

$\nu^{235} = 2.42$	$RI_f^{235} = 280$ b
$\nu^{239} = 2.90$	$RI_f^{239} = 288$ b
$\nu^{241} = 2.98$	$RI_f^{241} = 573$ b
$\nu^{238} = 2.87$	$\bar{\sigma}_{f,fast}^{238} = 0.306$ b

$\xi\Sigma_s = 0.18\ cm^{-1}$

$\tau_{ef} = 84.0\ cm^2$

$\lambda_f = 11.36$ cm

Table 4.3

RESULTS FOR THE FAST NEUTRON YIELD, η_L

Lattice	η	$\Delta\eta_{epi}$	$\Delta\eta_{fast}$	η_L
19-rod cluster 9.33 in. pitch	1.3645	0.0191	0.0014	1.385
31-rod cluster 9.33 in. pitch	1.4032	0.0320	0.0023	1.438
31-rod cluster 12.12 in. pitch	1.4032	0.0081	0.0006	1.412

In terms of the volume fraction of fuel, v_i, which in this case is:

$$v_i = \lim_{n\to\infty} \frac{6\pi a^2 \sum_{n=1}^{n} n}{\frac{3}{4}\pi p_0^2 n^2} = \frac{4a^2}{p_0^2}, \tag{4.28}$$

the result for the inscribed case is:

$$S_f < \left[\frac{4\lambda_f v_i}{\pi a^2} + \frac{\sqrt{3v_i}}{a} + \frac{\pi}{4\lambda_f} \right] e^{-\frac{\pi\sqrt{3}a}{\lambda_f\sqrt{v_i}}} + \frac{3\sqrt{v_i}}{a} e^{-\frac{\pi a}{\lambda_f\sqrt{v_i}}}. \tag{4.29}$$

The numerical results obtainable from Eqs. 4.25 and 4.29 give the necessary bounds for the value of S_f. Actually the two expressions derived above would be identical in terms of the volume fraction fuel, if the first ring in the "inscribed" case were not treated separately. Thus the value of S_f to be used in Eq. 4.9 may be obtained by using the actual volume fraction of fuel v ($=2\ a^2/\sqrt{3}p^2$) in Eq. 4.25.

4.4 RESONANCE ESCAPE PROBABILITY

A simple equation can be derived to relate the resonance escape probability, p, to the epithermal absorption parameter, A_L, for an infinite uniform lattice.

Equation 2.6 for the epithermal absorption parameter A corresponds to the case of an isolated single fuel element in an epithermal neutron flux which is constant in lethargy and space. To obtain a corresponding parameter, A_L, for a reactor cell, it is necessary, strictly speaking, to consider the energy depletion of the slowing-down neutrons at successive resonances, the spatial non-uniformity of the epithermal flux across the cell, and the Dancoff effect which results from the shadowing

of a fuel element by its neighbor. A discussion of the relation between A_L and the measured fuel parameter A is taken up in the following subsection.

For one neutron slowing down in the moderator volume V_m of a unit cell of unit height, the averaged slowing-down density in the moderator is $1/V_m$. The total epithermal absorption at the single effective resonance energy per cm-sec in the lattice cell is A_L/V_m. Consequently, the probability that a source neutron escapes epithermal absorption is:

$$p = 1 - \frac{A_L}{V_m} \tag{4.30}$$

A more rigorous derivation of the above expression is given by Klahr (K4). Equation 4.37 may be generalized to the case of many resonance levels; in that case, the simple derivation of Eq. 4.31 with a single equivalent resonance is correct to at least second order terms in a Taylor's expansion.

Table 4.5 shows the results of the calculation of the resonance escape probability, p, for the cluster-fuelled lattices considered in this study.

4.4.1 Relation between A_L and A

The epithermal absorption parameter, A_L, in a lattice cell may be deduced from the measured value of A by correcting the latter to account for the following effects:

1. flux depletion of the slowing-down neutrons in energy space,
2. Dancoff effect,

3. spatial non-uniformity of the neutron slowing-down density across the cell.

The effect of the changes in the energy spectrum of the epithermal neutrons on A has been discussed to some extent in Section 2.5.5. An approximate estimate of the decrease in ERI, and the corresponding decrease in A, due to epithermal flux depletion can be made on the basis of an approximate expression derived in an earlier work by the author (S1).

The effect of adding fuel in a lattice cell is to deplete the epithermal flux. This in turn decreases the ERI for the lattice. It has been shown (S1), under certain assumptions, that the lattice ERI decreases linearly with increasing volume fraction of fuel (V_f/V_m). The correction term (ΔERI) which must be subtracted from the ERI_{SE} of a single fuel element is given by the recipe:

$$\Delta ERI \simeq \left[n \frac{N_R \lambda_{sm}}{2} (ERI_{SE})^2 \right] \frac{V_f}{V_m} \quad , \tag{4.31}$$

where N_R is the concentration in fuel of the resonance absorbing atoms, λ_{sm} is the scattering mean free path of epithermal neutrons in the moderator (3.73 cm), and the index n, whose value depends on the ratio "S/M" of the fuel element, is about 0.3 in the present case of 19 and 31 rod cluster (S/M≃0.1). Further since A is directly proportional to ERI (Eq. 2.6), the correction (ΔA) in A to account for the flux depletion is:

$$\frac{\Delta A}{A} \simeq \frac{n \lambda_{sm}}{2 V_m} (N_R V_f ERI_{SE}), \tag{4.32}$$

or on simplifying with the use of Eq. 2.6,

$$\frac{\Delta A}{A} \simeq \frac{n\xi}{2} \frac{A}{V_m} . \qquad (4.33)$$

Application of either of the above equations to the lattices of the present study shows that the non-1/E effect on A is 0.75% for the 19-rod cluster lattice of 9.33 in. pitch and the 31-rod cluster lattice of 12.12 in. pitch, and 1.5% for the 31-rod cluster lattice of 9.33 in. spacing. The effect is thus small compared to the uncertainty in the experimental determination of A, and can therefore be neglected.

The Dancoff effect also tends to decrease the ERI and consequently the value of A. It depends among other factors, upon the fuel size and the fuel spacing (a/λ_{sm}, p_0/λ_{sm}). An estimate of the Dancoff shadowing on a fuel element is provided by looking up tables (R1) for the Dancoff-Ginsberg factors for the effect of neighboring fuel elements; tabulated values may be used to correct the surface area (S) of the fuel element. The reduced effective surface area causes the values of the single-element ERI and A to decrease. For the lattices of the present study, these calculations confirm the well known fact that the Dancoff shadowing effect is very small in widely spaced, D_2O-moderated lattices. Thus the maximum shadowing occurs in the case of the 9.33 in. spacing, 19-rod cluster lattice, the effect on the ERI or A being about 2.5%. For the 31-rod cluster lattices of 9.33 in. and 12.12 in. spacings, this result is 1.25% and 0.5% respectively. These corrections are also smaller than the error in A measurements and these have not been included in calculations of the buckling (Section 4.6).

The spatial non-uniformity of the epithermal neutron slowing-down density $q_{epi}(r,\tau_r)$ becomes important in those lattices for which the condition:

$$\frac{4\pi^2\tau_r}{V_c} >> 1 \tag{4.34}$$

is not met. Thus in lattices with large cell areas, particularly the 12.12 in. spacing lattice in the present study, the density of epithermal neutrons at the fuel may be significantly greater than that at the boundary of the cell. Denoting the ratio of the average epithermal flux in the fuel to that in the moderator by β, it follows that:

$$A_L = A\,\beta \ . \tag{4.35}$$

The excess of β over unity then measures the nonuniformity of the spatial flux (G3).

A method for calculating the advantage factor β is presented in the following subsection.

4.4.2 Calculation of β

The advantage factor β is determined by solving the age equation:

$$\nabla^2 q_{epi}(r,\tau) = \frac{\partial}{\partial\tau} q_{epi}(r,\tau), \tag{4.36}$$

for the epithermal neutron distribution in the lattice cell (radius = b), produced by a uniform cylindrical source (radius = a, a<b) of fast neutrons. Since there is no net current of epithermal neutrons across the boundary of the cell,

$$\left(\frac{\partial}{\partial r} q_{epi}(r,\tau)\right)_{r=b} = 0 \tag{4.37}$$

The manner of solving Eq. 4.36 is similar to that in Section 2.3.4, except that now the cell boundary (r=b) replaces the tank boundary ($r=\tilde{R}$) and the boundary condition is different.

The slowing down density at position r due to a unit source of unit height distributed on a cylindrical surface at r = r' is denoted by $q_{epi}(r',r,\tau)$. Then, as in Section 2.3.4,

$$\bar{q} = \bar{u} + \bar{w} , \tag{4.38}$$

and the arbitrary constant of Eq. 2.48 is obtained from the condition that:

$$\left(\frac{\partial \bar{q}}{\partial r}\right)_{r=b} = 0. \tag{4.39}$$

As a result:

$$\bar{q}(r',r,s) = \frac{I_0(sr')}{2\pi I_1(sb)} \{K_1(sb)I_0(sr) + I_1(sb)K_0(sr)\} . \tag{4.40}$$

Using the Inversion Theorem (Eq. 2.51) and applying methods of Ref. C1, it follows that:

$$q_{epi}(r'r,\tau) = \frac{1}{\pi b^2}\left[1 + \sum_{n=2}^{\infty} \frac{J_0(\alpha_n r')J_0(\alpha_n r)}{J_0^2(\alpha_n b)} e^{-\alpha_n^2 \tau}\right] , \tag{4.41}$$

where α_n (n=2,3...) are the positive roots of

$$J_1(\alpha b) = 0 . \tag{4.42}$$

Since the source extends from r = 0 to r = a, Eq. 4.41 is integrated between these limited to give:

$$q_{epi}(r,\tau) = \frac{1}{\pi b^2}\left[1 + 2\sum_{n=2}^{\infty}\frac{J_1(\alpha_n a)J_0(\alpha_n r)}{\alpha_n a\, J_0^2(\alpha_n b)}\, e^{-\alpha_n^2\tau}\right] . \tag{4.43}$$

If $\bar{q}_{epi}(x,\tau)$ denotes the average of $q_{epi}(r,\tau)$ over the cylinder of radius x, the definition of β is:

$$\beta(\tau) = \frac{\bar{q}_{epi}(a,\tau)}{\bar{q}_{epi}(b,\tau)} . \tag{4.44}$$

In this expression for β, the fuel has been replaced by the moderator for the sake of convenience and for taking into partial account the inelastic scattering in the fuel. When Eq. 4.43 is integrated over the limits: r = 0 to r = a, and r = 0 to r = b, the result is

$$\bar{q}_{epi}(a,\tau) = \frac{1}{\pi b^2}\left[1 + 4\sum_{n=2}^{\infty}\frac{J_1^2(\alpha_n a)}{(\alpha_n a)^2\, J_0^2(\alpha_n b)}\, e^{-\alpha_n^2\tau}\right], \tag{4.45}$$

and,

$$\bar{q}_{epi}(b,\tau) = \frac{1}{\pi b^2} ; \tag{4.46}$$

hence

$$\beta(\tau) = \left[1 + 4\sum_{n=2}^{\infty}\frac{J_1^2(\alpha_n a)}{(\alpha_n a)^2\, J_0^2(\alpha_n b)}\, e^{-\alpha_n^2\tau}\right] \tag{4.47}$$

The spatial distribution of slowing down neutrons is taken to be the weighted sum of two Gaussians (characterized by τ_1, τ_2). Thus the final value of β is evaluated from $\beta_1(\tau_1)$ and $\beta_2(\tau_2)$, and

$$\beta = B_1\beta_1 + B_2\beta_2 . \tag{4.48}$$

The values (G7) used for the fission-to-resonance ages τ_1 and τ_2 are 126.5 cm^2 and 40.5 cm^2, and those for the corresponding weighting factors B_1 and B_2 are 0.56 and 0.44. These factors are based upon measurements of slowing-down distributions at the indium resonance (G6), and the assumption that the single effective resonance energy (D2) is 30 ev.

The summation which appears in Eq. 4.47 converges very rapidly; only the first three terms are significant for the cases considered. The values of β calculated and used in the present study are shown in Table 4.4. These are compared with results, to be denoted by β_G obtained by using the same values for B's and τ's in a method given by Graves et al. (G7). This latter method does not take into consideration the effect of source size. Thus β_G compare very well with β_{line} calculated from Eqs. 4.48 and 4.49 in the limit of zero source size (a = 0).

4.5 INFINITE MEDIUM MULTIPLICATION FACTOR

The neutron balance in the thermal reactor lattices is described in terms of the conventional neutron cycle and the familiar four-factor formula for the neutron multiplication factor. However, the manner in which the heterogeneous fuel parameters Γ, η and A are defined, necessitates slight adjustments in the interpretation of the conventional four factors to which these parameters are directly related. Thus, f_Γ differs from the conventional definition of the thermal utilization in using the term "fuel" to include cladding, coolant and all other materials within the outermost boundary of the

Table 4.4

VALUES OF THE ADVANTAGE FACTOR β

Lattice	β	β_{line}	β_G
19-rod cluster 9.33 in. pitch	1.040	1.058	1.06
31-rod cluster 9.33 in. pitch	1.031	1.058	1.06
31-rod cluster 12.12 in. pitch	1.193	1.284	1.285

Table 4.5

RESULTS FOR RESONANCE ESCAPE PROBABILITY, p

Lattice	V_m, cm^2	A, cm^2	β	A_L, cm^2	p
19-rod cluster 9.33 in. pitch	436.7	58.0	1.040	60.32	0.8750
31-rod cluster 9.33 in. pitch	405.1	81.5	1.031	84.03	0.7926
31-rod cluster 12.12 in. pitch	739.3	81.5	1.193	97.25	0.8684

cluster. The factor η_L also differs from its conventional counterpart η': it accounts for the net fast neutron yield in the lattice due to all fissions - thermal, epithermal and fast, in all the fissionable isotopes per thermal neutron absorbed in the composite cluster fuel element. Thus,

$$f_\Gamma \ \eta_L = (f \eta \varepsilon) \text{ conventional} . \tag{4.49}$$

The expression for the infinite medium multiplication factor k_∞ may then be written as:

$$k_\infty = f_\Gamma \eta_L p . \tag{4.50}$$

4.6 MATERIAL BUCKLING B_m^2

The material buckling of the uniform lattices considered in this work is obtained from the infinite medium multiplication factor (k_∞), and the diffusion and slowing down areas (L^2, τ_L) of the lattice. The following modified one-group, two-group and age-diffusion equations have been used:

$$B_m^2 = \frac{(k_\infty - 1) + \ell n\, k_\infty}{2(L^2 + \tau_L)} , \text{ (modified one-group)} \tag{4.51}$$

$$B_m^2 = -\frac{1}{2}\left[\left(\frac{1}{\tau_L} + \frac{1}{L^2}\right)\right] + \left[\frac{1}{4}\left(\frac{1}{\tau_L} + \frac{1}{L^2}\right)^2 + \frac{k_\infty - 1}{L^2 \tau_L}\right]^{1/2} , \text{ (Two-group)} \tag{4.52}$$

$$k_\infty e^{-B_m^2 \tau_L} - (L^2 B_m^2 + 1) = 0. \quad \text{(Age-diffusion)} \tag{4.53}$$

In the above equations, the value of L^2 for the lattices is calculated from:

$$L^2 \simeq L_0^2(1-f_\Gamma). \tag{4.54}$$

which is a good approximation for loosely packed lattices. The neutron age, τ_L, is also obtained, from a simple recipe (D2):

$$\tau_L = \left(1 - \frac{V_{A\ell}}{V_c} - \frac{\varepsilon_n}{2}\frac{V_f}{V_c}\right)^{-2}, \tag{4.55}$$

where V_f is the volume of the fuel element, $V_{A\ell}$ is the volume of the cladding material (aluminum) within the fuel, and ε_n is the ratio of the concentration of fuel atoms (U, Pu) in the fuel element to that in natural uranium. The value of τ for the moderator (119 cm^2) is based on studies by Wade (W1) which indicate that the age decreases linearly by 4 cm^2 as the H_2O contamination in the moderator increases to 1 mole %. Values of L^2 and τ_L for the three cluster lattices are given in Table 4.6.

The determination of various reactor physics parameters and the calculation of the material bucklings therefrom, are carried out by a computer routine, HECKLE. All three expressions, Eq. 4.51 through Eq. 4.53, give values of material bucklings which agree with one another to within 2%. This report therefore presents only the age-diffusion results (Eq. 4.53).

The first application of the single-element method is made to the case of uniform lattices of 1.01 inch diameter natural uranium rods. This is important since the natural uranium single-rod has been used as a "reference element" for η and A measurements on the clusters.

Table 4.6

DIFFUSION AND SLOWING DOWN AREAS

Lattice	L^2 cm^2	τ_L cm^2
19-rod cluster 9.33 in. pitch	208.10	124.1
31-rod cluster 9.33 in. pitch	137.92	128.5
31-rod cluster 12.12 in. pitch	269.05	124.8

The curve of Fig. 4.3 shows the values of the buckling of 1.01 in. diameter natural uranium rod lattices calculated over a range of lattice spacings on the basis of the simple model outlined in this chapter, and taking for the values for the heterogeneous parameters η and A their "reference" values, 1.375 and 20.39 cm^2 (Appendices E, F) respectively. This result from the single-element parameters is compared with the extensive experimental studies on the same fuel rod in critical and exponential lattices. The experimental results presented in the graph of Fig. 4.3 are drawn (P1) from experiments at several laboratories: North American Aviation (exponential), Savannah River (critical and exponential), M.I.T. (exponential), Zebra (Swedish, exponential), and Aquilon (French, critical). The agreement evident in this figure provides an excellent check on the use of the 1.01 in. diameter natural uranium rod as a "reference" fuel, and on the single-element model.

The more important test of the methods proposed in this work lies in their application to the lattices composed of the tight clusters of 19 and 31-rods (Fig. 1.1) investigated as "single-elements", in the present study. As is pointed out earlier, the plutonium containing fuel within these clusters simulates natural UO_2 burned to 5000 MWD/ton. The clusters are typical of fuel designs for the pressure-tube type of D_2O-moderated power reactors. Table 4.7 gives values of the reactor lattice parameters f_Γ, η_L, p and B_m^2 calculated for 9.33 in. spacing lattice of the 19-rod clusters and 9.33 in. and 12.12 in. spacing lattices of the 31-rod clusters. The values taken for the heterogeneous fuel parameters Γ, η and A of these clusters

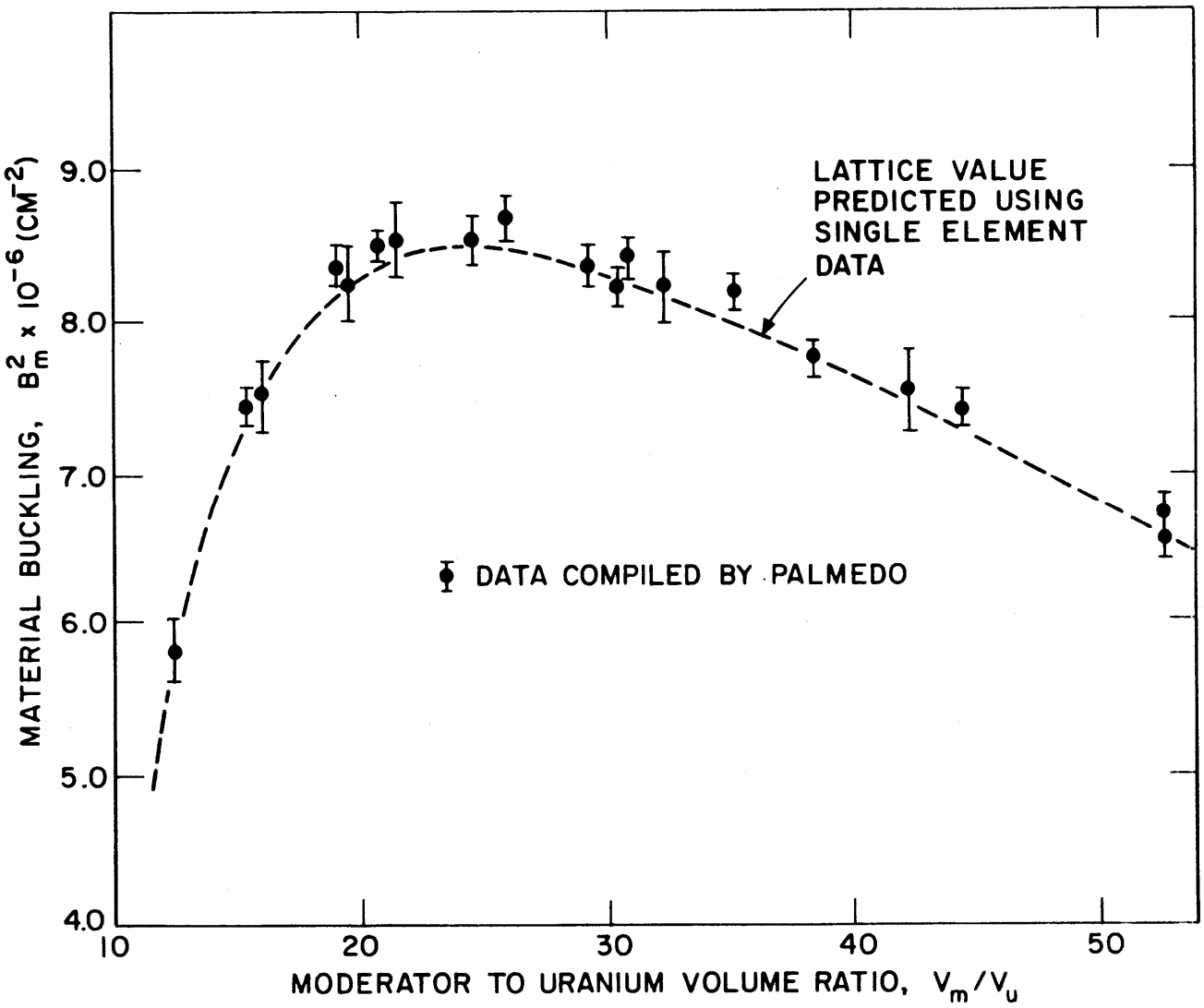

FIG. 4.3 BUCKLING OF 1.0 IN. DIAMETER, NATURAL URANIUM RODS IN D_2O

are those measured in single-element experiments described in the previous chapter. Also tabulated for comparison are results of the studies (B1) at Savannah River Laboratory (SRL) carried out as a part of the USAEC-AECL Cooperative Program. Each experimental result of SRL is the weighted average of substitution buckling measurements analyzed by: two-group, two region diffusion theory calculation; the successive substitution method; and by the heterogeneous reactor code HERESY-I. The SRL-calculations are made with the HAMMER code (S3) - a one-dimensional, multigroup (54 fast, 30 thermal), integral-transport, lattice-cell calculation.

The comparison of results obtained in the SRL and the M.I.T. single element studies is to be made in the light of slight differences in the definition of lattice parameters. These are referred to in Section 4.2. The slight differences in the cluster cladding have been noted earlier in Table 3.2. The effect of including epithermal neutron absorptions in the definition of neutron age causes the SRL values for τ_L to be lower by about 10 cm^2 than those used in the present study (Table 4.6). This use of somewhat higher values of τ_L in the single-element calculations is however almost exactly counterbalanced by the somewhat lower values (K1, K4) of L^2 resulting from the use of the approximate Eq. 4.54.

The accuracy of the single-element results and the general "state-of-the-art" of buckling calculations are discussed in the next section.

TABLE 4.7

COMPARISON OF SINGLE ELEMENT AND LATTICE RESULTS

FOR D_2O MODERATED AND COOLED, PLUTONIUM CONTAINING FUEL CLUSTERS

TYPE OF RESULT	η_L	p	f	k_∞	B_m^2, cm^{-2} $\times 10^6$
A. 19-ROD CLUSTER 9.33 in. Lattice Spacing					
(1) MIT Single Element	1.385	0.8750	0.9793	1.1868	540 ± 45
(2) SRL Calculation	1.407	0.8556	0.961	1.1566	484
(3) SRL Lattice Expt.	–	–	–	–	524 ± 15
B. 31-ROD CLUSTER 9.33 in. Lattice Spacing					
(1) MIT Single Element	1.438	0.7926	0.9863	1.1241	458 ± 43
(2) SRL Calculation	1.451	0.79	0.9621	1.1028	425
(3) SRL Lattice Expt.	–	–	–	–	501 ± 15
C. 31-ROD CLUSTER 12.12 in. Lattice Spacing					
(1) MIT Single Element	1.412	0.8684	0.9733	1.1937	472 ± 44
(2) SRL Calculation	1.419	0.8486	0.9513	1.1458	416
(3) SRL Lattice Expt.	–	–	–	–	429 ± 20

4.7 ACCURACY OF VALUES OF MATERIAL BUCKLING

The values of the buckling obtained in this study are a result of a combination of the single-element experiments, the heterogeneous theory, and the simple lattice calculations. The uncertainty associated with values of the material buckling calculated by the single element method is best obtained from the direct evaluation of the effect which the experimental errors have on the final buckling results. Figure 4.4 shows the sensitivity of the calculated values to the variation in the measured experimental parameters X, γ, R and F. These studies have been made through repeated calculations of B_m^2 for systematic variations in each of the experimental parameters. The figure aids in estimating the uncertainty in B_m^2 due to typical values of experimental errors (Table 3.4): that is, approximately, 1.5% in X, 0.5% in γ, 1% in R, and 2% in F. The result of compounding the separate uncertainties is a net error in the neighborhood of 8% for the values of buckling from the single-element method.

The extensive studies (B1, F4) of the Savannah River Laboratory (SRL) and the Atomic Energy of Canada Ltd. (AECL), done under the USAEC-AECL Cooperative Program, provide a good ground to assess the accuracy of the best present-day methods to determine the values of heterogeneous lattice buckling. The two studies cited above, put together, deal with 19 and 31-rod cluster fuelled lattices which involve five fuel rod-types, four coolants (D_2O, H_2O, HB-40 and air) and three lattice spacings. However, the work reported by AECL does not include theoretical cell calculations such as those done at SRL. Furthermore, there is very limited overlap between works of the two

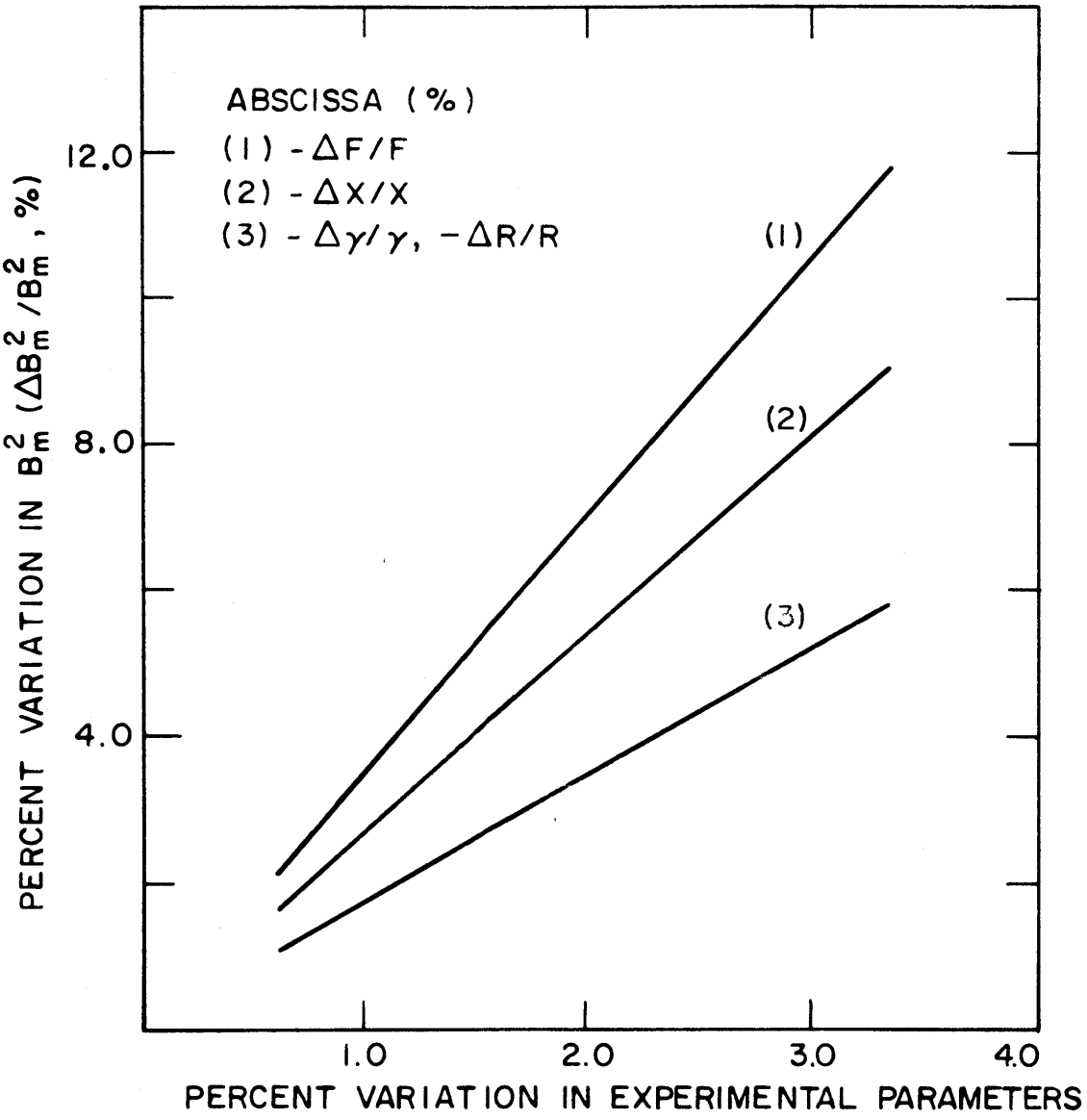

FIG. 4.4 SENSITIVITY OF B_m^2

laboratories. Thus, most of the AECL study pertains only to the 31-rod clusters with H_2O and air as coolants. On the other hand, the SRL study does not include H_2O-coolant. There are twelve lattices for which the SRL experiments and calculations, and the AECL experiments can all be compared.

In general, the experimental results have a good accuracy, the error being less than 5% in most cases. The quoted errors on AECL buckling results (~1%) tend to be unrealistically small; thus the corresponding SRL results for several of the twelve "common" cases fall far out of the uncertainty bounds shown by AECL. As for the accuracy of calculations, Baumann et al. (SRL) report the magnitude by which each measurement differs from the HAMMER-calculated value. Though the agreement between experiment and the calculations appears to be good for some of the 31-rod cluster fuelled lattices, errors on the order of 10% and more are quite common. It is interesting to note that when the experimental and calculated results of SRL are compared with the experimental results of AECL for the "common" lattices, only three out of these twelve cases show an agreement within 10%. In the case of the 9.33 in. spacing 31-rod cluster SRL lattice, which is also of direct interest to the present study, the discrepancy between the calculated and experimental values of buckling (Table 4.7) is in excess of 15%.

The comparable accuracy of the single element method in predicting the material buckling of lattices is seen from the comparison in Table 4.7. Thus the single-element results show excellent agreement with results of SRL experiments: the difference in the values of buckling being in the neighborhood of 5% for two of the lattices.

For the 12.12 in. spacing 31-rod cluster lattice, this discrepancy is about 10%.

Chapter 5

CONCLUSION

5.1 SUMMARY

The purpose of the present study has been the development of methods for the direct experimental determination of the heterogeneous fuel parameters Γ, η and A, based on the use of a single fuel element. This objective appears to have been accomplished satisfactorily. Three single-fuel assemblies have been investigated: a 1.01 in. diameter natural uranium fuel rod for use as a "reference element", and tight-clusters of 19 and 31-rods of UO_2-PuO_2 fuel which simulate natural uranium "burned" to 5000 MWD/ton. The cluster design is typical of those used in pressure-tube designs for D_2O moderated power reactors.

The test fuel assembly is placed at the center of a subcritical tank of heavy water moderator fed by thermal neutrons from the bottom of the tank. The theoretical formulation developed in Chapter 2 related the heterogeneous fuel parameters to four experimental quantities X, γ, R and F which are measured in the moderator surrounding the single fuel element. The experimental setup is very simple. All the necessary measurements are made outside the fuel element, thus obviating the need to cut into the radioactive fuel assembly. These single-element measurements were discussed in Chapter 3. The uncertainty associated with the measured heterogeneous parameters Γ, η and A is in the neighborhood of 5%, 3% and 4% respectively. Some suggested improvements in the experimental techniques are discussed in the following section.

Values of the heterogeneous fuel parameters Γ, η, A obtained from the experiments on the UO_2-PuO_2 fuel clusters and the natural uranium rod were tested in Chapter 4. Simple expressions relate Γ, η and A for a fuel element to the thermal utilization, fast neutron yield, resonance escape probability and multiplication constant of an infinite uniform lattice composed of the fuel element in question. Values of the material buckling of the lattices were derived from these reactor physics parameters through the use of age-diffusion theory. The accuracy of the values of the buckling obtained in this manner is estimated to be about 8%. The values of the buckling for uniform lattices of the natural uranium reference rod were compared (Fig. 4.4) with a compilation of experimental values for lattices of the same fuel rod obtained at several laboratories. The corresponding results for the 19 and 31-rod cluster-fuelled lattices were compared (Table 4.7) with numerical and experimental results obtained at the Savannah River Laboratory. The agreement between the results obtained in the present study and those obtained from conventional experimental and theoretical techniques demonstrates the feasibility and adequacy of the single-element method.

5.2 SUGGESTIONS FOR FUTURE WORK

The single-element method has been tested in this study by its application to uniform lattices. Future work should involve the determination of heterogeneous parameters for different fuel clusters and control elements which might be present in practical core configurations. These parameters should then be used with a "proven"

computer code based on the heterogeneous reactor theory, such as HERESY, to calculate reactor physics characteristics of nonuniform lattices. Problems like the absorption patterns in spiked lattices and control rod placement effects could also be investigated. The solutions to such problems are difficult or impossible by other methods.

In addition, an attempt should be made to find out how the single-element method could best be applied to study the change in physics characteristics of a reactor core due to fuel burn-up. Towards this end, it may be possible to obtain theoretical curves describing the change in heterogeneous fuel parameters due to fuel burn-up. These could then be normalized by experimental studies on "reference" fuel assemblies which simulate different degrees of burn-up.

Another interesting problem is the optimization of the cluster with respect to its internal arrangement. The single-element method should make it easier to obtain the heterogeneous parameters for different cluster-types at a very low cost. These single-element parameters can then be used to evaluate the physics characteristics of lattices made up of the particular fuel cluster. It would also be useful to find out the spacing of rods in a cluster ("looseness") at which the single-element model begins to break down.

There is evidence (H2) that the single-element method could be extended to H_2O-moderated reactor lattices. Experimental data on integral parameters of these lattices have been found to be interpretable in terms of heterogeneous reactor theory. The behavior of Γ, η and A calculated from these data does not appear to be any more

complex than that which has already been treated successfully in D_2O lattices. Therefore, if the single-element parameters can be measured in H_2O moderator, the necessary analytic formalism to characterize complete lattices of the subject fuel, can be developed. Numerical experiments to study the feasibility of single-element experiments in this case, show that measurements of η and A in H_2O should be no harder than in D_2O; but, owing to the greater importance of transport effects, additional theoretical work is needed to obtain Γ.

In parallel with the above efforts to widen the applicability of the single-element method, effort could also be directed towards improving the experimental techniques involved. Some specific suggestions to this effect have been discussed in earlier chapters.

The measurement of X could be accomplished by the use of short lengths of gold wire instead of foils as detectors. With the axis of the wires oriented parallel to the fuel axis, these will approximate point detectors. The number of flux detectors could also be increased simply by staggering the foil centers along different radii. Alternatively, a radial gold wire could be used. A remotely maneuverable fission-chamber was developed at the start of this experimental study to be used as a flux scanner. Though the effort was dropped owing to trouble with the fission-chamber, this technique could be applied successfully to the determination of X. It enables an on-the-spot evaluation of X, which would be more convenient than the tedious foil-irradiation and counting procedures.

Considerable additional work may be done to improve the measurement of A. The difficulties in the use of the ANISN computer code

for the present application have been indicated in Section 2.5.3. A good alternative procedure would be to generate the curves of f_c versus A experimentally: the epithermal flux ratio would then be measured for "reference" fuel elements with different known values of A, and which have the same diameter as the test fuel assembly. No normalization of data would then be necessary. A convenient reference fuel element could be an aluminum tube of the desired diameter packed with a dilute mixture of the fine UO_2-powder in lead oxide. The uniformity of packing could be verified by irradiating U-238 foils along a traverse through the tube and checking for the uniformity of the epithermal flux across the cross-section of the reference fuel. Since the concentration UO_2 in the tube is accurately known, the reference value of A can be easily calculated from the standard empirical equation for resonance integral (H3). The different values of A in the range of interest could then be obtained by varying the concentration of UO_2 within this tube. The use of such a reference fuel element with its diameter equal to that of the test element should also lead to improved accuracy of the η-measurements.

The use in the lattice calculations of the value of A measured in a single-element experiment assumes that A is insensitive to spectral differences (Section 2.5.5). Ideally this should be true only in the case of a single narrow resonance for epithermal neutron absorption. Evidence to support the assumption has been offered only for the case of the 1.01 in. diameter natural uranium rod. The general effect of spectral differences on A should be examined in greater detail. In the event that this effect turns out to be

important, measurement of A may have to be carried out in a 1/E-flux. One way to accomplish this in the framework of the single-element model would be to surround the test-fuel by a fuel ring of suitable diameter which would create a 1/E spectrum in the central region where the test element is placed. Cadmium rods clad in aluminum placed inside the ring (at a distance from the test element) can serve to deplete thermal neutrons and reduce the thermal U-238 capture in the fuel element. The resonance absorption parameter A is then directly related to the ratio of the neptunium-239 activity (in the case of U-238) of the test fuel assembly to that of an infintely dilute U-238 foil irradiated in place of the test fuel. The neptunium activities could be measured by Ge(li)-γ ray spectroscopy. A slight modification of this experimental set up can also lead to the direct measurement of the fast neutrons emitted per cm-sec by the test fuel assembly per epithermal neutron absorbed. This is related to $\Delta\eta_{epi}$ of Eq.(4.10) which accounts for most of the correction to η required to calculate η_L.

It was pointed out in Chapter 2 that, theoretically, only two of the three measurements X, $\bar{\gamma}$ and R are necessary for the determination of Γ and η. Since the composite uncertainty in determining Γ or η is smaller with fewer experimental parameters to measure, it would be advantageous, as well as convenient, to eliminate any extra measurement. The theoretical bases for the different ways of achieving this goal have been indicated in Section 2.4.3.

The heterogeneous fuel parameters Γ, η and A can also be obtained by more variations of the foil activation technique. These techniques also require only a single fuel element and involve measurements which

can be made outside the fuel. Thus, Γ of a test element could be obtained by measuring the ratio (ϕ_1/ϕ_2) of the thermal neutron activities at two radial positions in the moderator surrounding the fuel; the value of Γ is then given by a suitably normalized curve which describes the variation of ϕ_1/ϕ_2 with Γ. The parameter η could be evaluated by irradiating a pair of indium foils, with cadmium between them, on the fuel surface; the fast neutron yield parameter is then related to the ratio of the fast neutron induced activity of In-115 (isomeric state) to the difference of the thermal neutron activities of In-113 in the two foils. Likewise, A could be measured by irradiating a sandwich of cadmium covered depleted U-238 foils on the fuel surface; A is then proportional to the ratio of the difference of the neptunium-239 activities in the two foils to the sum of these activities. All these methods make use of an activity ratio which is normalized by the use of a "reference" fuel assembly. The above methods may not necessarily be more accurate than those discussed in this report, but are indicated here because they have not been investigated previously.

Appendix A

PERTURBATION IN RADIAL BUCKLING

The thermal neutron flux distribution in the cylindrical tank containing only the moderator has a J_0-shape. The unperturbed radial buckling, α_0^2, of the moderator tank is obtained from the condition that the flux (fundamental mode) vanishes at the outer boundary ($r = \tilde{R}$) of the tank. Thus,

$$\alpha_0 = \frac{\nu_0}{\tilde{R}} , \tag{A.1}$$

where ν_0 (= 2.405) is the argument of J_0 corresponding to its first zero. Insertion of a fuel element in the center of the moderator increases the radial buckling to α (increased radial leakage). Useful approximate expressions are now derived for the perturbation, $\Delta\alpha$, in radial buckling;

$$\Delta\alpha = \alpha - \alpha_0 . \tag{A.2}$$

One such expression is obtained by simplifying Eq. 2.68. For elements of small size,

$$\begin{aligned} &J_0(\alpha a) \simeq 1, \; J_1(\alpha a) \simeq \frac{\alpha a}{2} , \\ &Y_0(\alpha a) \simeq \frac{2}{\pi} \ell n(\alpha a), \; Y_1(\alpha a) \simeq - \frac{2}{\pi \alpha a} . \end{aligned} \tag{A.3}$$

Equation 2.68 then reduces to:

$$\eta = \frac{\left(\frac{J_0(\alpha\tilde{R})}{Y_0(\alpha\tilde{R})} - \frac{J_1(\alpha X)}{Y_1(\alpha X)} \right)}{\left(\frac{J_0(\alpha\tilde{R})}{Y_0(\alpha\tilde{R})} I_1 - \frac{J_0(\alpha X)}{Y_1(\alpha X)} \right)}, \tag{A.4}$$

where I_1 is given by Eq. 2.69.1. Expanding $J_0(\alpha\tilde{R})$ in a Taylor Series and making the following substitution:

$$J_0(\alpha\tilde{R}) \simeq -R\Delta\alpha\, J_1(\nu_0) = -\frac{\Delta\alpha}{\alpha_0}\, \nu_0 J_1(\nu_0), \tag{A.5}$$

Equation A.4 yields:

$$\frac{\Delta\alpha}{\alpha_0} \simeq \frac{Y_0(\alpha\tilde{R})}{J_1(\nu_0)} \frac{J_1(\alpha X)}{Y_1(\alpha X)} \frac{(\eta+1)}{(\eta I_1 - 1)}. \tag{A.6}$$

The right hand side of the above expression involves α, which is here an unknown quantity unless it is measured (Section 3.5). Only a few iterations are, however, necessary to calculate $\Delta\alpha$.

Another useful approximation for $\Delta\alpha$ which does not involve X is obtained more directly. Simplifying Eq. 2.26 with the value of S_r from Eq. 2.11, and that of L from Eq. 2.19, it follows that

$$\left(1 - \frac{J_0(\alpha\tilde{R})}{Y_0(\alpha\tilde{R})} \frac{Y_0(\alpha a) + 2\pi D\, \Gamma\, \alpha a\, Y_1(\alpha a)}{J_0(\alpha a) + 2\pi D\, \Gamma\, \alpha a\, J_1(\alpha a)} \right) = \eta \frac{\left(I_J(a,\tilde{R}) - \frac{J_0(\alpha\tilde{R})}{Y_0(\alpha\tilde{R})} I_Y(a,\tilde{R}) \right)}{\left(J_0(\alpha a) + 2\pi D\, \Gamma\, \alpha a\, J_1(\alpha a) \right)}. \tag{A.7}$$

Again, making the substitution from Eq. A.5 in the left-hand side of Eq. A.7, the result is

$$\frac{\Delta\alpha}{\alpha_0} = \frac{Y_o(\alpha\tilde{R})}{J_1(\nu_0)} \frac{\eta I_2 - \{J_0(\alpha a) + 2\pi D\, \Gamma\, \alpha a\, J_1(\alpha a)\}}{\nu_0\{Y_0(\alpha a) + 2\pi D\, \Gamma\, \alpha a\, Y_1(\alpha a)\}}, \tag{A.8}$$

where

$$I_2 = \left(I_J(a,\tilde{R}) - \frac{J_0(\alpha\tilde{R})}{Y_0(\alpha\tilde{R})} I_Y(a,\tilde{R})\right). \tag{2.69.2}$$

Equation A.8 can be simplified by making several assumptions. First, it can be shown that when the line-source, infinite-medium age kernel (Eq. 2.56) is used for $q_r(r,\tau)$ in the integral I_J, and the integration (G5) approximated to range from 0 to ∞, the value of I_J is very close to unity. Further, if the contribution of the second term in I_2 is neglected, $I_2 \simeq 1$. Then for elements of small size (Eqs. A.3), it follows that:

$$\frac{\Delta\alpha}{\alpha_0} \simeq \frac{Y_0(\alpha\tilde{R})}{J_1(\nu_0)} \frac{(\eta-1)}{\nu_0\{Y_0(\alpha a) - 4D\Gamma\}}, \tag{A.9}$$

Again, only a few iterations on α are necessary to obtain $\Delta\alpha$.

In the case of the perturbation due to the 1.01 in. diameter natural uranium rod, the calculated value for $\Delta\alpha$ agrees with the experimental results to within 5%.

Appendix B

UNCOLLIDED FLUX KERNEL

The uncollided flux, $\phi_f(r)$, at a point P which is a distance r from an infinitely long line source of fast neutrons of unit intensity is approximately given by

$$\phi_f(r) = \phi_0(r)\, e^{-\bar{\ell}/\lambda_f}, \tag{B.1}$$

where $\phi_0(r)$ is the value of $\phi_f(r)$ in a fully transparent medium ($\lambda_f = \infty$), and

$\bar{\ell}$ is the mean chord length of uncollided fast neutrons inside a transparent cylinder of radius r.

$\phi_0(r)$ is obtained by summing the contribution from infinitesimal source elements of length $d\ell$. If the direction of the normal to the element $d\ell$ subtends an angle θ with the line joining the element to the point P, then it follows that

$$d\ell = r\sec^2\theta\, d\theta \tag{B.2}$$

and the contribution of the element $d\ell$ to the uncollided flux at point P is given by

$$\Delta\phi_0 = \frac{d\ell}{4\pi(r\sec\theta)^2} = \frac{d\theta}{4\pi r}. \tag{B.3}$$

Hence,

$$\phi_0(r) = \int_{-\pi/2}^{\pi/2} \frac{d\theta}{4\pi r} = \frac{1}{4r} \tag{B.4}$$

The mean chord length, $\bar{\ell}$, is obtained by expressing the flux, $\phi_0(r)$ as the total number of chord lengths per cm^3-sec. If $d\bar{\ell}$ is the differential chord length of fast neutrons in a cylindrical shell of thickness dr at the point P, then $\phi_0(r)$ may be written as

$$\phi_0(r) = \frac{d\bar{\ell}}{2\pi r dr} . \tag{B.5}$$

Then from Eqs. B.4 and B.5, it follows that

$$d\bar{\ell} = \frac{\pi}{2} dr, \tag{B.6}$$

and integrating the last equation gives

$$\bar{\ell} = \frac{\pi r}{2} . \tag{B.7}$$

The required flux of uncollided neutrons is then given by the substitution of Eqs. B.4 and B.7 in Eq. B.1. This result is

$$\phi_f(r) = \frac{1}{4r} e^{-\frac{\pi}{2}\frac{r}{\lambda_f}} \tag{B.8}$$

The last equation has been compared with experimental and numerical data by Higgins (H5).

Appendix C

CORRECTION OF DETECTOR RESONANCE INTEGRALS

In the derivation of the epithermal flux at a certain neutron energy from the activity of a resonance foil detector irradiated on the fuel surface (Section 3.7.3), it is necessary to correct the infinite-dilution resonance integral of the detector for the $1/\tau(u)$ flux spectrum at the fuel element. The necessary correction factor is obtained in this appendix.

Under the assumptions stated in Section 2.5.1, the slowing-down density of neutrons of age τ at the fuel surface is

$$q(\tau) = \frac{1}{4\pi\tau} \simeq \frac{1}{4\pi} \frac{\xi\Sigma_t}{D} \frac{1}{u} \tag{C.1}$$

Since the age (τ_1) of neutrons after one collision is approximately given by

$$\tau_1 \simeq \frac{D}{\xi\Sigma_t} \quad \xi \simeq \frac{D}{\Sigma_t}, \tag{C.2}$$

it follows that

$$q_1(\tau_1) \simeq \frac{1}{4\pi} \frac{\Sigma_t}{D}. \tag{C.3}$$

Hence the probability that a neutron will slow down to age τ at the fuel surface is equal to:

$$\frac{q(\tau)}{q_1(\tau_1)} \simeq \frac{\xi}{u} \tag{C.4}$$

The resonance integral of the foil-detector irradiated on the fuel surface should be weighted with the probability derived in the last equation. Thus

$$RI_{1/\tau} = \int_{\xi}^{u_{cd}} \sigma_a(u) \frac{\xi}{u} du, \tag{C.5}$$

where u_{cd} is the lethargy of neutrons at the cadmium resonance energy (0.4 ev). The resonance integral is the sum of the contributions of 1/v-absorption and resonance absorption in the detector material. The 1/v-part of the absorption in the present case may be estimated with the following substitution for $\sigma_a(u)$:

$$\sigma_a = \sigma_0 \sqrt{\frac{E_0}{E}} = \sigma_0 \sqrt{\frac{E_0}{E^*}}\ e^{u/2}, \tag{C.6}$$

where σ_0 and E_0 correspond to the absorption cross-section and neutron energy at 2200 m/s, and

E^* is such that $u = \ln(E^*/E)$.

Substitution for σ_a in Eq. C.5 gives

$$RI_{1/\tau}(1/v\text{-part}) = \sigma_0 \sqrt{\frac{E_0}{E^*}}\ \xi \left[E_1\left(\frac{u_{cd}}{2}\right) - E_1\left(\frac{\xi}{2}\right)\right], \tag{C.7}$$

where

$$E_1(x) = \int_{-\infty}^{x} \frac{e^t}{t}\ dt \tag{C.8}$$

The numerical value of the right-hand side of Eq. C.7 is obtained by substituting for the values of the constants ($u_{cd} = 17$, $\xi = 0.51$). The result is

$$RI_{1/\tau}\ (1/v\text{-part}) \simeq 2 \times 10^{-4} \sigma_0. \tag{C.9}$$

The 1/v-contribution calculated above is negligible compared to the contribution of the resonance absorption; consequently,

$$RI_{1/\tau} \simeq \frac{\xi}{u_r} \int_{\text{resonance}} \sigma_a(u)\, du, \tag{C.10}$$

where u_r is the lethargy of neutrons at the resonance energy of the detector. For a large value of resonance cross-section of the detector (RI/σ_0, large),

$$RI_{1/\tau} \simeq \frac{\xi}{u_r} RI \tag{C.11}$$

The above equation explains why the resonance integrals of gold-197 and molybdenum-98 are weighted with the value of their inverse resonance lethargy ($1/u_r$) in Section 3.7.3.

Appendix D

SAMPLE DATA

Table D.1 shows the radial distribution of corrected gold foil activities measured in a typical experiment on each of the three fuel elements investigated in this study. The value of X for each radial traverse is obtained by curve-fitting the measured activities to Eq. 3.2. Values of X are tabulated in Table D.2.

Typical values of the corrected gold foil activities along axial traverses and the value of γ^2 corresponding to the best curve-fit of each set of data, are given, respectively, in Tables D.3 and D.4.

Tables D.5 and D.6 list the results, respectively, of measurements for R and F. Further details regarding these are to be found in Refs. L9 and M2.

Table D.1

TYPICAL GOLD FOIL ACTIVITIES FOR

RADIAL TRAVERSES

Nat. Uranium Rod		19-Rod Cluster		31-Rod Cluster	
Radial Distance (cm)	Corrected Activity per mgm	Radial Distance (cm)	Corrected Activity per mgm	Radial Distance (cm)	Corrected Activity per mgm
6.41	3320	9.24	2967	10.15	2836
7.05	3340	9.87	2980	10.79	2855
7.68	3369	10.51	3029	11.42	2881
8.32	3368	11.14	3030	12.06	2881
8.95	3371	11.78	3074	12.69	2883
9.59	3432	12.41	3088	13.32	2917
10.22	3435	13.05	3073	13.96	2981
10.86	3389	13.68	3081	14.59	2885
11.49	3380	14.31	3104	15.23	2919
12.13	3385	14.95	3073	15.86	2953
12.76	3326	15.59	3030	16.50	2919
13.40	3304	16.22	3047	17.13	2903
14.03	3322	16.86	3075	17.77	2896
14.67	3293	17.49	3027	18.40	2816

Table D.2

VALUES OF X (CM)

Nat. Uranium Rod	19-Rod Cluster	31-Rod Cluster
9.574	13.396	14.411
9.557	12.482	15.366
9.542	13.282	14.192
9.84	12.967	14.587
10.05	13.337*	15.263*
9.673	13.08*	15.666*
	13.03*	13.895*

* Cluster rotated through 30°

Table D.3

TYPICAL CORRECTED GOLD FOIL

ACTIVITIES[1] FOR AXIAL TRAVERSES

Axial Distance[2] (cm)	Nat. Uranium Rod	19-Rod Cluster	31-Rod Cluster
46.51	4716	4295	4762
51.59	3634	3332	3723
56.67	2822	2570	2895
61.75	2198	1986	2257
66.83	1693	1574	1767
71.91	1331	1228	1397
76.99	1022	953	1077
82.07	797	744	848
87.15	626	583	661
92.23	488	447	512
97.31	373	344	402
102.39	287	272	310
107.47	222	209	239

(1) per milligram

(2) measured from the bottom of the tank

Table D.4

VALUES OF γ^2 ($\times 10^{-6}$ CM^{-2})

Nat. Uranium Rod	19-Rod Cluster	31-Rod Cluster
2510	2442	2433
2501	2413	2371
2460	2410	2356
2478	2401	2372
2513	2432*	2434*
2469	2400*	2401*
	2395*	2348*
	2444*	2388*

* Cluster rotated through 30°

Table D.5

VALUES OF R

Nat. Uranium Rod	19-Rod Cluster	31-Rod Cluster
97.11	78.25	57.08
130.06	76.88	59.82
120.53	79.89	57.60
128.32	76.62	60.56
121.76	78.53	55.86
133.24	77.9	59.08
117.42	75.92	57.77
126.68	77.52	59.52

Table D.6

VALUES OF F AND f_e

Fuel Type	F	f_e	Average f_e
Natural Uranium Rod	361.8 361.4	0.9516 0.9505	0.9510
19-Rod Cluster	407.8 386.5	1.072 1.016	1.044
31-Rod Cluster	394.75 385.04	1.038 1.013	1.025

Appendix E

η OF NATURAL URANIUM ROD

The natural uranium rod has been used as a "reference element" in the experimental determination of heterogeneous fuel parameters of single clusters. The reference value of η is calculated from the "accepted" value of η' of a 1.0 in. diameter natural uranium rod. η' is defined as the number of neutrons due to thermal fission in U-235 per thermal neutron absorbed in the fuel. It is necessary to correct η' for the effects of epithermal and fast fissions in the fuel rod in order to obtain η. The correction is based upon the values of δ_{25} and δ_{28} measured (S1) for a single 1.01 in. diameter natural uranium rod in D_2O. Equation 2.4 gives the necessary relation for the calculation of η from η'. Values used for the constants appearing in Eq. 2.4 are as follows:

$\eta' = 1.315$ (K2)	$\nu_{28,f} = 2.7$ (K1)
$\delta_{25} = 0.008$ (S1)	$\alpha_{28,f} = 0.107$ (K1)
$\delta_{28} = 0.058$ (S1)	$\nu_{25,th} = 2.47$ (K1)

The resulting reference value of η obtained for the natural uranium rod is 1.375.

Appendix F

ERI^{238} AND A OF SINGLE ELEMENTS

The values of the ERI^{238} are calculated from Hellstrand's empirical correlations (H3):

$$ERI^{238} = 4.25 + 26.8\sqrt{\frac{S}{M}} \quad \text{(metal)}, \tag{F.1}$$

and

$$ERI^{238} = 5.6 + 26.3\sqrt{\frac{S}{M}} \quad \text{(oxide)}, \tag{F.2}$$

Equation F.1 is used for the natural uranium rod, and Eq. 4.2 is used for the UO_2-PuO_2 clusters. All the data necessary for this calculation are given in Fig. 1.1 and Table 3.1. In the case of cluster, the values of ERI have been calculated by two methods. In one of the methods, S is taken as the effective surface area (H1) of the fuel rods within the cluster. In the other, the cluster is homogenized and M taken to be the mass of all U-238 atoms. Both procedures given approximately the same results (for example, 14.25b versus 14.06b for the 19-rod cluster).

The epithermal absorption parameter, A, of the fuel elements is evaluated by substituting the calculated values of ERI^{238} in the following equation.

$$A = \frac{V_f}{\xi\Sigma_s}\left[N^{238}\, ERI^{238} + \sum_{i,i\neq U\text{-}238} N^i RI^i_\infty\right]. \tag{F.3}$$

The summation in the section term of Eq. F.3 extends over all uranium and plutonium isotopes with the exception of U-238. Their low concentration in the fuel permits the use of infinite dilution

values for their resonance integrals (D5). The concentration of various isotopes in the fuel and the epithermal nuclear data used in the calculation of A are given in Appendix G and Table 4.2.

The values of ERI^{238}, and A calculated for the natural uranium rod ("reference element") and the two UO_2-PuO_2 clusters are tabulated in Table F.1. Also shown in the table is the contribution to A of the epithermal absorption in U-238 (A^{238}). In the present work, the calculated values of A of the fuel clusters have been used only to estimate the range over which the values of A should be varied in order to generate the curves of f_c versus A (Fig. 2.4). They are, however, in good agreement with the experimentally determined values (Table 3.6).

Table F.1

CALCULATED VALUES OF ERI^{238} AND A

Fuel Type	$\sqrt{S/M}$	ERI^{238}	A^{238}	A
Nat. U rod	0.28	11.95	16.3	20.4
19-rod cluster	0.32	14.06	42.2	54.2
31-rod cluster	0.28	12.95	64.1	83.2

Appendix G

CONCENTRATION OF NUCLIDES IN THE UO_2-PuO_2 FUEL CLUSTERS*

Nuclide	Nuclei/cm^3 × 10^{-24}	
	19-Rod Cluster	31-Rod Cluster
O^{16}	0.02224	0.02215
Al^{27}	0.00984	0.00877
U^{235}	0.03348 × 10^{-3}	0.03334 × 10^{-3}
U^{238}	0.01106	0.01101
Pu^{239}	0.02661 × 10^{-3}	0.02650 × 10^{-3}
Pu^{240}	0.01758 × 10^{-4}	0.01750 × 10^{-4}
Pu^{241}	0.02241 × 10^{-5}	0.02232 × 10^{-5}
Pu^{242}	0.01128 × 10^{-6}	0.01124 × 10^{-6}

Appendix H

NOMENCLATURE

Superscripts

238	uranium-238
epi	epithermal neutrons
fast	fast neutrons
i	nuclide type
st	standard value; refers to the "reference" fuel element

Subscripts

25	uranium-235
28	uranium-238
∞	infinite dilution
Au	resonance energy of gold-197
a	absorption (cross-section)
c	unit cell
cd	cadmium cut-off energy (0.4 ev)
ef	effective resonance energy for epithermal fission
epi	epithermal neutrons
f	fuel (includes cladding and coolant)
f	fission (cross-section)
f	fast neutrons
L	lattice
Mo	resonance energy of molybdenum-98
m	moderator
r	effective resonance energy for epithermal absorption
r	radial component
SE	single element
s	scattering (cross-section)
st	standard value; refers to the "reference" fuel element
t	total (cross-section)

th	thermal neutrons
tr	transport of thermal neutrons
z	axial component

Arabic

A	epithermal absorption parameter, cm^2
a	radius of the smallest circle which completely encloses the single fuel assembly, cm
B_m^2	material buckling, cm^{-2}
b	radius of unit cell, cm
D	diffusion coefficient of thermal neutrons in the moderator, cm
E	energy of neutron, ev
ERI	effective resonance integral of the fuel element, barns
ERI(u)	partial ERI evaluated from lethargy, u, barns
F	ratio of the epicadmium activities of unit isotopic weights of Au-197 and Mo-98 irradiated on the fuel surface; obtained experimentally
f	thermal utilization (conventional)
f_Γ	thermal utilization (derived from Γ; cladding and coolant included in the fuel)
f_c	ratio of the neutron flux in group-12 ($3 \leq E \leq 10$ev) to that in group-9 ($100 \leq E \leq 550$ev); obtained from the ANISN computer program
f_e	ratio of the neutron flux at Au-197 resonance to that at Mo-98 resonance, obtained from F; obtained experimentally
I_0, I_1	modified Bessel functions of the first kind, zero and first order respectively
J_0, J_1	Bessel functions of the first kind, zero and first order respectively
K_0, K_1	modified Bessel functions of the second kind, zero and first order respectively
L	diffusion length of thermal neutrons in a lattice, cm
L_0	value of L in the moderator, cm
N	number density of nuclide, cm^{-3}
p	resonance escape probability
p_0	spacing between neighboring fuel elements in a lattice, cm

$q(r,z,\tau)$	asymptotic slowing-down density of neutrons of age τ at a point (r,z), cm^{-3} sec^{-1}
R	cadmium ratio (ratio of the bare to the cadmium-covered activity) of gold at r = Y; obtained experimentally
$\tilde{R}$	extrapolated radius of the moderator tank at which neutron fluxes of all energies vanish, cm
RI	resonance integral, barns
r	radial distance from the axis of the moderator tank, cm
S/M	surface-to-mass ratio of the fuel element, cm^2/gm
u	lethargy of neutron
V	volume, cm^3
v	volume fraction of fuel
v	velocity of neutron, cm/sec
X	radial distance of the peak of the asymptotic thermal neutron flux in the moderator, cm; obtained experimentally
Y	radial distance at which R is measured, cm
Y_0, Y_1	Bessel functions of the first kind, zero and first order respectively
z	axial distance from the bottom of the tank cm

Greek

α	related to γ (Eq. 2.10), cm^{-1}
α	capture-to-fission ratio
β	ratio of the average epithermal flux in the fuel to that in the moderator
Γ	thermal constant, cm^{-1}
γ	inverse relaxation length of the axial flux, cm^{-1}; obtained experimentally
η	fast neutron yield factor
η'	conventional η
λ	mean-free-path of thermal neutrons in the moderator ($1/\Sigma$), cm
λ_f	mean-free-path of fast neutrons in the moderator, cm
ν	average number of neutrons produced per fission
ξ	average loss in lethargy per collision
ξ	dummy variable
Σ	macroscopic nuclear cross-section, cm^{-1}

σ	microscopic nuclear cross-section, barns
τ	age of neutron, cm^2
ϕ	total neutron flux, cm^{-2} sec^{-1}
$\phi(r,z)$	asymptotic thermal neutron flux at a point (r,z) in the moderator, cm^{-2} sec^{-1}
$\phi_{epi}(r,z)$	asymptotic epithermal flux at a point (r,z) in the moderator, cm^{-2} sec^{-1}
$\hat{\phi}_r(r)$	relative value of the radial component of $\phi(r,z)$ with respect to its value on the fuel surface

Appendix I

BIBLIOGRAPHY OF PUBLICATIONS ON HETEROGENEOUS REACTOR THEORY

This bibliography contains a selection of references which deal with various aspects of heterogeneous reactor theory and single fuel element neutronics. A brief comment is included on each.

1. Barden, S. E. et al., "Some Methods of Calculating Nuclear Parameters for Heterogeneous Systems," Proc. Intern. Conf. Peaceful Uses At. Energy, Geneva, P/272 (1958). Application of heterogeneous method to finite arrays of rectangular shape.

2. Bernard, E. A. and R. B. Perez, "Determination of Heterogeneous Parameters by the Neutron Wave Technique," Trans. Am. Nucl. Soc., 12, No. 1, 663 (1969). Measurement of the thermal constant in a single element experiment; analysis by age-diffusion theory.

3. Blaesser, G., "An Application of Heterogeneous Reactor Theory to Substitution Experiments," P/42/52, IAEA Symposium, Amsterdam (1963). The method avoids many difficulties which are typical of homogenized treatment as, for example, determination of coupling constants.

4. Corno, S. E., "Interpretazione Teorica delle Esperienze di Moltiplicazione Neutronica su un Solo Elemento di Combustible," Energia Nucleare, 10, 11 (1963). A highly theoretical application of small source theory to the problem of a single rod in an exponential pile. (Series of three articles.)

5. Corno, S. E., "Theory of Pulsed Neutron Experiments in Highly Heterogeneous Multiplying Media," in Pulsed Neutron Research, Vol. II, IAEA, Vienna (1965). A theory of pulsed neutron experiments applicable to a single fuel element.

6. Donovan, R. "Measurement of Heterogeneous Parameters," MIT-2344-12 (1967). Calculations based on measurements on a single element using foil techniques.

7. Durrani, S., E. Etherington and J. Ford, "Determinations of Reactor Lattice Parameters from Measurements on a Single Fuel Element Channel," APC/TN 1054. Another application of the method in (30) below.

8. Estabrook, F. B., "Single Rod Exponential Experiments," NAA-SR-925, P13. Reports other data on some experiments as in (14).

9. Feinberg, S. M., "Heterogeneous Methods for Calculating Reactors," Proc. Intern. Conf. Peaceful Uses At. Energy, Geneva, P/669 (1955). One of the original and basic theoretical papers on heterogeneous methods.

10. Galanin, A. D. "The Thermal Coefficient in a Heterogeneous Reactor," and, "Critical Size of Heterogeneous Reactors with Small Number of Rods," loc. cit. 8, P/666 and P/663. Two of the original and basic theoretical papers on heterogeneous methods.

11. Graves, W. E. et al., "A Comparison of Heterogeneous Nuclear-Reactor Lattice Theory with Experiment," Nucl. Sci. Eng., 31, 57 (1968). Comparison is made for thermal neutron densities and critical geometric bucklings.

12. Hamilton, G. T., "Application of the Single Element Method to Light Water Lattices," MIT-3944-4 (1969). Data on H_2O-moderated lattices shown to be interpretable in terms of heterogeneous reactor theory.

13. Hassit, A., "Methods of Calculation of Heterogeneous Reactors," Progress in Nuclear Energy, Series I, Vol. II, P271 (1958). Describes the "mesh method" of solving the two group diffusion theory equations within the moderator region of the heterogeneous system using finite difference equations.

14. Heinzman, O. W. and S. W. Kash, "Intracell Flux Distributions for an Extensive Series of Heavy Water, Uranium Rod Lattices," NAA-SR-1548 (1956). Reports radial flux traverses about 1-inch diameter single rods.

15. Higgins, M. J., "Fuel Rod Interaction Kernels," MIT-2344-12 (1967). Describes experimental determination of the rod interaction kernels and methods that can use these kernels to predict integral parameters for entire lattices.

16. Horning, W. A., "Small Source Model of a Thermal Pile," HW-24282 (1952). An early attempt at an analysis that could be used to relate theory and experiment.

17. Jonsson, A., "Heterogeneous Calculation of Fast Fission," AE-42 (1961). An exact calculation of the collision probabilities is included.

18. Jonsson, A. and G. Naslund, "Heterogeneous Two Group Diffusion Theory for a Finite Cylindrical Reactor," AE-57 (1961). Describes the basis for the computer code HETERO.

19. Jonsson, A., G. Naslund et al., "Theory of Application of Heterogeneous Methods for D_2O Reactor Calculations," Proc. Intern. Conf. Peaceful Uses At. Energy, Geneva, P/683 (1964). Extension of heterogeneous methods to finite cylindrical systems.

20. Klahr, C. N. et al., "Heterogeneous Calculation Methods," NYO-2680 (1961). A final report on small source reactor physics calculations using the HERESY code.

21. Lanning, D. D. "Heterogeneous Reactor Critical Conditions Using Small Source Theory," TID-7532, Part I (1957). The application of heterogeneous analysis using age theory, to reactors containing control rods.

22. Meetz, K., "Exact Treatment of Heterogeneous Core Structures," loc. cit. 1, P/968. A theoretical paper which develops a mathematical formalism for such problems.

23. Papay, L. T., "Fast Neutron Fission Effect for Single Slightly Enriched Uranium Rods in Air and Heavy Water," MIT-2344-4 (1965). Describes the determination of δ_{28} for small diameter single rods.

24. Pershagen, B., G. Anderson and I. Carlvik, "Calculation of Lattice Parameters for Uranium Rod Clusters in Heavy Water and Correlation with Experiments," loc. cit. 1, P/151. An example of the application of the Poisson summation in heterogeneous lattices.

25. Pilat , E. E. et al., "The Use of Experiments on Single Fuel Elements to Determine the Nuclear Parameters of Reactor Lattices," MIT-2344-10 (1967). Combines experiments on a single element with a theory which describes a lattice of such elements.

26. Rodeback, G. W., C. H. Skeen and J. W. Zink, "Single Element Measurements," Trans. Amer. Nucl. Soc., 2, 1 (1959). A preliminary report on (30).

27. Saji, G. and A. Axford, "Space-Time Kinetics for Heterogeneous Reactor Models," Nucl. Sci. Eng., 35, 319 (1969). A new theoretical formalism of the space-time kinetics is developed for heterogeneous reactor models.

28. Seth, S. S., "Measurement of Integral Parameters," MIT-2344-9 (1966) and MIT-2344-12 (1967). Reports include techniques to obtain single element integral parameters.

29. Stewart, J. D. et al., "MICRETE: A G-20 Program for Calculating Finite Lattices by the Microscopic Discrete Theory," AECL 2547 (1966). Description of the program MICRETE for solving 2D reactor lattice problem using heterogeneous theory.

30. Zink, J. and G. Rodeback, "The Determination of Lattice Parameters by Means of Measurements on a Single Fuel Element," NAA-SR-5392 (1960). Actual experiments on a single fuel rod are used to infer parameters of graphite uranium lattices, with best results in the thermal energy region. Also reported in Nucl. Sci. Eng., 9, 16 (1961).

Appendix J

REFERENCES

A1. Albertoni, S., G. Blaesser, G. D'Amico, "HET-B2: A Heterogeneous Method for Reactor Calculations," Eur. 1839-C (1964).

B1. Baumann, N. P., J. L. Crandall, et al., "Lattice Experiments with Simulated Burned-up Fuel for D_2O Power Reactors," DP-1122 (1968).

B2. Bernard, E. A., R. B. Perez, "Determination of Heterogeneous Parameters by the Neutron Wave Technique," Trans. Am. Nucl. Soc., 12, No. 1, 663 (1969).

B3. Bierens De Haan, D., "Nouvelles Tables D'intégrales définies de m.," New York Stechert (1969).

B4. Blaesser, G., G. Casini, G. D'Amico, "Studies in the Field of Heterogeneous Reactor Theory," Eur-2105-E (1964).

B5. Boling, M. A., W. A. Rhoades, "ANISN/DTF II Conversion to IBM System 360," AI-66-Memo 171 Vol. 1 (1967).

B6. Brooks, W. L., H. Soodak, "Resonances Absorption in D_2O Lattice Reactors," NDA-2131-19 (1960).

C1. Carslaw, H. S., J. C. Jaeger, "Conduction of Heat in Solids," 2nd ed., Clarendon Press, Oxford (1959).

C2. Crandall, J. L., "D_2O Power Reactor Physics," Letter to Dr. H. Harty, Manager, Pacific Northwest Laboratory, Battelle Memorial Institute (September 18, 1967).

D1. Davis, H. T., "The Summation of Series," Principia Press, Trinity University (1962).

D2. Dessauer, G., "Physics of Natural Uranium Lattices in Heavy Water," Proc. Intern. Conf. Peaceful Uses At. Energy, Geneva, 12, 320 (1958).

D3. Donohew, J. N., J. D. Eckard, "Numerical Methods," loc. cit., ref. D6, Chapter 7.

D4. Donovan, R. E., "Determination of the Heterogeneous Parameters Γ, A and η by Measurements on a Single Fuel Element," S.M. Thesis, Department of Nuclear Engineering, M.I.T. (1967).

D5. Drake, M. K., "A Compilation of Resonance Integrals," Nucleonics (August, 1966).

D6. Driscoll, M. J., T. J. Thompson, Eds. "Reactor Physics Project Progress Report," MIT-3944-1, MITNE-96 (1968).

D7. Driscoll, M. J., I Kaplan, D. D. Lanning, Eds. "Reactor Physics Project Progress Report, No. 2," MIT-3944-4, MITNE-111 (1969).

E1. Engel, W. W., M. A. Boling, B. W. Colston, "DTF II, A One-Dimensional, Multigroup, Neutron Transport Program," NAA-SR-10951 (1966).

E2. Engel, W. W., "A User's Manual for ANISN," K-1693 (1967).

F1. Feinberg, S. M., "Heterogeneous Methods for Calculating Reactors: Survey of Results and Comparison with Experiment," Proc. Intern. Conf. Peaceful Uses At. Energy, Geneva, 5, 484 (1955).

F2. Finch, D. R., "User's Manual for SRL-HERESY I," DP-1027 (1966).

F3. Frech, D., "Neutron Temperature Measurements Inside Fuel Rods," Chapter 5, Heavy Water Lattice Project Final Report, MIT-2344-12, MITNE-86 (1967).

F4. French, P. M., R. Solheim, "Experimental Bucklings of Simulated Burned-up Natural Uranium Clusters in Heavy Water," ANS/CNA Trans., 11, No. 1 (1968).

G1. Galanin, A. D., "The Thermal Coefficient in a Heterogeneous Reactor," loc. cit., ref. F1, p. 477.

G2. Galanin, A. D., "Critical Size of Heterogeneous Reactors With Small Number of Rods," loc. cit., ref G1, p. 462.

G3. Gibson, I. H., "The Physics of LATREP," AECL-2548, CRRP-1235 (1966).

G4. Gosnell, J. W., "Studies of Two-Region Subcritical Uranium Heavy Water Lattices," Sc.D. Thesis, Department of Nuclear Engineering, M.I.T. (1969).

G5. Gradshteyn, I. S., I. M. Ryzhik, "Table of Integrals, Series, and Products," 4th et., Academic Press, New York (1965).

G6. Graves, W. E., "Measured Slowing Down Distribution at the Indium Resonance from a Line Source of Fission Neutrons in Heavy Water," Nucl. Sci. Eng., 12, 439 (1962).

G7. Graves, W. E., F. D. Benton, R. M. Satterfield, "A Comparison of Heterogeneous Nuclear Reactor Lattice Theory and Experiment," Nucl. Sci. Eng., 31, 57 (1968).

H1. Halsall, M. J., "The Effective Surface Area of Fuel Clusters for Resonance Integral Calculations," AECL-2775 (1967).

H2. Hamilton, G. T., "Application of the Single Element Method to Light Water Lattices," S.M. Thesis, Department of Nuclear Engineering, M.I.T. (1969).

H3. Hellstrand, E., "Measurement of Resonance Integrals," in Reactor Physics in the Resonance and Thermal Regions, Eds. A. J. Goodjohn and G. C. Pomraning, Vol. 2, The M.I.T. Press (1966).

H4. Hemmig, P. B., Ed. "Conference on Neutron Cross-Section Technology," P148, CONF-660303 (1966).

H5. Higgins, M. J. "Determination of Reactor Lattice Parameters Using Experimentally Measured Kernels," S.M. Thesis, Department of Nuclear Engineering, M.I.T. (1968).

H6. Hildebrand, F. B., "Methods of Applied Mathematics," 2nd ed., Prentice-Hall, Inc., Englewood Cliffs, N. J. (1965).

H7. Hildebrand, F. B., "Introduction to Numerical Analysis," McGraw-Hill, New York (1956).

H8. Honeck, H. C., J. L. Crandall, "The Physics of Heavy Water Lattices," in Reactor Technology - Selected Reviews, Ed. L. E. Link, Argonne National Laboratory (1965).

H9. Horning, W. A., "Small Source Model of a Thermal Pile," HW-24282 (1952).

K1. Kaplan, I., "Nuclear Reactor Physics (II)," Course 22.22 Lecture Notes, Department of Nuclear Engineering, M.I.T. (1965).

K2. Kaplan, I., J. Chernick, "Uranium-Graphite Lattices - The Brookhaven Reactor," loc. cit., ref. (G1), p. 295.

K3. Klahr, C. N., J. Heitner, N. Stein, "Test and Verification of Heterogeneous Reactor Calculation Methods," NYO-3194-1 (1964).

K4. Klahr, C. N., L. B. Mendelsohn, J. Heitner, "Heterogeneous Reactor Calculation Methods," NYO-2680 (1961).

L1. Leung, T. C., "Measurement of η Using Foil Activation Technique," S.M. Thesis, Department of Nuclear Engineering, M.I.T. (1969).

M1. McFarland, E., "Experimental Determination of the Epithermal Absorption Parameter, A," S.M. Thesis, Department of Nuclear Engineering, M.I.T. (1969).

N1. Näslund, G., "HETERO, Description of the IBM 7044 Program," TPM-RFN-176, AB Atomenergi, Sweden (1964).

O1. Ortiz, N. R., T. C. Leung, "Pulsed Neutron and Buckling Methods," loc. cit., ref D6, Chapter 5.

P1. Palmedo, P. F., I. Kaplan, T. J. Thompson, "Measurements of the Material Bucklings of Lattices of Natural Uranium in D_2O," NYO-9660, MITNE-13 (1962).

P2. Pilat, E. E., M. J. Driscoll, I. Kaplan, T. J. Thompson, "The Use of Experiments on a Single Fuel Element to Determine the Nuclear Parameters of Reactor Lattices," MIT-2344-10, MITNE-81 (1967).

P3. Poncelet, C. G., "LASER - A Depletion Program for Lattice Calculations Based on MUFT and THERMOS, WCAP-6073 (1966).

R1. "Reactor Physics Constants," ANL-5800, Argonne National Laboratory (1963).

S1. Seth, S. S. "Measurement of Integral Parameters," Chapter 3, Heavy Water Lattice Project Final Report, MIT 2344-12, MITNE-86 (1967).

S2. Stewart, J. D., J. M. Kennedy, (Mrs.) S. J. Cowley, "MICRETE: A G-20 Program for Calculation of Finite Lattices by the Microsopic-Discrete Theory," AECL-2547 (1966).

S3. Suich, J. E., H. C. Honeck, "The HAMMER System," DP-1064 (1967).

T1. Tanner, C. J., D. G. Andrews, "Buckling Measurements in a Heavy-Water Super Lattice," Trans. Am. Nucl. Soc., 11, No. 1, 252 (1968).

T2. Thompson, T. J., I. Kaplan, Eds., "Heavy Water Lattice Project Annual Report," NYO-9658 (1961).

W1. Wade, J. W. "Neutron Age in Mixtures of D_2O and H_2O," Nucl. Sci. Eng., 4, 12 (1958).

W2. Weinberg, A. M., E. P. Wigner, "The Physical Theory of Neutron Chain Reactors," University of Chicago Press, Chicago, Ill. (1958).